UNIVERSITY OF TASMANIA

Rapid Mass Spectrometry Approaches for Wine Industry Quality Control Applications

by

Ross R. Farrell (BSc., MSc.)

A thesis submitted in fulfilment of the requirements for the degree of Doctor of Philosophy

Australian Centre for Research On Separation Science (ACROSS)
School of Natural Sciences

University of Tasmania
July 2018

Declaration

This thesis contains no material which has been accepted for a degree or diploma by the University or any other institution, except by way of background information and duly acknowledged in the thesis, and to the best of my knowledge and belief no material previously published or written by another person except where due acknowledgement is made in the text of the thesis, nor does the thesis contain any material that infringes copyright.

The publishers of the papers comprising Chapters 2 and 3 hold the copyright for that content, and access to the material should be sought from the respective journals. The remaining non-published content of the thesis may be made available for loan and limited copying and communication in accordance with the Copyright Act 1968.

Ross R. Farrell

July 2018

Acknowledgments

Throughout my PhD Candidature I have been fortunate to meet extraordinary people who have inspired, guided and assisted me in this incredible journey into Mass Spectrometry – thank you.

I would like to extend my gratitude to my supervisors for sparking my interest in Analytical Chemistry and accommodating my PhD with the Australian Centre for Research On Separation Science (ACROSS) and the University of Tasmania. To Noel Davis, thank you for your time and enthusiasm and for the enlightening discussions on mass spectrometry. I gratefully acknowledge financial support from an Australian Postgraduate Award and a PhD scholarship from the Australian Grape and Wine Authority.

To my collaborators at ETH-Zurich, special thanks to Renato Zenobi for welcoming me to his group. I am indebted to many members of the Zenobi group who have shared their knowledge and passion for mass spectrometry, particularly Jan-Christoph Wolf.

To my collaborators at Zurich University of Applied Science, special thanks to Chahan Yeretzian for sharing his experience of “direct” mass spectrometry. Thanks to Marco Wellinger, Alexia Gloess, José Antonio Sánchez-López and Samo Smrke for their time and advice.

To my friends in SoHo, thank you for seeing me through those early days.

To Kaja, what can I say? Thank you for your enthusiasm, patience, unwavering support, the “positive rays” and Richard Feynman!

“You must expect failure after failure after failure before you succeed.”

Edwin Land

Statement of co-authorship

The following people and institutions have contributed to the publication of work undertaken as a part of this thesis:

Ross R Farrell, ACROSS, School of Natural Sciences, UTAS: Candidate
Renato Zenobi, Department of Chemistry and Applied Biosciences, ETH-Zurich
Pablo Martinez-Lozano Sinues, Department of Chemistry and Applied Biosciences, ETH-Zurich
Diego García-Gómez, Department of Chemistry and Applied Biosciences, ETH-Zurich
Johannes Fahrentrapp, Institute of Natural Resource Sciences, Zurich University of Applied Sciences
Chahan Yeretzian, Institute of Chemistry and Biological Chemistry, Zurich University of Applied Sciences
Alexia N. Gloess, Institute of Chemistry and Biological Chemistry, Zurich University of Applied Sciences
Marco Wellinger, Institute of Chemistry and Biological Chemistry, Zurich University of Applied Sciences
Michael C Breadmore, ACROSS, School of Natural Sciences, UTAS
Robert A Shellie, Trajan Medical and Scientific and ACROSS, School of Physical Sciences, UTAS
David S Nichols, Central Science Laboratory, Division of Research, UTAS

Author contributions

1. Rapid fingerprinting of grape volatile composition using secondary electrospray ionization orbitrap mass spectrometry: A preliminary study of grape ripening
Presented in Chapter 2

Candidate was the primary author and performed all the experiments and data analysis (65%) while JF (10%), PMLS (10%), RZ (10%) and DGG (5%) helped with the formation of the idea, presentation and refinement of the published work.

2. Real-Time Mass Spectrometry Monitoring of Oak Wood Toasting: Elucidating Aroma Development Relevant to Oak-aged Wine Quality

Presented in Chapter 3

Candidate was the primary author and performed all the experiments and data analysis (70%) while MW (10%), ANG (7%) and CY (7%) helped with the formation of the idea, presentation and refinement. MCB, RAS and DSN contributed to refinement and presentation of the published work (total of 6%).

We the undersigned agree with the above stated contributions by the candidate for each of the published manuscripts contributing to this thesis.

Signed:

Prof. Michael Breadmore
Supervisor
School of Natural Sciences
University of Tasmania

Date: 5/7/2018

Signed:

Prof. Mark Hunt
Head of School
School of Natural Sciences
University of Tasmania

Date: 5/7/18

List of publications and presentations

1. R.R. Farrell, J. Fahrentrapp, D. Garcia-Gomez, P. Martinez-Lozano Sinues, R. Zenobi. Rapid Fingerprinting of Grape Volatile Composition Using Secondary Electrospray Ionization Orbitrap Mass Spectrometry: A Preliminary Study of Grape Ripening. *Food Control* 81: 107–12. [Research Article]

2. R.R. Farrell, M. Wellinger, A.N. Gloess, D.S. Nichols, R.A. Shellie, M.C. Breadmore, C. Yeretzian. 2015. Real-Time Mass Spectrometry Monitoring of Oak Wood Toasting: Elucidating Aroma Development Relevant to Oak-Aged Wine Quality. *Scientific Reports* 5 (17334): 1–13. [Research Article]

3. R.R. Farrell, Robert A. Shellie and M.C. Breadmore, 2013. Optimising Oak Aromas Through Near Real-Time Analysis. 15th Australian Wine Industry Technical Conference, Sydney. [Poster presentation]

4. R.R. Farrell, 2013. Optimising Oak Aromas Through Near Real-Time Analysis. 15th Australian Wine Industry Technical Conference, Sydney. ["in the wine light" student forum oral presentation]

5. R.R. Farrell, R. Wilson, D.S. Nichols, M.C. Breadmore, 2014. Direct infusion and paper spray ionisation mass spectrometry for high-throughput screening of rapid oak extracts. 20th international mass spectrometry conference, Geneva. [Poster presentation]

6. R.R. Farrell, J.C. Wolf, R. Zenobi, 2015. Online monitoring of oak wood volatiles by active capillary plasma ionization mass spectrometry.10th international symposium of oenology, Bordeaux. [Poster presentation]

7. R.R. Farrell, D. Stadler, J. Krismer, R. Zenobi, 2017. Rapid screening of non-volatile oak wood components of oenological importance. 26th The Australian and New Zealand society for mass spectrometry (ANZSMS) conference. Adelaide. [Poster presentation]

Abstract

The work presented in this thesis investigates the utility of direct mass spectrometry (MS) approaches for wine industry quality control applications.

Chapter 1 provides an insight into the evolution of direct mass spectrometry from the beginnings of mass spectrometry in 1913, to the development of proton transfer reaction mass spectrometry in 1995 and the breakthrough invention of desorption electrospray ionisation in 2004. The latter represents the birth of "ambient mass spectrometry" marking a new approach to mass spectrometry – the pursuit of direct, *in situ* analysis on unprocessed samples in their natural environment.

High-variability is a natural characteristic of grapes and oak-aging processes and thus presents challenges from a wine quality perspective. These aspects of wine quality are introduced, highlighting how new analytical approaches based on direct mass spectrometry could be of benefit to the wine industry.

Chapter 2, introduces a secondary electrospray ionization mass spectrometry (SESI-MS) approach to monitor grape ripening by analysing volatile organic compounds (VOC's) directly from intact berries of non-Muscat grape cultivars (Pinot Noir, Chardonnay and Sauvignon Blanc). The method does not require sample preparation or concentration steps. Grape volatiles were tentatively identified based on soft ionisation and accurate mass, the related elemental composition and literature. Approximately 300 peaks were detected in positive ion mode, and fewer (70-100) in negative ion mode. Peaks assigned to C_{13}-norisoprenoids and benzenoid derivatives have shown similar trends during ripening in previous studies using offline gas chromatography (GC) approaches.

Considering the high sensitivity and speed of analysis, SESI-MS holds promise as a tool for the rapid screening of grape volatiles that could be useful for a number of significant applications including ripeness monitoring and disease detection.

Chapter 3, introduces a real-time method to monitor the evolution of oak aromas during the oak toasting process. French and American oak wood boards were toasted in an oven at three different temperatures, while the process-gas was continuously transferred to the inlet of a proton-transfer-reaction time-of-flight mass spectrometer for online monitoring. Oak wood aroma compounds important for their sensory contribution to oak-aged wine, were tentatively identified based on soft ionisation, molecular mass and the literature. Their time-intensity profiles revealed toasting process dynamics and illustrated in real-time how different compounds evolve from the oak wood during toasting. The study demonstrated a new analytical approach for research on oak wood toasting which circumvents limitations associated with previous gas chromatography based approaches.

In **Chapter 4**, a thermal desorption dielectric barrier discharge ionisation mass spectrometry system (TD-DBDI-MS) for rapid analysis of volatile organic compounds (VOC's) from oak wood shavings was developed. Oak VOC's were tentatively identified based on soft ionisation, accurate mass and the literature. Known oak wood VOC's from different chemical classes were detected including furanic aldehydes, volatile phenols, phenolic aldehydes, oak lactones and norisoprenoids. 287 peaks were detected across all oak samples. Screening of oak VOC's could be conducted with an analysis time of ten seconds. The system was also used to monitor the oak toasting process. Continuous infusion of an internal standard and appropriate dilution strategies demonstrated how ion suppression or enhancement phenomena could be minimised and accounted for in this ambient mass spectrometry approach.

Finally, **Chapter 5** of this thesis examines the findings of the three studies presented in Chapters 2, 3 and 4 and discusses directions for future research.

List of Abbreviations

AHC	Agglomerative hierarchical clustering
APTDI	Atmospheric pressure thermal desorption/ionisation
APGDDI	Atmospheric pressure glow discharge desorption ionisation
ASAP	Atmospheric solids analysis probe
APCI	Atmospheric pressure chemical ionisation
APPI	Atmospheric pressure photon ionisation
CI	Chemical ionisation
CID	Collision induced dissociation
DAPCI	Desorption atmospheric pressure chemical ionisation
DAPPI	Desorption atmospheric pressure photon ionisation
DART	Direct analysis in real time
DBDI	Dielectric barrier discharge ionisation
DeSSI	Desorption sonic spray ionisation
DESI	Desorption electrospray ionisation
EASI	Easy ambient sonic-spray ionisation
EESI	Extractive electrospray ionisation
EI	Electron ionisation
ELDI	Electrospray-assisted laser desorption ionisation
ESI	Electrospray ionisation
FAPA	Flowing atmospheric-pressure afterglow
FA-APGDI	Flowing afterglow-atmospheric pressure glow discharge
FD-ESI	Fused-droplet ESI
GC	Gas chromatography
GDI	Glow discharge ionisation
IR-LADESI	Infrared laser-assisted desorption ESI
JEDI	Jet desorption electrospray ionisation
LAESI	Laser ablation electrospray ionisation
LA-FAPA	Laser ablation FAPA
LIAD	Laser-induced acoustic desorption
LDI	Laser desorption ionisation
LDTD	Laser diode thermal desorption
LOD	Limits of detection
LTP	Low temperature probe
MALDI	Matrix-assisted laser desorption ionisation
MALDESI	Matrix-assisted laser desorption electrospray ionisation
MFC	Mass flow controller
MS	Mass spectrometer
ND-EESI	Neutral desorption EESI

PADI	Plasma-assisted desorption/ionisation
PCA	Principal component analysis
PI	Photon ionisation
PSI	Paper spray ionisation
PTR	Proton transfer reaction
RSD	Residual standard deviation
SESI	Secondary electrospray ionisation
SPME	Solid phase microextraction
SRM	Single reaction monitoring
SSI	Supersonic spray ionisation
TD-APCI	Thermal desorption APCI
TDU	Thermal desorption unit
TIC	Total ion current
UA-EESI	Ultrasonically assisted EESI
V-EASI	Venturi easy ambient sonic-spray ionisation
VOC	Volatile organic compound
AHC	Agglomerative hierarchical clustering
ASAP	Atmospheric solids analysis probe
CID	Collision induced dissociation
DART	Direct analysis in real time
DBDI	Dielectric barrier discharge ionisation
DESI	Desorption electrospray ionisation
ESI	Electrospray ionisation
GC	Gas chromatography
LAESI	Laser ablation electrospray ionisation
LOD	Limits of detection
MFC	Mass flow controller
MS	Mass spectrometer
PCA	Principal component analysis
PTR	Proton transfer reaction
RSD	Residual standard deviation
SESI	Secondary electrospray ionisation
SPME	Solid phase microextraction
SRM	Single reaction monitoring
TDU	Thermal desorption unit
TIC	Total ion current
VOC	Volatile organic compound

Table of Contents

Chapter 1: Introduction and Literature Review

1.1 Introduction

Ernest Hemingway once said that wine "offers a greater range of enjoyment and appreciation than, possibly, any other purely sensory thing"[1]. Flavour, in general refers to the entirety of sensations including smell, taste and touch and is related to both volatile and non-volatile compounds. Whilst non-volatile compounds are an important flavour component and interact with the volatile composition, wine aroma is considered the major contributor to overall flavour perception and perceived wine quality[2–4]. The research in this thesis focuses on the volatile compounds.

The volatile compounds in wine arise from several sources[4]:

- directly from the grape berry;
- indirectly from the grape arising from a non-volatile precursor, released during processing and/or storage;
- from yeast and bacterial metabolism;
- from oak wood extraction during aging; and
- from chemical reactions upon storage.

The sensory experience of wine thus relates primarily to the interplay of aromas derived from the grape, from fermentation processes and from compounds extracted during maturation in contact with oak wood. Numerous chemical classes are present in wines, including esters, alcohols, terpenes, C13-norisoprenoids, and sulphur compounds[2,3]. Gas chromatography (GC) is the routine analytical technique to analyse the chemical components involved in wine aroma[3]. GC, is frequently coupled with flame ionisation detectors (FID) or mass spectrometry (GC-MS), the

latter providing superior identification of compounds based on both retention time and mass. GC-MS has been used for grape and wine research at the Australian Wine Research Institute (AWRI) since 1971[5]. However, whilst GC techniques have played a pivotal role in wine and vine science they also have significant limitations:

- analyses are slow, typically requiring > 30 min per sample[6].
- they require laborious and / or time-consuming sample preparation techniques.
- they are not readily amenable to portable or point-of-need applications.

Direct mass spectrometry (MS) techniques provide a suite of alternative analytical approaches that separate compounds by mass alone. With the omission of chromatographic separation, analytical throughput can be greatly expedited, facilitating real-time analysis[7]. By utilising "soft" ionisation as opposed to "hard" ionisation (typically electron ionisation employed in GC-MS), mass spectra and subsequent compound identification in complex mixtures can be simplified. Furthermore, high sensitivity ionisation techniques (e.g. ambient ionisation) permit real-time analysis without requiring pre-concentration steps.

1.2 Direct Mass Spectrometry

1.2.1 Birth of Mass Spectrometry

The field of mass spectrometry was born following J.J. Thomson's report on experiments with "Rays of positive electricity and their application to chemical analyses" in 1913[8]. Mass spectrometers analyse molecules according to the mass-to-charge ratio (m/z) of constituent molecules allowing both qualitative and quantitative analyses. This is achieved by firstly ionising the chemical compounds, then separating the resultant ions (based on m/z), and finally detecting the ions to produce a meaningful output, typically visualised as a mass spectrum[9] (Figure 1). A mass spectrum is a plot of relative abundance (signal intensity) versus m/z on the x-axis. The separation and (typically) the ionization processes are carried out under vacuum.

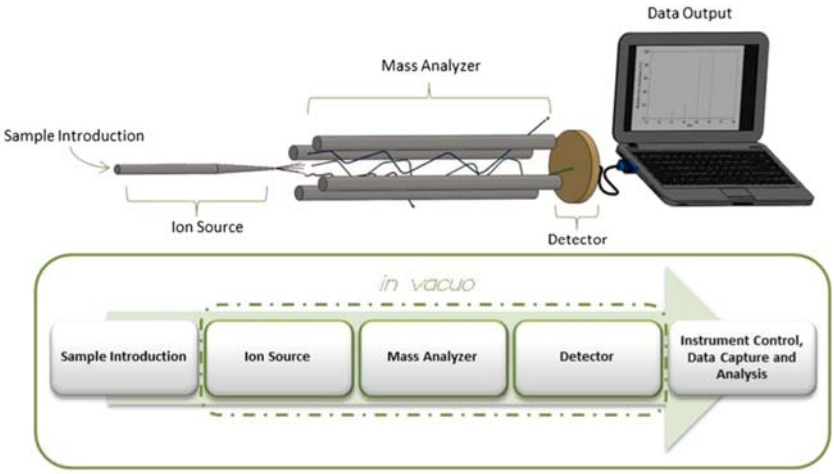

Figure 1: The stages of mass spectrometry. Reproduced with permission from reference [9]. Copyright © 2015, American Physical Society.

1.2.2 The Quest for Simplicity

The first report of electrospray ionisation (ESI) with mass spectrometry by Malcolm Dole in 1968 was a significant breakthrough in the evolution of MS (Figure 2). This removed a limitation of mass spectrometry, namely, the difficulty in transferring analyte molecules from the "real-world" to the high vacuum environment of the MS where traditional MS ionisation, for example, electron ionisation (EI), chemical ionisation (CI) and secondary ion MS (SIMS), had to be performed on pure gaseous molecules[10]. Since then, several atmospheric pressure ionisation (API) sources have been developed, including atmospheric pressure chemical ionisation (APCI) and atmospheric pressure photoionisation (APPI)[11].

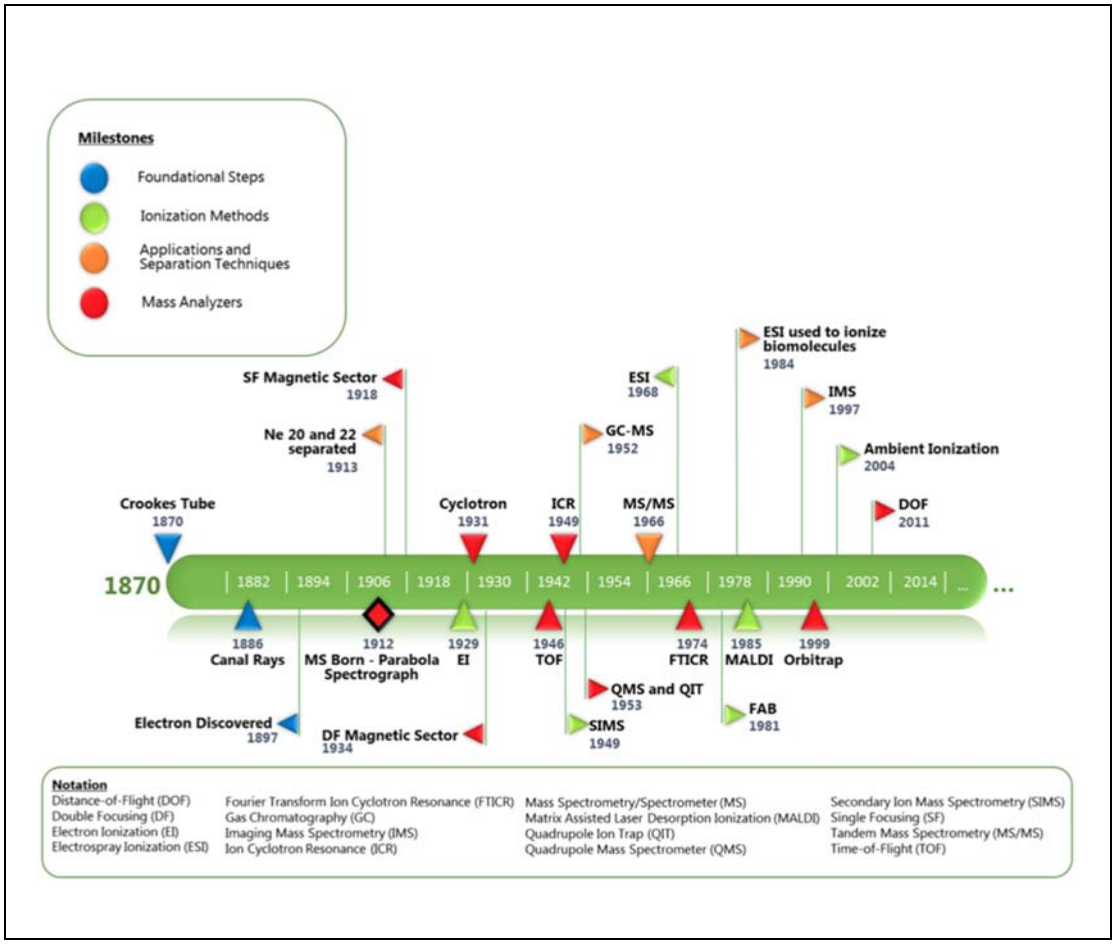

Figure 2: Summary time line of major advances in mass spectrometry. Reproduced with permission from reference[9]. Copyright © 2015, American Physical Society.

1.2.3 Ambient Mass Spectrometry

Although API methods were a revolutionary concept[10], they still required extensive sample preparation steps before the sample could be introduced to the MS. Ambient MS as demonstrated by Cooks' ground-breaking work on desorption electrospray ionisation MS (DESI-MS) in 2004[12] created a new revolution in pursuit of "simplified" MS. The essence of ambient MS is the direct, *in situ* analysis of unprocessed samples in their natural environment[9]. Ambient MS is thus distinguished from API by "the direct analysis of untreated samples or objects in the open environment, whilst largely maintaining the native condition and spatial integrity of the sample. Here, analyte molecules derived from the sample, but not the whole sample itself, are transferred into the mass spectrometer[13]."

Whilst previous attempts had been made to handle molecules directly in the "real-world"[14], the quest for simplicity was clearly kick-started by the invention of DESI in

2004, closely followed by the invention of direct analysis in real time (DART) in 2005[10]. Since the introduction of DESI, almost thirty new ambient MS techniques have been developed[13]. The diverse field of ambient MS has been thoroughly reviewed by several authors[7,10,11,13,15–22]. Fernandez[23] recently noted that some of the most cited approaches (other than DESI) include DART[24], laser ablation electrospray ionization (LAESI)[25], low temperature plasma probe (LTP)[26], atmospheric pressure solids analysis probe (ASAP)[27], electrospray-assisted laser desorption/ionization (ELDI)[28], dielectric barrier discharge ionisation (DBDI)[29], desorption sonic spray ionization (DeSSI, later relabelled EASI)[30], flowing atmospheric pressure afterglow (FAPA)[31], and paper spray[32]. At least six of these (DART, DESI, LAESI, ASAP, DBDI and paper spray) are now commercially available.

Alberici et al.[10] proposed that ambient MS methods are best understood and categorised according to the basis of their method of ionization (Figure 3).

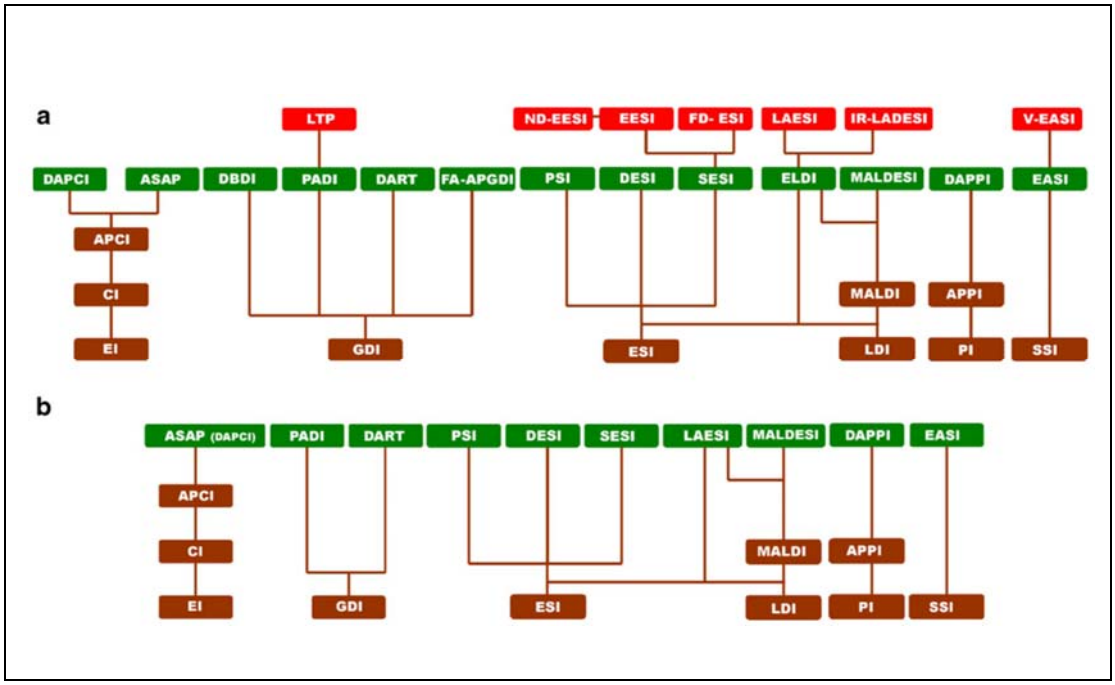

Figure 3: The ionisation tree in mass spectrometry showing the "root" technique (*brown*) and the major ambient mass spectrometry techniques (the branches in *green*) and some of their variants (the leaves in *red*). (**a**) Full view according to the present "acronym zoo". (**b**) Proposed simplified view with merging of closely related techniques into the one that best describes the desorption/ionisation principle. Reproduced with permission from reference[10]. Copyright © 2010, Springer-Verlag.

Chen et al[15] also proposed a concept to reduce the number of different acronyms describing very similar embodiments of ambient mass spectrometry (Table 1).

Table 1: Classification of ambient ionization methods according to the dominant desorption / volatilization and ionization mechanisms. Boxes shaded in grey indicate clusters of acronyms that could be replaced by a single acronym. Reproduced with permission from reference[15]. Copyright © 2009, American Society for Mass Spectrometry.

Dominant desorption/volatilization method	Dominant ionization/post-ionization method				
	Direct	**ESI Spray**	**Chemical post-ionization**	**Plasma, Penning, electrons**	**Laser or lamp post-ionization**
(Gas-phase introduction)		SESI EESI		FAPA	
(Aerosol introduction)		EESI SESI			
Liquid spray/nebulization		EESI			
Momentum transfer (liquid or gas jet)		ND-EESI, JEDI			DAPPI
ESI (including sonic spray)	DESI, EASI, DeSSI				
Laser desorption		LAESI, ELDI, (IR)-LADESI	LD/APCI	LA-FAPA	
Energetic particles	DART			PADI, FAPA (?)	
Plasma	LTP		DART, DAPCI, DBDI, LTP, PADI, DAPI, APGDDI	PADI, DART (?)	
Thermal desorption		APTDI	DART, ASAP, TD-APC, LDTD, DAPCII	DART, FAPA, APGD	DAPPI
Acoustic desorption		UA-EESI, RADIO	LIAD		

1.2.3.1 Secondary Electrospray Ionisation Mass Spectrometry

The name secondary electrospray ionisation (SESI) was first reported by Wu, Siems, & Hill, 2000[33] referring to the use of electrosprayed solvent droplets to ionize sample molecules in the gas phase. However, Fenn et al had previously noted that vapours put in contact with an electrospray cloud were ionized[34]. Whilst the ionisation mechanisms are not fully understood, ionisation is thought to mostly occur through ion-molecule reactions[35].

SESI is a soft ionisation process, producing little fragmentation. The ionisation efficiency is high, leading to excellent sensitivity and limits of detection that are commonly in the part-per-trillion (PPT) or even below PPT levels[36]. A schematic of a SESI source is shown in Figure 4 below.

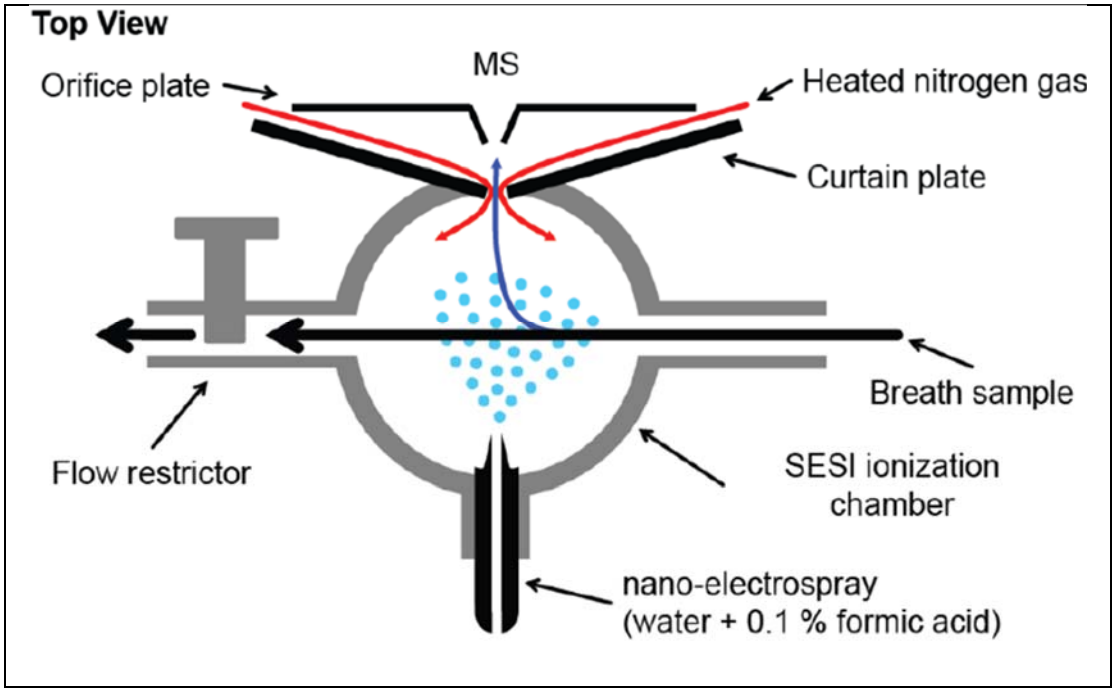

Figure 4: Scheme of the lab-built secondary electrospray ionization chamber coupled to a mass spectrometer to allow for the real-time breath analysis. Reproduced with permission from reference[37]. Copyright © 2016, British Thoracic Society and BMJ.

1.2.3.2 Dielectric Barrier Discharge Ionisation Mass Spectrometry

A dielectric barrier discharge is obtained at atmospheric pressure when alternating voltage is applied to two electrodes separated by a dielectric barrier[38] producing a stable low-temperature plasma.

The ionisation processes in DBDI are complex and affected by several parameters including the proton affinity and ionization energy of the analyte as well as the polarity of the discharge gas[39]. In positive ion mode, protonated analyte $[M+H]^+$ and/or radical cation $[M]^{+\bullet}$ are predominantly formed, either through water clusters[40] or via a radical mediated pathway[41].

DBDI, is a highly sensitive ionisation source with limits-of-detection similar to that of SESI[42]. It has the advantages of not requiring an electrosprayed solvent, is compact in size and of simple design. A schematic of a DBDI source in the so called "Active-Capillary" configuration is provided in Figure 5 below.

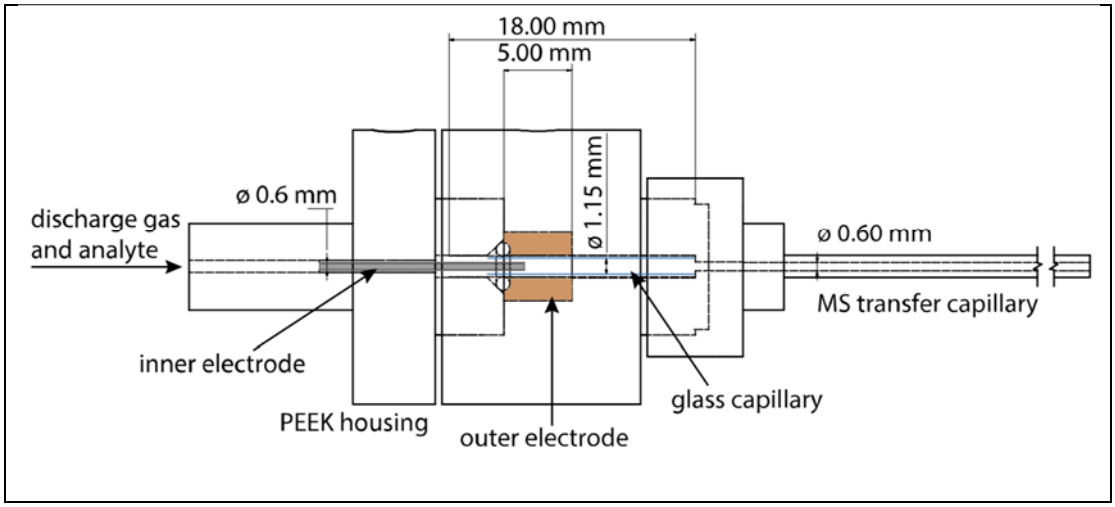

Figure 5: Schematic of the cross section of the active capillary plasma ionization source with the transfer capillary to the mass spectrometer. Reproduced with permission from reference[39]. Copyright © 2018, American Chemical Society.

1.2.4 Proton Transfer Reaction Mass Spectrometry

Proton Transfer Reaction Mass Spectrometry (PTR-MS) was first described in 1995 by scientists at the Leopold-Franzens University in Innsbruck, Austria utilizing a quadrupole mass analyser[43]. A simplified schematic of quadrupole PTR-MS is shown in Figure 6. The first reported description of a PTR-MS with time-of-flight (TOF) mass analyser was given by Blake et al. in 2004[44]. PTR-TOF-MS was a significant advancement as it facilitates high-speed measurements due to the multichannel nature of TOF mass analysers and furthermore, much greater mass resolution (R) can be achieved with a TOF (R = 5,000-10,000) compared to unit mass quadrupole analyser (R ≈ 1,000).

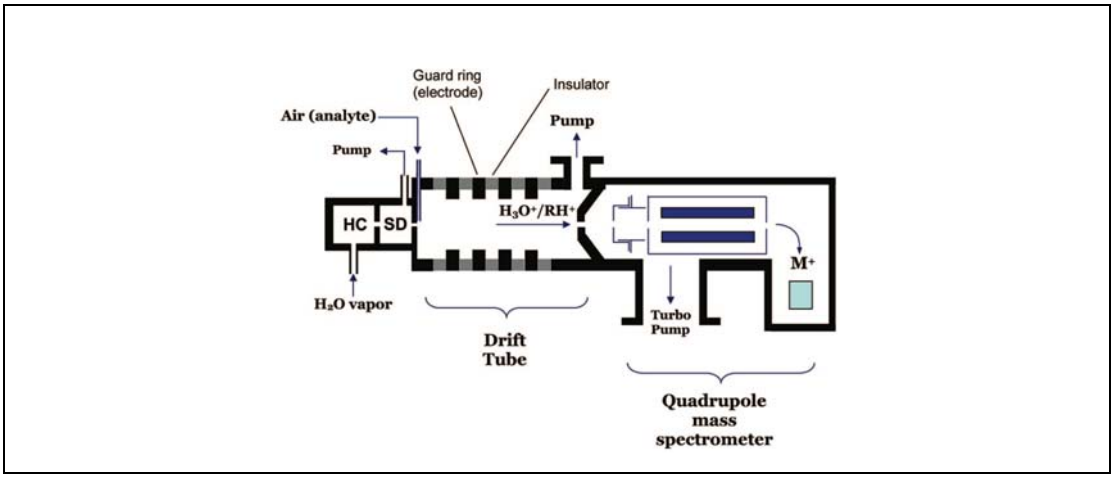

Figure 6: Simplified representation of a proton-transfer-reaction mass spectrometer utilising a quadrupole mass analyser: HC = hollow cathode discharge source and SD – source drift region. Reprinted with permission from reference [45]. Copyright © 2009 American Chemical Society.

Today, PTR-MS is the most widely used method for real-time monitoring of volatile organic compounds (VOC's) at low concentrations[46]. Whilst PTR is not an ambient ionisation approach (PTR reaction cell is typically around 2 mbar) it does share common traits with ambient approaches that exemplify its utility as a direct mass spectrometry approach:

- requires no or little sample preparation.
- real-time detection of hundreds of VOC's.
- soft ionisation.

Soft ionisation is a critical aspect of both ambient MS and PTR-MS because of the simultaneous detection of hundreds to potentially thousands of ions from different compounds present in the sample. Soft ionisation reduces fragmentation and therefore spectral complexity by reducing the m/z signals from each sample component.

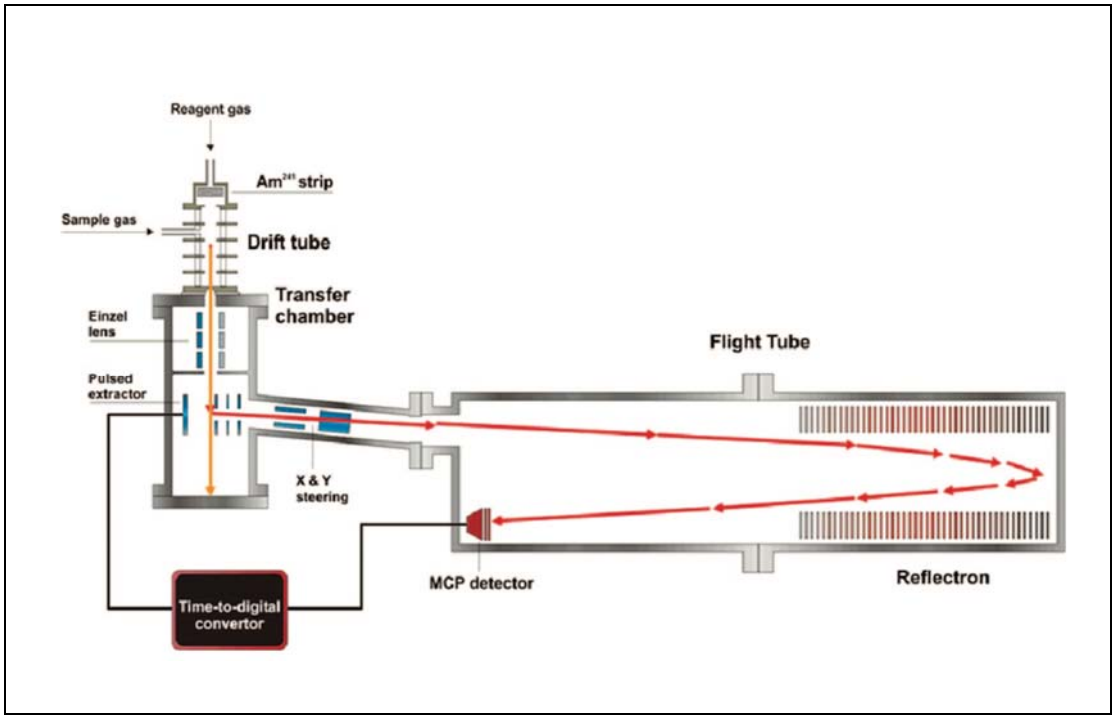

Figure 7: Schematic representation of the first published description of a PTR-TOF-MS. Reprinted with permission from reference[44]. Copyright © 2004 American Chemical Society.

PTR-MS is primarily a tool for VOC analysis that can be adopted to semi-volatile compounds by using appropriate sample introduction interfaces[47]. This is in contrast to ambient MS methods that can be used to analyse an enormous range of compounds spanning from volatile to large non-volatile compounds. PTR-MS further differs from ambient MS due to the reduced pressure reaction cell and the reliance on a single (PTR) ionisation pathway typically via high purity H_3O^+ (hydronium) ions[45]:

$$VOC + H_3O^+ \rightarrow VOC \cdot H^+ + H_2O$$

This is in contrast to the plethora of different ionisation pathways prevalent in ambient MS (Table 1). For proton transfer reactions to occur, the VOC molecule must have a higher proton affinity than that of water (proton affinity of H_2O: 166.5 kcal/mol)[48,49]. Many VOC's undergo an efficient proton-transfer reaction with H_3O^+, whereas the major component of clean air (N_2, O_2) do not because their reaction with H_3O^+ is not thermodynamically favourable.

PTR-MS is an inherently semi-quantitative or quantitative technique with highly controlled ionisation reaction conditions that facilitate direct quantification based on kinetic theory[50]. This means that (at least theoretically), quantification can be

achieved without calibration or standards. Blake et al.[45] indicate that quantitative accuracies of 10-15% can be achieved. The inherent quantitative ability of PTR-MS provides an advantage over ambient methods that can suffer from ion suppression and ion enhancement phenomena that complicate quantitation[16]. Accurate absolute quantitation is still considered an issue in ambient MS[23].

Recent advancements in PTR-MS include the ability to utilise different reagent ions such as O_2^+ and NO^+ through a "switchable ion source"[51]. The different ionisation induced by different precursor ions can facilitate the separation of isomeric compounds[52], but also enables the ionisation of molecules with a proton affinity lower than water, expanding the range of amenable compounds that can be analysed[45].

1.2.5 Ionisation methods used

Three different ionisation methods were used with mass spectrometry in this thesis. Namely, (i) proton-transfer-reaction (PTR), (ii) secondary electrospray ionisation and (iii) dielectric barrier discharge ionisation. PTR was selected as it is a well-established approach, generally regarded as the most widely used method for real-time monitoring of volatile organic compounds (VOC's) at low concentrations[46].

SESI was selected as an emerging approach that has been growing in popularity since it was named by Wu in 2000. SESI-MS has already demonstrated promise in the real-time analysis of VOC's[33,53], including monitoring VOC emissions from plants[54]. Furthermore, a similar technique was previously shown to discriminate different stages of ripeness in a variety of fruits including table grapes[55].

DBDI was selected as the third ionisation approach, representing a new technology with several key advantages: (i) simplicity, (ii) compact size (iii) low part-per-trillion sensitivity and (iv) solvent free. These characteristics indicate that DBDI is an excellent candidate ion-source technology that may ultimately prove suitable for portable, point-of-need analysis.

1.3 Grape Ripening and its Relation to Wine Quality

1.3.1 Grape Ripening

Grape ripeness is a critical issue in winemaking because the grape chemical composition at harvest time is a key determinant of the resultant wine quality[56–59]. The optimal time to harvest grapes is dependent on the grape variety, the growing conditions, management practices and the style of the target wine. The growth period from post-véraison (i.e. colour change) to harvest is the most critical stage of grape ripening, where grape berries rapidly accumulate sugar, change colour, shift metabolism and accumulate flavour compounds[60].

The simplest and most widely used indicator of grape maturity is based on the ratio of sugar to acidity. Generally, the grape ripening process (post-véraison) includes a decrease in organic acids and an increase in sugars[61]. However, as there is no physiological basis for this inverse correlation between sugar and acidity many exceptions have been observed[62]. Accordingly, it is widely recognized that the sugar to acidity ratio is of limited utility, lacking information on the flavour potential of the grapes[63]. This has provided the rationale for studies on the evolution of grape VOC's seeking an objective measure of grape ripeness that would better reflect wine quality[57,64].

However, it has been difficult to investigate grape volatile emissions from non-floral varietals (accounting for > 90% of the worlds wine production)[65] due to their low VOC concentrations[64,66]. Consequently, few studies have examined the evolution of VOC's from non-floral grape varietals[66]. Recent studies have begun to address this subject using different sample concentration methods and gas chromatography[66–68] however, the approaches are time-consuming, creating a potential barrier to future studies. Furthermore, although tentative trends for the evolution of some compounds exist, contradictory findings in the literature highlight the complex nature of the grape ripening process and indicate the need for further research.

To this end, complimentary analytical approaches are required to provide rapid measurement of grape VOC's without sample preparation steps. This could

ultimately allow grape VOC composition to be analysed on-site at the winery gate providing a means to rapidly monitor grape ripening.

1.3.2 Grape Volatiles

1.3.2.1 C13-Norisoprenoids

The C_{13}-norisoprenoids are an important component of aroma in non-muscat grape varietals[69–71]. C_{13}-norisoprenoids have low (< µg/L) sensory thresholds[72] and contribute a range of floral, violet, tobacco or camphorous aromas[73]. β-ionone has been found in Pinot Noir grapes at higher concentrations than α-ionone[68] and was observed to decrease in concentration in the latter stages of ripening. In contrast, the same authors found α-ionone concentrations to remain static throughout grape ripening, and vitispirane was not detected in free form by these authors. A decreasing trend for free β-ionone in the latter stages of ripening was also observed in an earlier study of Pinot Noir grapes[74], and in a recent study of other non-floral grape varietals; Nebbiolo, Dolcetto and Barbera[67]. Evidence of a decreasing trend for β-ionone has also been observed in other grape varietals[57,58], indicating similar trends across different varietals and geographic locations.

A decrease in both the number and intensity of volatiles in some grape varietals as ripening progresses may relate to glycosylation of the free volatiles[75]. Razungles, Baumes, Dufour, & Bayonove (1998)[76], had previously suggested this hypothesis as an explanation for the decrease in certain free C_{13}-norisoprenoids with ripening, however, few studies have yet confirmed this hypothesis. Carlomagno et al., (2016)[67], provide some supporting evidence of such an inverse-relation between the free and bound states via their observation of a corresponding increase in the bound form of β-ionone in Dolcetto grapes. However, they found no supporting evidence for the other grape varietals studied.

Taking a broader perspective on ripeness signaling, Carlomagno et al., (2016)[67] did not find β-ionone in leaves of *Vitis vinifera*, but in the tendrils (homologous organs to flowers). Such findings highlight this compound as an indicator for signaling ripeness not only in grapes but in *Vitis vinifera* reproductive tissues, similar to patterns already observed in tomatoes and other plants[77].

1.3.2.2 Monoterpenes

Monoterpenes are generally much more abundant in aromatic muscat grape varietals[58]. A general trend has been observed by some authors that monoterpenes increase during ripening but may decrease at late stage maturity[58,74]. Similar trends were observed for several monoterpenes in the final stages of ripening in *Vitis vinifera* L. cv Fernao-Pires grapes[57]. Some monoterpenes continue to increase during ripening demonstrating a potential varietal-specific behaviour[66,67]. It should also be noted, that the influence of climatic factors can cause inconsistencies in observed trends[78].

Monoterpenes with two isoprene units $[C_{10}H_{16}]^+$ including limonene have been previously identified in grapes[79]. A number of isobaric monoterpene alcohols $[C_{10}H_{18}O_1]^+$, including linalool, α-terpineol, nerol, geraniol and eucalyptol in addition to the cyclic ether *cis/trans*-rose oxide, have all been identified as potent grape-derived odorants in wine[79,80]. Other monoterpene alcohols include citronellol, dihydromyrcenol and isomenthol.

Cis/trans-linalool oxide was generally observed to decrease during ripening in Pinot Noir grapes[68]. The evolution of geranylacetone has been observed to be distinct from the other monoterpene-related peaks. This unique profile (among monoterpenes) has been related to the different biosynthetic origin of this compound[67]. E-geranylacetone has been suggested as a potential stress marker[67], indicative of vine response to abiotic conditions as it is derived from carotenoid degradation[81,82] meriting attention in further studies.

1.3.2 3 Sesquiterpenes

Sesquiterpenes are difficult to investigate due to the close similarity of GC elution times, mass spectra, and their low volatility[78]. Although receiving little attention in the past sesquiterpenes are of increasing interest following the discovery of rotundone as the impact compound responsible for “black pepper” aroma in red wine[83].

The evolution profile of sesquiterpenes has been observed to be similar to the general profile for monoterpenes in several non-floral grapes (Shiraz and Cabernet

Sauvignon)[84], Dolcetto[67] and that of the Baga grape, a varietal rich in sesquiterpenes[85], increasing to a maximum in the late stages of ripening, followed by a decrease towards harvest date.

1.3.2.4 C_6 Compounds

C_6 compounds are generally associated with "green" or herbaceous odours in wine[57,68]. (E)-2-hexenal (leaf aldehyde) was among the most abundant compounds detected in grapes in previous studies[57,58,66,68]. Different trends have been observed regarding the evolution of C_6 compounds[66,68,74]. These compounds originate via the lipoygenase pathway and diversity in their evolution profile may be due to the existence of lipoxygenases with different activity[67].

A number of isomeric C_6 compounds have been found in grapes including 1-hexanal, and the isomers cis-2-hexenol, (E)-2-hexenol, and cis-3-hexenol[79]. Direct MS approaches cannot separate these isomers thus C_6 compounds are of limited value as grape ripeness indicators via the direct MS approaches.

1.3.2.5 Benzene Derivatives

Volatile phenols and other benzene derivatives are another group of compounds important for the primary aroma of wine[86]. Even though the majority of these compounds in wine are generated during fermentation[68], their evolution profile in grapes may still provide useful information on the ripening process. Generally a decreasing trend has been observed with ripening[58,86].

Benzyl alcohol and 2-phenylethanol peaked two weeks after véraison and then decreased until harvest in Pinot Noir grapes[68]. Benzaldehyde (m/z 107.0491) concentrations were observed to increase in the final week of ripening in three out of four varietals in the study by Vilanova et al., 2012.

Although eugenol has been detected in both Chardonnay[71] and Dolcetto grapes [67], there is little published information on its evolution during ripening. The major source of eugenol in wine is from oak wood[87] rather than from grapes. As potential isobaric compounds have been reported in grapes for several benzene derived compounds, caution should be exercised regarding tentative compound assignment

from direct MS. Potential isobaric compounds include benzyl acetate [$C_9H_{10}O_2$][88] methyl salicylate [$C_8H_8O_3$][58,89] and 2-phenylethyl acetate [$C_{10}H_{12}O_2$][88].

1.3.2.6 Volatile Fatty Acids

There is limited published data regarding the evolution of volatile fatty acid components in grapes. Salinas et al., (2004)[64] observed no significant variation in acetic acid during ripening and Mar Vilanova et al., (2012)[58] observed an increase in hexanoic acid at a later stage of grape ripening. Varietal specific trends have also been observed[58].

1.4 Oak Wood and its Relation to Wine Quality

1.4.1 Oak Aging of Wine

Oak wood enhances wine quality through an "aging process" providing improved stability, clarity, balance and increased complexity[90]. Gougeon et al. 2009[91], revealed that "10-year-old wines still express a metabologeographic signature of the forest location where oaks of the barrel in which they were aged have grown". Barrel making is thought to have been introduced by the Romans around 2000 years ago and oak wood was used primarily because of its availability[92]. Oak persisted as the primary wood for aging wine because of its natural abundance in the "old world" wine producing regions[93] and due to suitable physical and chemical properties[94]. The tradition of oak aging has created a high level of expertise regarding the production and utilisation of the oak species and "oak expression" has become characteristic of wine styles such as Bordeaux and Burgundy[95] – factors likely to perpetuate the dominance of oak cooperage.

The extraction of oak 'flavour compounds' is influenced by many variables including species, site and tree factors, cooperage processing conditions (seasoning and toasting), volume of barrel or size of wood piece (affecting surface area to volume ratio), the duration of aging and previous use of oak barrels. These variables are discussed below.

1.4.2 Oak Species

Wine is predominantly aged in barrels (or barrel alternatives) made from American oak (*Quercus alba)* or European oak *Quercus petraea* (synonym *Quercus sessiliflora*, sessile oak) and *Quercus robur* (pedunculate oak) sourced from France and to a lesser extent from Hungary and Russia[96]. The former (sessile oak), is considered superior for aging wine due to finer grain and greater complexity of aromatic constituents. Limited volumes are also sourced from Eastern European countries such as Moldova and Romania[97]. Oak species from other countries are also being used for cooperage purposes including *Quercus pyrencaica* found in Spain and Portugal[98,99].

1.4.3 Oak Compounds of Oenological Importance

Approximately 90% of the oak wood mass is composed of complex carbohydrates (hexoses and pentoses) that provide structural integrity; cellulose, hemicellulose and lignin. These complex organic polymers are mostly insoluble in hydro-alcoholic solutions[94]. The remaining 10% (approximately) of oak wood mass are extractible substances[100] – representing the compounds of highest oenological importance[95,101].

However, knowledge of the basic wood structure is important to understand the chemical changes that occur during cooperage production processes (particularly seasoning and toasting) and how these variables can influence the sensory profile. Wood can also be divided into sapwood and heartwood. Only heartwood is used for aging wine or spirits due to the significantly higher extractive component and (critically for barrels), the presence of tyloses (gums) that effectively block wood vessels preventing liquid penetration and therefore barrel leakage[94].

A great deal of consumer interest in wine is generally derived from the subtle aroma characteristics of the product[4]. Naturally, sensory perception is a complex phenomenon and arises from the totality of our sensory experience. We now appreciate not only the additive and suppressive effects among volatile compounds, but also the interactions between volatile and non-volatile components that may affect sensory perception[3,102]. Ideally, both volatile and non-volatile components

should be considered concurrently to garner a more holistic understanding of flavour impact.

Flamini and Traldi 2009[90] provide an extensive summary of oak extractives - a range of compounds including ellagitannins, polysaccharides, furan compounds, aldehydes, ketones, alcohols, phenols, acids and esters, lactones, coumarins, hydrocarbons, fatty acids, terpenes, steroids, carotenoids and norisoprenoids. Of these compounds, the most important non-volatiles are the ellagitannins (affecting colour, stability and perception of astringency[103]), coumarins (bitter / acidic[104]) and triterpenes, recently identified as contributing to wine sweetness[105].

During the aging of wine in barrels a progressive solubilisation of ellagitannins occurs. The presence of small amounts of oxygen (barrels provide a micro-oxidative environment, allowing small amounts of oxygen to contact wine) facilitates polymerisation with anthocyanin increasing colour intensity and wine stability[106,107]. This rapid absorption of dissolved oxygen by the oak ellagitannins has a protective effect against phenolic oxidation during the wine aging process[108].

Oak aging is known to have a sweetening effect on wine[108] but until recently non-volatile compounds with a sweet taste had yet to be identified. Marchal and Waffo-Teguo 2011[105], identified a new sweet triterpenoid called Quercotriterpenoside I from oak extract, thus helping elucidate the perception of sweetness in aged wine.

1.4.3.1 Oak Impact Aroma Compounds

Of the approximately 200 volatile compounds identified in oak[94], only a few are considered to be impact compounds[109], generally present above their sensory thresholds and thought to have a significant influence on wine flavour and quality. These impact aroma compounds include the oak lactones (*cis* and *trans* β-methyl-γ-octalactone, formed through lipid oxidation[94]), furanic aldehydes (furfural and 5-methylfurfural formed through degradation of hemicellulose[110]), volatile phenols (eugenol, guaiacol and 4-methylguaiacol from lignin degradation[95]) and phenolic aldehydes such as vanillin and syringaldehyde, also formed through lignin degradation[111].

As volatile compounds may have additive or suppressive effects, their impact on wine cannot be fully understood by considering the odour active values of each compound in isolation. Correlation of the analytical data to sensory attributes is ultimately required to better understand the impact of flavour compounds on aroma attributes. Such analyses reveal that the sensory impact in wine is not always that of the compound in its pure state. For example, furanic compounds considered sweet and almond like in pure state have been positively correlated with smoky[112], oak[109] and vanilla[112] attributes. Vanillin does not always correlate with vanilla, having been also correlated to cinnamon and smoky[112] attributes in white wine. In red wine the vanilla descriptor has been often correlated with cis-oak-lactone[109,112]. Prida and Chatonnet 2010[109], found no correlation between guaiacol, 4-methylguaiacol and eugenol (described as smoky and spicy in their pure state) and the respective sensory descriptors in wine.

These studies correlating analytical and sensory data confirm the impact compounds important for the sensory attributes of the resultant oak-aged wines[109,112–114]. For Pinot Noir wines aged in different woods, Sauvageot and Feuillat 1999[115] found those rated highest for woody, toasted, vanilla and coconut attributes contained the highest levels of *cis*-Oak lactone. The oak lactones (otherwise known as the "whisky lactones" as they were first discovered in that spirit[92]) are considered the signature compounds of oak-aged wines. They are only found in oak wood[116] and are substantial contributors to oak wood aroma in wine[95,100,109,113,117].

As summarised by Wilkinson et al. 2013[118] the oak lactones typically impart 'woody', 'coconut', 'vanilla', and 'dark chocolate' attributes. Prida et al. 2009[113], found *cis*-lactone the most significant factor explaining sensory perception in wines correlating significantly with 'caramel' and 'milk' sensory descriptors[113]. Oak lactones are generally considered a positive contribution to wine aroma and quality but can be detrimental at high levels by dominating flavour complexity and subtlety[92,119]. Chardonnay wines aged in Hungarian and Russian oak with low oak lactone content scored well for oak wood sensory attributes. Eugenol, guaiacol and related compounds contributed to the spicy, clove, cinnamon, oaky attributes, whilst the lactones contributed sweet, vanilla and oak aromas[120].

Oak impact aroma compounds have been widely discussed and summarised by several authors[95,98,101,112,121–124]. Prida and Chattonnet 2010[109], also indicate the transformations of some of these compounds in a wine medium. For example, decreased vanillin levels have been observed during barrel fermentation and maturation in contact with yeast lees and furfurylthiol and 5-methyl-2-furanmethanthiol (coffee-smelling compounds with very low odor thresholds of 0.4 and 50 ng/L, respectively) have been identified as products of transformation of furfural and 5-methylfurfural, respectively, in a wine medium.

β-Ionone is not generally referenced as an impact compound but is included here to convey the range of sensory attributes that may be attributed to wood. Furthermore, compounds conveying floral attributes are important for maturation of certain varietals (particularly white wines) where preservation of fruit character and subtle complex aroma are highly desirable. β-Ionone is a primary aroma compound in violet flowers and the scarcity of reports for this compound in oak wood may be due to its presence in grapes and thus their source in wine possibly attributed to grapes rather than oak[95]. Figure 8 illustrates the chemical structure and sensory attribute associated with each oak impact compound.

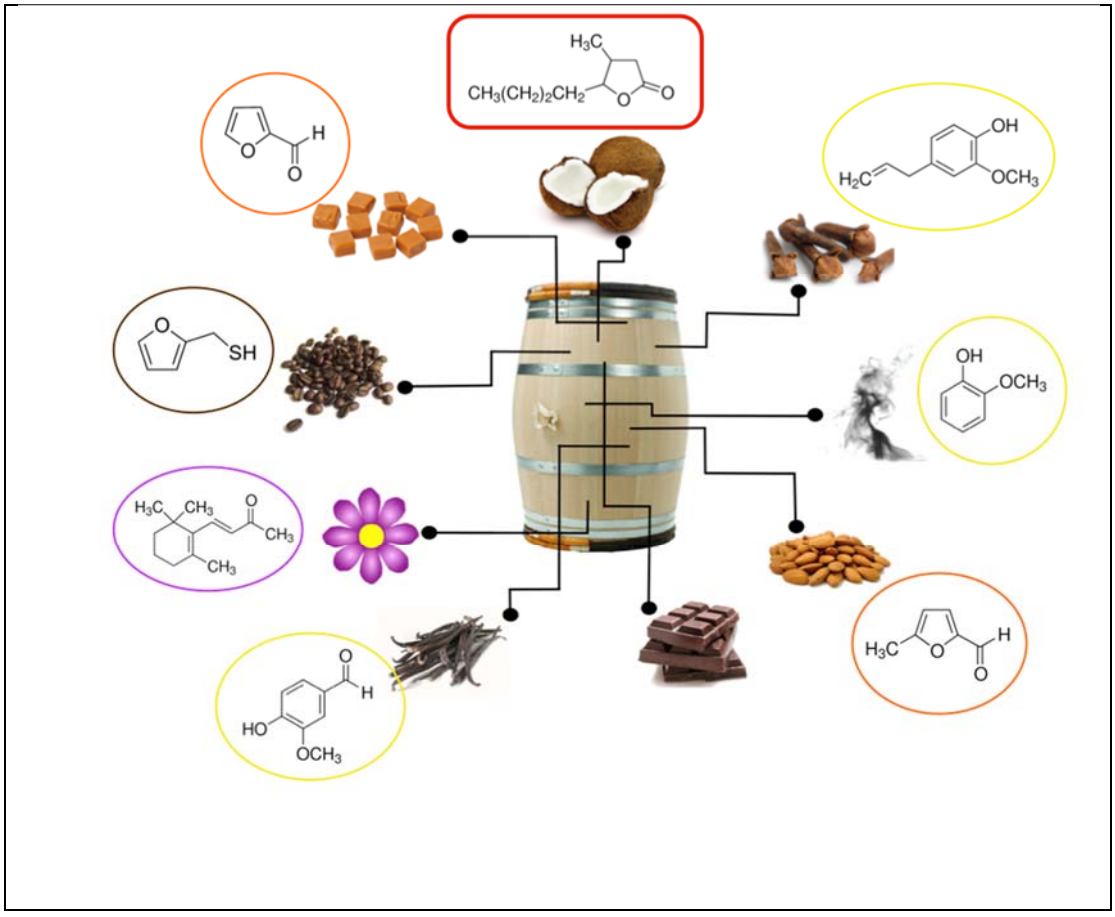

Figure 8: Impact aroma compounds in oak, chemical structure and associated sensory attributes. Original figure.

As summarised by De Simon et al. 2009[125], only some of these impact compounds are originally present in oak wood in significant amounts, i.e. the oak lactones, eugenol and vanillin. The oak "flavour profile" undergoes significant development during the cooperage processes of seasoning and particularly the toasting process.

1.4.4 Oak Wood Seasoning

Vivas et al. 1997[126] provide an extensive review of the seasoning process outlining its significance in the preparation of oak wood for aging wine. This essential step is required firstly to reduce the moisture content of stave wood to approximately 15-18% ensuring a dimensionally stable product – an essential requirement for manufacturing leak-free barrels. Beyond this physical need, the oak chemistry is modified through leaching of compounds by rain (particularly the ellagitannins) and biological activity by a wide variety of microflora.

The microflora populate the wood surface and through time breakdown some of the cell wall structure, likely increasing the aromatic potential of the wood. Wood is generally seasoned in the open environment for two to three years, and certain cooperages utilise irrigation systems to spray the wood stacks ensuring optimal rainfall levels. Stave position in the stack may also be rotated to ensure equal exposure to the environment and therefore more uniform flavour profiles[127].

In the wine industry air seasoned wood is preferred to kiln dried material likely due to a reduced microfloral population in the latter and suggested impact on sensory quality[128]. As discussed by Canas et al. 2006[127], seasoning is considered a refining stage where the wood undergoes chemical and biochemical transformations that contribute to its "maturation".

Seasoned wood generally contains lower levels of the water soluble ellagitannins likely to contribute reduced astringency and bitterness to oak aged wine[129]. This sensory observation is also related to the hydrolysis of glycosylated coumarins (bitter taste), generating their aglycones (more neutral flavour)[101]. Interestingly, Chira and Teissedre 2013[130], noted that guaiacol and furfural (normally associated with smoky and sweet attributes) play some role in the perception of astringency. As reported by several authors the impact of seasoning on individual oak wood volatiles is ambiguous with contradictory results finding levels of oak lactones, eugenol and vanillin to increase, to decrease or remain constant[118,124,131]. It is unclear whether these contradictory results are related to artefact creation during analysis[123], a consequence of exact experimental methodologies or even attributed to potential errors in traceability and identification of wood pieces[131].

Considering the importance of the seasoning stage and lengthy timelines involved, it is not surprising to encounter research focused on accelerated methods, for example Petruzzi et al. 2012[132], inoculated oak chips with mould (*Penicillium purpurogenum*) to rapidly invoke desirable characteristics. Such work indicates the potential to utilise specific fungal inocula to enrich specific compounds.

1.4.5 Oak Wood Toasting

Although seasoning is essential to produce oak staves of suitable organoleptic quality, toasting may be considered to have the biggest single effect on oak wood flavour profile[125,133,134]. During toasting a variety of hydrothermolysis and pyrolysis reactions occur resulting in thermodegradation of hemicellulose, cellulose, lignin, polyphenols and lipids. A dramatic increase in the variety and intensity of volatile compounds is evident.

Oak toasting has been extensively studied and is reviewed in recent work conducted by Duval et al. 2013[124]. They discuss the general trends that exist as well as the limitations of the research to date, namely the difficulty in comparing different experimental conditions where these are defined using subjective descriptors such as 'intensity' rather than explicit statements of temperature and time. Comparison is further complicated by the diversity of conditions used (model *vs* real wine) and sizes of the wood samples (powders, staves, barrels).

Generally, trends do exist however. Guaiacol, eugenol and vanillin result from the breakdown of lignin and their concentration tends to increase with heating. Furfural is produced from the depolymerisation of hemicelluloses catalysed by acetic acid that is also formed during thermal treatment and thus generally increases with temperature. The authors suggest: "Oak lactones are certainly the compounds for which the literature shows greatest discrepancies in terms of the evolution of their concentrations with heat treatments." They summarise research showing (lactone) levels to remain constant, to decrease at high temperature, to increase then decrease, or finally to decrease then increase.

Wilkinson et al. 2013[118] provide some clarification on these phenomena, also referencing work where oak lactone is found to increase as a function of toasting intensity and where very high temperatures or prolonged toasting periods reduce oak lactone (likely) through volatilisation. Their research on oak lactone glycoconjugate precursors (oak lactone occurs in both free and precursor forms) demonstrated the thermal stability of the precursors finding that 200 °C for 30 min would not generate significant quantities of oak lactone. The authors conclude that

oak lactone can be generated from glycoconjugates by thermal degradation during toasting, where both temperature and duration influence yield. As an aside, they also indicate that oak lactone levels can continue to increase in bottle (after removal from oak contact) following extraction of the precursor forms.

Returning to the findings of Duval et al. 2013[124] who used Headspace solid phase microextraction (HS-SPME) combined with GC-MS to investigate the effect of moisture content on the modulation of oak volatiles during toasting (using oak extracted in model wine). The authors found that when oak is not previously soaked, temperature has a high impact on concentration of furfural, guaiacol and vanillin (i.e. higher temperature = higher concentration). In contrast, lactone levels were constant up to 200 °C and decreased (45%) at the 240 °C treatment. Eugenol levels remained constant for the 10 min heating trials across all temperatures, however, decreased significantly at 240 °C for the longer 25 min heating trial.

For soaked woods, concentrations of all extracted compounds tend to be lower, suggesting a delaying effect of water on thermal degradation of wood biopolymers and lipids. However, beyond 200 °C alternative mechanisms seem to exist that now promote the formation of furfural and hinder degradation of eugenol and the oak lactones. As suggested by the authors themselves, lower lactone levels (in soaked wood) up to 200 °C, compared to dry wood is likely due to the soaking process itself (rather than a delaying effect of water) that would already extract a fraction of the available pool of lactones.

Related work was conducted by Chira & Teissedre 2013[130], investigating the impacts of volatiles and ellagitannins on sensory perception with eight different toast levels (including untoasted). They found lactone levels for toasted wood to be lower than untoasted wood for all treatments except 'Noisette' (a long toast at relatively low temperatures, 175 °C). The 'special' toast (180 °C and a water soaking treatment) resulted in high lactone level among all treatments excluding Noisette, with levels similar to Light Toast+ (2hrs at 170 °C).

This result where *water treatment enhances lactone extraction* seems to contradict findings of Duval et al. 2013[124] i.e. *soaked wood treatment lowers lactone*

concentrations. However, the latter study involved extraction in model wine for 48hrs, whilst the former study examined levels at a variety of time points up to a maximum extraction period of 3 months. Likely, the longer time period allows greater extraction of 'free' lactone as well as increased lactone generation from the precursor form. The duration of the extraction period is another critical factor influencing extraction of oak compounds into wine[118,124,135]. The difficulty in comparing previous studies is evident.

1.4.6 Variability in Oak Wood Chemistry

The previous discussion illustrated how the oak wood chemical composition may be modulated during the production processes of seasoning and in particular, toasting.

Reflecting on the many publications regarding oak wood extractives and wine, the one unifying theme may be the inherent variability of oak wood as a natural material. Oak wood is a complex natural product, exhibiting variation between geographical locations, species, management practices, within trees and between individual trees as summarised by the following authors among many others[96,97,117,124,131]. Experiments by Campbell et al. 2005[136], demonstrate the high degree of variation of *cis*-Oak lactone in model wine extracts of individual staves before toasting. In samples taken from three French oak staves *cis*-Oak lactone varied by up to 400% (73-295 µg/L), whilst the American oak staves varied by up to 440% (211-930 µg/L)

Considering the many variables that effect oak extraction, the processing (seasoning and toasting) and utilisation variables (volume and duration etc.) *can* be controlled. However, even though silvicultural forest management practices can influence wood chemistry, natural variation will always be present due to differences in site environments and variation within (and between) individual trees. Consequently, natural variation in the chemical composition of oak wood remains the key challenge in producing cooperage products with predictable properties[137,138]. This is important from a wine quality and economic perspective because after grapes, oak is the greatest expense in the production of many quality wines[139].

1.4.6.1 Barrel Alternatives

Barrel alternatives (i.e. wood pieces such as staves or chips placed in stainless steel tanks with wine) were approved for use in the European Union in 2006[140]. However, these products were commonly used prior to 2006 in other countries were there was no legal requirement for barrel aging wine. There is a great need for objective measurements of quality for oak-based barrel alternatives because:

- There is a vast array of different products available (e.g. powders, shavings, blocks, staves).
- They are not subject to the same processing steps (particularly toasting) as their barrel counterparts.
- They can be produced from a wide variety of different wood pieces including off-cuts and rejects.
- They are marketed under a plethora of different grade names that may describe the product in qualitative terms (species, seasoning and toasting intensity) or under proprietary names such as "original blend, sweet granular, spice, intense, high vanilla, high mocha, premium dark, etc."[141] meaning there is a great difference between different brands.

1.5 Thesis Aims

The overall aim of this thesis is to investigate the utility of direct MS approaches for wine industry quality control applications. Objective measures of quality are important for the wine industry sector in order to measure and ultimately control variation at the different stages of wine production. High-variability is a natural characteristic of grapes, fermentation and oak-aging processes.

Whilst optical spectroscopy has been widely studied as a potential quality control tool[142], the exploration of state-of-the-art, direct mass spectrometry approaches for wine quality control applications is only beginning. Some examples to date include: Trace-level volatile quantitation by direct analysis in real time mass spectrometry following headspace extraction: optimization and validation in grapes[143], Direct determination of multi-pesticides in wine by ambient mass spectrometry[144] and Fast

quantitation of pyrazole fungicides in wine by ambient ionization mass spectrometry[145].

The revolution in ambient mass spectrometry and related technologies promises to simplify MS analysis, thus creating the "four-S trademark" of mass spectrometry (sensitivity, selectivity, speed and simplicity)[146]. Ultimately, direct MS approaches may be deployed using simplified, miniaturised MS devices providing the wine industry with powerful, point-of-need analytical tools.

1.6 Thesis Structure

Three different direct MS approaches are investigated in this thesis covering both ambient and reduced-pressure ionisation methods. Chapter 2 explores the direct analysis of grape volatiles from the intact berries of non-Muscat grape cultivars using a highly sensitive and selective ambient ionisation approach, namely, secondary electrospray ionisation mass spectrometry (SESI-MS). A secondary goal of the work in Chapter 2 was to monitor changes in grape berry volatile composition during the ripening process as a preliminary screening for ripeness markers.

Chapter 3 aims to monitor the oak wood toasting process on-line, in real-time, using proton transfer reaction mass spectrometry (PTR-MS). PTR-MS is a reduced-pressure ionisation technique that can provide direct, quantitative data[48]. The primary goal of Chapter 3 is to elucidate aroma development during the oak wood toasting process relevant to wine quality and to offer better methods for future optimisation of the oak toasting process.

Chapter 4 introduces a second ambient ionisation approach based on dielectric barrier discharge ionisation mass spectrometry (DBDI-MS). The goal is to develop a rapid approach for screening oak wood volatile composition. Sample gas dilution and internal standard infusion is explored as a strategy to reduce and account for ion suppression phenomena that may occur under ambient ionisation conditions.

References

(1) Hemingway, E. *Death in the Afternoon*; Charles Scribner's Sons: New York, 1932.

(2) Villamor, R. R.; Ross, C. F. Wine Matrix Compounds Affect Perception of Wine Aromas. *Annu. Rev. Food Sci. Technol.* **2013**, *4* (1), 1–20.

(3) Polášková, P.; Herszage, J.; Ebeler, S. Wine Flavor: Chemistry in a Glass. *Chem. Soc. Rev.* **2008**, 2478–2489.

(4) Francis, I. L.; Newton, J. L. Determining Wine Aroma from Compositional Data. *Aust. J. Grape Wine Res.* **2005**, *11* (2), 114–126.

(5) Hayasaka, Y.; Baldock, G. a.; Pollnitz, A. P. Contributions of Mass Spectrometry in the Australian Wine Research Institute to Advances in Knowledge of Grape and Wine Constituents. *Aust. J. Grape Wine Res.* **2005**, *11* (2), 188–204.

(6) Taylor, A. J.; Linforth, R. S. T. Direct Mass Spectrometry of Complex Volatile and Non-Volatile Flavour Mixtures. *Int. J. Mass Spectrom.* **2003**, *223–224*, 179–191.

(7) Li, L.-P.; Feng, B.-S.; Yang, J.-W.; Chang, C.-L.; Bai, Y.; Liu, H.-W. Applications of Ambient Mass Spectrometry in High-Throughput Screening. *Analyst* **2013**, *138* (11), 3097–3103.

(8) Thomson, S. J. J. *Rays of Positive Electricity and Their Application to Chemical Analyses*; Longmans, Green and Co., 1913.

(9) Maher, S.; JJunju, F. P. M.; Taylor, S. Colloquium: 100 Years of Mass Spectrometry: Perspectives and Future Trends. *Rev. Mod. Phys.* **2015**, *87* (1), 113–135.

(10) Alberici, R.; Simas, R.; Sanvido, G. Ambient Mass Spectrometry: Bringing MS into the "Real World." *Anal. Bioanal. Chem.* **2010**, *398* (1), 265–294.

(11) Venter, A.; Nefliu, M.; Cooks, R. G. Ambient Desorption Ionization Mass Spectrometry. *TrAC Trends Anal. Chem.* **2008**, *27* (4), 284–290.

(12) Takáts, Z.; Wiseman, J. M.; Gologan, B.; Cooks, R. G. Mass Spectrometry Sampling Under Ambient Conditions with Desorption Electrospray Ionization. *Science (80-.).* **2004**, *306* (5695), 471–473.

(13) Weston, D. J. Ambient Ionization Mass Spectrometry: Current Understanding of Mechanistic Theory; Analytical Performance and Application Areas. *Analyst* **2010**, *135* (4), 661–668.

(14) Berkel, G. J. Van; Pasilis, S. P.; Ovchinnikova, O. Established and Emerging Atmospheric Pressure Surface Sampling/Ionization Techniques for Mass Spectrometry. *J. Mass Spectrom.* **2008**, *43* (9), 1161–1180.

(15) Chen, H.; Gamez, G.; Zenobi, R. What Can We Learn from Ambient Ionization Techniques? *J. Am. Soc. Mass Spectrom.* **2009**, *20* (11), 1947–1963.

(16) Black, C.; Chevallier, O. P.; Elliott, C. T. The Current and Potential Applications of Ambient Mass Spectrometry in Detecting Food Fraud. *TrAC Trends Anal. Chem.* **2016**, *82*, 268–278.

(17) Monge, M. E.; Harris, G. a.; Dwivedi, P.; Fernandez, F. M. Mass Spectrometry: Recent Advances in Direct Open Air Surface Sampling/Ionization. *Chem. Rev.* **2013**, *113* (4), 2269–2308.

(18) Ding, X.; Duan, Y. Plasma-Based Ambient Mass Spectrometry Techniques: The Current Status and Future Prospective. *Mass Spectrom. Rev.* **2015**, *34* (4), 449–473.

(19) Chen, J.; Tang, F.; Guo, C.; Zhang, S.; Zhang, X. Plasma-Based Ambient Mass Spectrometry: A Step Forward to Practical Applications. *Anal. Methods* **2017**, *9* (34), 4908–4923.

(20) Yang, Y.; Deng, J. Analysis of Pharmaceutical Products and Herbal Medicines Using Ambient Mass Spectrometry. *TrAC Trends Anal. Chem.* **2016**, *82*, 68–88.

(21) Buhr, K.; Buettner, A.; Schieberle, P. Analysis of Lactones by Proton Transfer Reaction - Mass Spectrometry (PTR-MS). Fragmentation Patterns and Detection Limits. In *3rd International Conference on Proton Transfer Reaction Mass Spectrometry and Its Applications*; Armin, H., Timann, M., Eds.; innsbruck university press: Innsbruck, 2007; pp 149–153.

(22) Cooks, R. G.; Mueller, T. Through a Glass Darkly: Glimpses into the Future of Mass Spectrometry. *Mass Spectrom. (Tokyo, Japan)* **2013**, *2* (Spec Iss), S0001.

(23) Garcia-reyes, J. F.; Fernandez, F. M. Ambient Mass Spectrometry. *Anal. Methods* **2017**, *9*, 4894–4895.

(24) Cody, R. B.; Laramée, J. A.; Durst, H. D. Versatile New Ion Source for the Analysis of Materials in Open Air under Ambient Conditions. *Anal. Chem.* **2005**, *77* (8), 2297–2302.

(25) Nemes, P.; Vertes, A. Laser Ablation Electrospray Ionization for Atmospheric Pressure, in Vivo, and Imaging Mass Spectrometry. *Anal. Chem.* **2007**, *79* (21), 8098–8106.

(26) Harper, J. D.; Charipar, N. A.; Mulligan, C. C.; Zhang, X.; Cooks, R. G.; Ouyang, Z. Low-Temperature Plasma Probe for Ambient Desorption Ionization. *Anal. Chem.* **2008**, *80* (23), 9097–9104.

(27) McEwen, C. N.; McKay, R. G.; Larsen, B. S. Analysis of Solids, Liquids, and Biological Tissues Using Solids Probe Introduction at Atmospheric Pressure on Commercial LC/MS Instruments. *Anal. Chem.* **2005**, *77* (23), 7826–7831.

(28) Shiea, J.; Huang, M.-Z.; Hsu, H.-J.; Lee, C.-Y.; Yuan, C.-H.; Beech, I.; Sunner, J. Electrospray-Assisted Laser Desorption/Ionization Mass Spectrometry for Direct Ambient Analysis of Solids. *Rapid Commun. Mass Spectrom.* **2005**, *19* (24), 3701–3704.

(29) Na, N.; Zhao, M.; Zhang, S.; Yang, C.; Zhang, X. Development of a Dielectric Barrier Discharge Ion Source for Ambient Mass Spectrometry. *J. Am. Soc. Mass Spectrom.* **2007**, *18* (10), 1859–1862.

(30) Haddad, R.; Sparrapan, R.; Eberlin, M. N. Desorption Sonic Spray Ionization for (High) Voltage-Free Ambient Mass Spectrometry. *Rapid Commun. Mass Spectrom.* **2006**, *20* (19), 2901–2905.

(31) Andrade, F. J.; Shelley, J. T.; Wetzel, W. C.; Webb, M. R.; Gamez, G.; Ray, S. J.; Hieftje, G. M. Atmospheric Pressure Chemical Ionization Source. 1. Ionization of Compounds in the Gas Phase. *Anal. Chem.* **2008**, *80* (8), 2646–2653.

(32) Wang, H.; Liu, J.; Cooks, R. G.; Ouyang, Z. Paper Spray for Direct Analysis of Complex Mixtures Using Mass Spectrometry. *Angew. Chem. Int. Ed. Engl.* **2010**, *49* (5), 877–880.

(33) Wu, C.; Siems, W. F.; Hill, H. H. Secondary Electrospray Ionization Ion Mobility Spectrometry/Mass Spectrometry of Illicit Drugs. *Anal. Chem.* **2000**, *72* (2), 396–403.

(34) Fenn, J. B.; Mann, M.; Meng, C. K.; Wong, S. F.; Whitehouse, C. M. Electrospray Ionization for Mass Spectrometry of Large Biomolecules. *Science* **1989**, *246* (4926), 64–71.

(35) Vidal-De-miguel, G.; Macía, M.; Pinacho, P.; Blanco, J. Low-Sample Flow Secondary Electrospray Ionization: Improving Vapor Ionization Efficiency. *Anal. Chem.* **2012**, *84* (20), 8475–8479.

(36) Martínez-Lozano, P.; Rus, J.; Fernández de la Mora, G.; Hernández, M.; Fernández de la Mora, J. Secondary Electrospray Ionization (SESI) of Ambient Vapors for Explosive Detection at Concentrations Below Parts Per Trillion. *J. Am. Soc. Mass Spectrom.* **2009**, *20* (2), 287–294.

(37) Schwarz, E. I.; Martinez-Lozano Sinues, P.; Bregy, L.; Gaisl, T.; Garcia Gomez, D.; Gaugg, M. T.; Suter, Y.; Stebler, N.; Nussbaumer-Ochsner, Y.; Bloch, K. E.; et al. Effects of CPAP Therapy Withdrawal on Exhaled Breath Pattern in Obstructive Sleep Apnoea. *Thorax* **2016**, *71* (2), 110–117.

(38) Sonnenfeld, A.; Tun, T. M.; Zajíčková, L.; Kozlov, K. V; Wagner, H.-E.; Behnke, J. F.; Hippler, R. Deposition Process Based on Organosilicon Precursors in Dielectric Barrier Discharges at Atmospheric Pressure---A Comparison. *Plasmas Polym.* **2001**, *6* (4), 237–266.

(39) Gyr, L.; Wolf, J.-C.; Franzke, J.; Zenobi, R. Mechanistic Understanding Leads to Increased Ionization Efficiency and Selectivity in Dielectric Barrier Discharge Ionization Mass Spectrometry: A Case Study with Perfluorinated Compounds. *Anal. Chem.* **2018**, *90* (4), 2725–2731.

(40) Cunningham, A. J.; Payzant, J. D.; Kebarle, P. Kinetic Study of the Proton Hydrate H+(H2O)n Equilibriums in the Gas Phase. *J. Am. Chem. Soc.* **1972**, *94* (22), 7627–7632.

(41) Wolf, J.-C.; Gyr, L.; Mirabelli, M. F.; Schaer, M.; Siegenthaler, P.; Zenobi, R. A Radical-

Mediated Pathway for the Formation of [M + H](+) in Dielectric Barrier Discharge Ionization. *J. Am. Soc. Mass Spectrom.* **2016**, *27* (9), 1468—1475.

(42) Wolf, J.-C.; Schaer, M.; Siegenthaler, P.; Zenobi, R. Direct Quantification of Chemical Warfare Agents and Related Compounds at Low Ppt Levels: Comparing Active Capillary Dielectric Barrier Discharge Plasma Ionization and Secondary Electrospray Ionization Mass Spectrometry. *Anal. Chem.* **2015**, *87* (1), 723–729.

(43) Hansel, A.; Jordan, A.; Holzinger, R.; Prazeller, P.; Vogel, W.; Lindinger, W. Proton Transfer Reaction Mass Spectrometry: On-Line Trace Gas Analysis at the Ppb Level. *Int. J. Mass Spectrom. Ion Process.* **1995**, *149–150*, 609–619.

(44) Blake, R. S.; Whyte, C.; Hughes, C. O.; Ellis, A. M.; Monks, P. S. Demonstration of Proton-Transfer Reaction Time-of-Flight Mass Spectrometry for Real-Time Analysis of Trace Volatile Organic Compounds. *Anal. Chem.* **2004**, *76* (13), 3841–3845.

(45) Blake, R. S.; Monks, P. S.; Ellis, A. M. Proton-Transfer Reaction Mass Spectrometry. *Chem. Rev.* **2009**, *109*, 861–896.

(46) Tofwerk. What is Proton Transfer Reaction Mass Spectrometry (PTR-MS)? https://www.tofwerk.com/proton-transfer-reaction-mass-spectrometry/ (accessed Jun 16, 2018).

(47) Materić, D.; Peacock, M.; Kent, M.; Cook, S.; Gauci, V.; Röckmann, T.; Holzinger, R. Characterisation of the Semi-Volatile Component of Dissolved Organic Matter by Thermal Desorption – Proton Transfer Reaction – Mass Spectrometry. *Sci. Rep.* **2017**, *7* (1), 15936.

(48) Lindinger, W.; Hansel, A.; Jordan, A. On-Line Monitoring of Volatile Organic Compounds at Pptv Levels by Means of Proton-Transfer-Reaction Mass Spectrometry (PTR-MS) Medical Applications, Food Control and Environmental Research. *Int. J. Mass Spectrom.* **1998**, *173*, 191–241.

(49) Jordan, A.; Haidacher, S.; Hanel, G.; Hartungen, E.; Märk, L.; Seehauser, H.; Schottkowsky, R.; Sulzer, P.; Märk, T. D. A High Resolution and High Sensitivity Proton-Transfer-Reaction Time-of-Flight Mass Spectrometer (PTR-TOF-MS). *Int. J. Mass Spectrom.* **2009**, *286*, 122–128.

(50) Beauchamp, J.; Herbig, J.; Dunkl, J.; Singer, W.; Hansel, A. On the Performance of Proton-Transfer-Reaction Mass Spectrometry for Breath-Relevant Gas Matrices. *Meas. Sci. Technol.* **2013**, *24* (12), 125003.

(51) Jordan, A.; Haidacher, S.; Hanel, G.; Hartungen, E.; Herbig, J.; Märk, L.; Schottkowsky, R.; Seehauser, H.; Sulzer, P.; Märk, T. D. An Online Ultra-High Sensitivity Proton-Transfer-Reaction Mass-Spectrometer Combined with Switchable Reagent Ion Capability (PTR+SRI−MS). *Int. J. Mass Spectrom.* **2009**, *286* (1), 32–38.

(52) Sulzer, P.; Petersson, F.; Agarwal, B.; Becker, K. H.; Jurschik, S.; Mark, T. D.; Perry, D.; Watts, P.; Mayhew, C. A. Proton Transfer Reaction Mass Spectrometry and the Unambiguous Real-Time Detection of 2,4,6 Trinitrotoluene. *Anal. Chem.* **2012**, *84* (9), 4161–4166.

(53) Sinues, P. M.-L.; Alonso-Salces, R. M.; Zingaro, L.; Finiguerra, A.; Holland, M. V; Guillou, C.; Cristoni, S. Mass Spectrometry Fingerprinting Coupled to National Institute of Standards and Technology Mass Spectral Search Algorithm for Pattern Recognition. *Anal. Chim. Acta* **2012**, *755*, 28–36.

(54) Barrios-Collado, C.; García-Gómez, D.; Zenobi, R.; Vidal-de-Miguel, G.; Ibanez, A.; Martínez-Lozano Sinues, P. Capturing in Vivo Plant Metabolism by Real Time Analysis of Low to High Molecular Weight Volatiles. *Anal. Chem.* **2016**.

(55) Chen, H.; Sun, Y.; Wortmann, A.; Gu, H.; Zenobi, R. Differentiation of Maturity and Quality of Fruit Using Noninvasive Extractive Electrospray Ionization Quadrupole Time-of-Flight Mass Spectrometry. *Anal. Chem.* **2007**, *79* (4), 1447–1455.

(56) Aleixandre, M.; Santos, J.; Sayago, I.; Cabellos, J.; Arroyo, T.; Horrillo, M. A Wireless and Portable Electronic Nose to Differentiate Musts of Different Ripeness Degree and Grape Varieties. *Sensors* **2015**, *15* (4), 8429–8443.

(57) Coelho, E.; Rocha, S. M.; Barros, A. S.; Delgadillo, I.; Coimbra, M. A. Screening of Variety- and Pre-Fermentation-Related Volatile Compounds during Ripening of White Grapes to Define Their Evolution Profile. *Anal. Chim. Acta* **2007**, *597*, 257–264.

(58) Vilanova, M.; Genisheva, Z.; Bescansa, L.; Masa, A.; Oliveira, J. M. Changes in Free and Bound Fractions of Aroma Compounds of Four Vitis Vinifera Cultivars at the Last Ripening Stages. *Phytochemistry* **2012**, *74*, 196–205.

(59) Giovenzana, V.; Civelli, R.; Beghi, R.; Oberti, R.; Guidetti, R. Testing of a Simplified LED Based Vis/NIR System for Rapid Ripeness Evaluation of White Grape (Vitis Vinifera L.) for Franciacorta Wine. *Talanta* **2015**, *144*, 584–591.

(60) Geffroy, O.; Dufourcq, T.; Carcenac, D.; Siebert, T.; Herderich, M.; Serrano, E. Effect of Ripeness and Viticultural Techniques on the Rotundone Concentration in Red Wine Made from Vitis Vinifera L. Cv. Duras. *Aust. J. Grape Wine Res.* **2014**, *20* (3), 401–408.

(61) Jackson, R. S. 3 - Grapevine Structure and Function. In *Wine Science (Third Edition)*; Jackson, R. S., Ed.; Food Science and Technology; Academic Press: San Diego, 2008; pp 50–107.

(62) Chapter 10 - The Relationship between Must Composition and Quality. In *Enological Chemistry*; Moreno, J., Peinado, R., Eds.; Academic Press: San Diego, 2012; pp 137–156.

(63) Šuklje, K.; Antalick, G.; Meeks, C. B.; Blackman, J. W.; Deloire, A.; Schmidtke, L. M. Optimising Harvest Date through Use of an Integrated Grape Compositional and Sensory Model: A Proposed Approach for a Better Understanding of Ripening of Autochthonous Varieties? *Oenoviti Int. Netw.* **2014**, 44–49.

(64) Salinas, M. R.; Zalacain, A.; Pardo, F.; Alonso, G. L. Stir Bar Sorptive Extraction Applied to Volatile Constituents Evolution during Vitis Vinifera Ripening. *J. Agric. Food Chem.* **2004**, *52* (15), 4821–4827.

(65) Gomez, E.; Martinez, A.; Laencina, J. Localization of Free and Bound Aromatic

Compounds among Skin, Juice and Pulp Fractions of Some Grape Varieties. *Vitis* **1994**, *4*, 1–4.

(66) Kalua, C. M.; Boss, P. K. Comparison of Major Volatile Compounds from Riesling and Cabernet Sauvignon Grapes (Vitis Vinifera L.) from Fruitset to Harvest. *Aust. J. Grape Wine Res.* **2010**, *16* (2), 337–348.

(67) Carlomagno, A.; Schubert, A.; Ferrandino, A. Screening and Evolution of Volatile Compounds during Ripening of 'Nebbiolo,' 'Dolcetto' and 'Barbera' (Vitis Vinifera L.) Neutral Grapes by SBSE–GC/MS. *Eur. Food Res. Technol.* **2016**.

(68) Yuan, F.; Qian, M. C. Development of C13-Norisoprenoids, Carotenoids and Other Volatile Compounds in Vitis Vinifera L. Cv. Pinot Noir Grapes. *Food Chem.* **2016**, *192*, 633–641.

(69) Fang, Y.; Qian, M. C. Quantification of Selected Aroma-Active Compounds in Pinot Noir Wines from Different Grape Maturities. *J. Agric. Food Chem.* **2006**, *54* (22), 8567–8573.

(70) Marais, J. Sauvignon Blanc Cultivar Aroma: A Review. *South African J. Enol. Vitic.* **1994**, *15* (2), 41–45.

(71) Sefton, M. A.; Francis, I. L.; Williams, P. J. The Volatile Composition of Chardonnay Juices: A Study by Flavor Precursor Analysis. *Am. J. Enol. Vitic.* **1993**, *44* (4), 359–370.

(72) Ferreira, V.; López, R.; Cacho, J. F. Quantitative Determination of the Odorants of Young Red Wines from Different Grape Varieties. *J. Sci. Food Agric.* **2000**, *80* (11), 1659–1667.

(73) Mendes-Pinto, M. M. Carotenoid Breakdown Products The-Norisoprenoids-in Wine Aroma. *Arch. Biochem. Biophys.* **2009**, *483* (2), 236–245.

(74) Yuan, F.; Qian, M. Development of C6 and Other Volatile Compounds in Pinot Noir Grapes Determined by Stir Bar Sorptive Extraction-GC-MS. In *Flavor Chemistry of Wine and Other Alcoholic Beverages*; American Chemical Society, 2012; pp 81–99.

(75) Kalua, C. M.; Boss, P. K. Evolution of Volatile Compounds during the Development of Cabernet Sauvignon Grapes (Vitis Vinifera L.). *J. Agric. Food Chem.* **2009**, *57* (9), 3818–3830.

(76) Razungles, A. J.; Baumes, R. L.; Dufour, C.; Bayonove, C. L. Effect of Sun Exposure on Carotenoids and C13-Norisoprenoid Glycosides in Syrah Berries (Vitis Vinifera L.). *Sci. Aliments* **1998**, *18* (4), 361–373.

(77) Goff, S. A.; Klee, H. J. Plant Volatile Compounds: Sensory Cues for Health and Nutritional Value? *Science* **2006**, *311* (5762), 815–819.

(78) Black, C. A.; Parker, M.; Siebert, T. E.; Capone, D. L.; Francis, I. L. Terpenoids and Their Role in Wine Flavour: Recent Advances. *Aust. J. Grape Wine Res.* **2015**, *21* (S1), 582–600.

(79) González-Barreiro, C.; Rial-Otero, R.; Cancho-Grande, B.; Simal-Gándara, J. Wine Aroma Compounds in Grapes: A Critical Review. *Crit. Rev. Food Sci. Nutr.* **2013**, *8398* (April 2014), 37–41.

(80) Fischer, U. Wine Aroma. In *Flavours and Fragrances Chemistry, Bioprocessing and Sustainability*; Berger, R. G., Ed.; Springer, 2007; pp 241–267.

(81) Berli, F. J.; Moreno, D.; Piccoli, P.; Hespanhol-Viana, L.; Silva, M. F.; Bressan-Smith, R.; Cavagnaro, J. B.; Bottini, R. Abscisic Acid Is Involved in the Response of Grape (Vitis Vinifera L.) Cv. Malbec Leaf Tissues to Ultraviolet-B Radiation by Enhancing Ultraviolet-Absorbing Compounds, Antioxidant Enzymes and Membrane Sterols. *Plant. Cell Environ.* **2010**, *33* (1), 1–10.

(82) Ferrandino, A.; Lovisolo, C. Abiotic Stress Effects on Grapevine (Vitis Vinifera L.): Focus on Abscisic Acid-Mediated Consequences on Secondary Metabolism and Berry Quality. *Environ. Exp. Bot.* **2014**, *103*, 138–147.

(83) Wood, C.; Siebert, T. E.; Parker, M.; Capone, D. L.; Elsey, G. M.; Pollnitz, A. P.; Eggers, M.; Meier, M.; Vössing, T.; Widder, S.; et al. From Wine to Pepper: Rotundone, an Obscure Sesquiterpene, Is a Potent Spicy Aroma Compound. *J. Agric. Food Chem.* **2008**, *56* (10), 3738–3744.

(84) May, B.; Wüst, M. Temporal Development of Sesquiterpene Hydrocarbon Profiles of Different Grape Varieties during Ripening. *Flavour Fragr. J.* **2012**, *27* (4), 280–285.

(85) Coelho, E.; Rocha, S. M.; Delgadillo, I.; Coimbra, M. A. Headspace-SPME Applied to Varietal Volatile Components Evolution during Vitis Vinifera L. Cv. 'Baga' Ripening. *Anal. Chim. Acta* **2006**, *563* (1–2), 204–214.

(86) Garcia, E.; Chacon, J. L.; Martinez, J.; Izquierdo, P. M. Changes in Volatile Compounds during Ripening in Grapes of Airen, Macabeo and Chardonnay White Varieties Grown in La Mancha Region (Spain). *Food Sci. Technol. Int.* **2003**, *9*, 33–41.

(87) Farrell, R. R.; Wellinger, M.; Gloess, A. N.; Nichols, D. S.; Breadmore, M. C.; Shellie, R. A.; Yeretzian, C. Real-Time Mass Spectrometry Monitoring of Oak Wood Toasting : Elucidating Aroma Development Relevant to Oak-Aged Wine Quality. *Sci. Rep.* **2015**, 1–13.

(88) Skogerson, K. J. Metabolomics in Agricultural Research: Expanded Applications and Database Capabilities for Volatile Compound Capture and Tracking, University of California Davis, 2011.

(89) Fenoll, J.; Manso, A.; Hellín, P.; Ruiz, L.; Flores, P. Changes in the Aromatic Composition of the Vitis Vinifera Grape Muscat Hamburg during Ripening. *Food Chem.* **2009**, *114* (2), 420–428.

(90) Flamini, R.; Traldi, P. *Mass Spectrometry in Grape and Wine Chemistry*; 2009.

(91) Gougeon, R. D.; Lucio, M.; De Boel, A.; Frommberger, M.; Hertkorn, N.; Peyron, D.; Chassagne, D.; Feuillat, F.; Cayot, P.; Voilley, A.; et al. Expressing Forest Origins in the Chemical Composition of Cooperage Oak Woods and Corresponding Wines by Using

FTICR-MS. *Chemistry* **2009**, *15* (3), 600–611.

(92) Maga, J. A. Oak Lactones in Alcoholic Beverages. *Food Rev. Int.* **1996**, *12* (1), 105–130.

(93) Nixon, K. C. Global and Neotropical Distribution and Diversity of Oak (Genus Quercus) and Oak Forests. In *Ecology and Conservation of Neotropical Montane Oak Forests*; Kappelle, M., Ed.; Ecological Studies; Springer Berlin Heidelberg, 2006; Vol. 185, pp 3–13.

(94) Maga, J. A. The Contribution of Wood to the Flavor of Alcoholic Beverages. *Food Rev. Int.* **1989**, *5* (1), 39–99.

(95) Phillip John Spillman. Oak Wood Contribution to Wine Aroma, University of Adelaide, 1997.

(96) Díaz-Maroto, M. C. Fast Screening Method for Volatile Compounds of Oak Wood Used for Aging Wines by Headspace SPME-GC-MS (SIM). *J. Agric. Food Chem.* **2004**, *52*, 6857–6861.

(97) Prida, A.; Puech, J. Influence of Geographical Origin and Botanical Species on the Content of Extractives in American, French, and East European Oak Woods. *J. Agric. Food Chem.* **2006**, *54*, 8115–8126.

(98) De Simón, B. F.; Cadahía, E.; Jalocha, J. Volatile Compounds in a Spanish Red Wine Aged in Barrels Made of Spanish, French, and American Oak Wood. *J. Agric. Food Chem.* **2003**, *51* (26), 7671–7678.

(99) Jordão, A. M.; Ricardo-da-silva, J. M.; Laureano, O. Comparison of Volatile Composition of Cooperage Oak Wood of Different Origins (Quercus Pyrenaica vs. Quercus Alba and Quercus Petraea). *Mitteilungen Klosterneub.* **2005**, *55*, 22–31.

(100) Mosedale, J. R.; Puech, J.-L. Barrels: Wines, Spirits, and Other Beverages. In *Encyclopedia of food science, food technology and nutrition*; Caballero, B., Finglas, P., Trugo, L., Eds.; Academic Press, London, 2003; pp 393–403.

(101) Bosso, a; Petrozziello, M.; Santini, D.; Motta, S.; Guaita, M.; Marulli, C. Effect of Grain Type and Toasting Conditions of Barrels on the Concentration of the Volatile Substances Released by the Wood and on the Sensory Characteristics of Montepulciano d'Abruzzo. *J. Food Sci.* **2008**, *73* (7), S373-82.

(102) Delwiche, J. The Impact of Perceptual Interactions on Perceived Flavor. *Food Qual. Prefer.* **2004**, *15* (2), 137–146.

(103) Michel, J.; Jourdes, M.; Silva, M. a; Giordanengo, T.; Mourey, N.; Teissedre, P.-L. Impact of Concentration of Ellagitannins in Oak Wood on Their Levels and Organoleptic Influence in Red Wine. *J. Agric. Food Chem.* **2011**, *59* (10), 5677–5683.

(104) Oberholster, A. UC Davis Examines Oak Management and Wune Sensory Issues. *Wine Bus. Mon.* **2012**, *12* (December), 40–44.

(105) Marchal, A.; Waffo-Téguo, P. Identification of New Natural Sweet Compounds in

Wine Using Centrifugal Partition Chromatography-Gustatometry and Fourier Transform Mass Spectrometry. *Anal. Chem.* **2011**, *83* (24), 9629–9637.

(106) Vivas, N.; Glories, Y. Role of Oak Wood Ellagitannins in the Oxidation Process of Red Wines During Aging. *Am. J. Enol. Vitic.* **1996**, *46* (1), 103–107.

(107) Perez-Prieto, L. J.; la Hera-Orts, M. L.; López-Roca, J. M.; Fernández-Fernández, J. I.; Gómez-Plaza, E. Oak-Matured Wines: Influence of the Characteristics of the Barrel on Wine Colour and Sensory Characteristics. *J. Sci. Food Agric.* **2003**, *83* (14), 1445–1450.

(108) Ribéreau-Gayon, P.; Glories, Y.; Maujean, A. and Dubourdieu, D. Aging Red Wines in Vat and Barrel: Phenomena Occurring during Aging. In *Handbook of enology: The chemistry of wine stabilization and treatments*; John Wiley & Sons, Ltd.: Chichester, 2006; pp 387–428.

(109) Prida, A.; Chatonnet, P. Impact of Oak-Derived Compounds on the Olfactory Perception of Barrel-Aged Wines. *Am. J. Enol. Vitic.* **2010**, *3*, 408–413.

(110) Cutzach, I.; Chatonnet, P.; Henry, R.; Dubourdieu, D. Identifying New Volatile Compounds in Toasted Oak. *J. Agric. Food Chem.* **1999**, *47* (4), 1663–1667.

(111) Pollnitz, A. P. The Analysis of Volatile Wine Components Derived from Oak Products during Winemaking and Storage, University of Adelaide, 2000.

(112) Phillip John Spillman; Sefton, M. A.; Gawel, R. The Contribution of Volatile Compounds Derived during Oak Barrel Maturation to the Aroma of a Chardonnay and Cabernet Sauvignon Wine. *Aust. J. Grape Wine Res.* **2004**, *10* (3), 227–235.

(113) Prida, A.; Heymann, H.; Balanuta, A.; Puech, J.-L. Relation between Chemical Composition of Oak Wood Used in Cooperage and Sensory Perception of Model Extracts. *J. Sci. Food Agric.* **2009**, *89* (5), 765–773.

(114) Aznar, M.; López, R.; Cacho, J.; Ferreira, V. Prediction of Aged Red Wine Aroma Properties from Aroma Chemical Composition. Partial Least Squares Regression Models. *J. Agric. Food Chem.* **2003**, *51* (9), 2700–2707.

(115) Sauvageot, F.; Feuillat, F. The Influence of Oak Wood (Quercus Robur L., Q. Petraea Liebl.) on the Flavor of Burgundy Pinot Noir. An Examination of Variation Among Individual Trees. *Am. J. Enol. Vitic.* **1999**, *50* (4), 447–455.

(116) Masuda, M.; Nishimura, K. Branched Nonalactones from Some Quercus Species. *Phytochemistry* **1971**, *10* (6), 1401–1402.

(117) Spillman, P. J.; Sefton, M. A.; Gawel, R. The Effect of Oak Wood Source, Location of Seasoning and Coopering on the Composition of Volatile Compounds in Oak-matured Wines. *Aust. J. Grape Wine Res.* **2004**, *10*, 216–226.

(118) Wilkinson, K. L.; Prida, A.; Hayasaka, Y. Role of Glycoconjugates of 3-Methyl-4-Hydroxyoctanoic Acid in the Evolution of Oak Lactone in Wine during Oak Maturation. *J. Agric. Food Chem.* **2013**, *61* (18), 4411–4416.

(119) Chatonnet, P.; Dubourdieu, D. Identifcation of Substances Responsible for the 'Sawdust ' Aroma in Oak Wood. *J. Sci. Food Agric.* **1998**, *76*, 179–188.

(120) Díaz-maroto, M. C.; Guchu, E.; Castro-vázquez, L.; Torres, C. De; Pérez-coello, M. S. Aroma-Active Compounds of American , French , Hungarian and Russian Oak Woods , Studied by GC – MS and GC – O. **2008**, No. February, 93–98.

(121) Cabrita, M. J. B.; Garcia, R.; Martins, N.; Gomes da Silva, M. D. R.; Freitas, A. M. C. Gas Chromatography in the Analysis of Compounds Released from Wood into Wine. In *Advanced gas chromatography - Progress in agricultural, biomedical and industrial applications*; Mohd, M. A., Ed.; 2012; pp 185–208.

(122) Doussot, F.; Pardon, P.; Dedier, J.; Jeso, B. De. Individual, Species and Geographic Origin Influence on Cooperage Oak Extractible Content (Quercus Robur L. and Quercus Petraea Liebl.). *Analusis* **2000**, *28*, 960–965.

(123) Pollnitz, A. P.; Pardon, K. H.; Sykes, M.; Sefton, M. a. The Effects of Sample Preparation and Gas Chromatograph Injection Techniques on the Accuracy of Measuring Guaiacol, 4-Methylguaiacol and Other Volatile Oak Compounds in Oak Extracts by Stable Isotope Dilution Analyses. *J. Agric. Food Chem.* **2004**, *52* (11), 3244–3252.

(124) Duval, C. J.; Sok, N.; Laroche, J.; Gourrat, K.; Prida, A.; Lequin, S.; Chassagne, D.; Gougeon, R. D. Dry vs Soaked Wood : Modulating the Volatile Extractible Fraction of Oak Wood by Heat Treatments. *Food Chem.* **2013**, *138* (1), 270–277.

(125) De Simón, B. F.; Esteruelas, E.; Muñoz, A. M.; Cadahía, E.; Sanz, M. Volatile Compounds in Acacia, Chestnut, Cherry, Ash, and Oak Woods, with a View to Their Use in Cooperage. *J. Agric. Food Chem.* **2009**, *57* (8), 3217–3227.

(126) Vivas, N.; Saint-Cricq De Gaulejac, N.; Doneche, B.; Glories, Y. The Duration Effect of Natural Seasoning of Quercus Petraea. Liebl. and Quercus Robur L. on the Diversity of Existin Fungi FLora. *J. des Sci. Tech. la tonnellerie* **1997**, *3*, 27–35.

(127) Canas, S.; Caldeira, I.; Mateus, A. M.; Belchior, A. P.; Climaco, M. C.; Bruno-De-Sousa, R. Effect of Natural Seasoning of the Chemical Composition of Chestnut Wood Used for Barrel Making. *Ciência e Técnica Vitivinic.* **2006**, *21* (1), 1–16.

(128) Ward, A.; Hale, D. M.; Cardias-Williams, F. C. The Isolation of Fungi from Air and Kiln Drying Oak Wood Used for the Maturation of Alcoholic Beverages. *Holzforschung - International Journal of the Biology, Chemistry, Physics and Technology of Wood*. 1998, pp 359–364.

(129) Sáenz-Navajas, M.-P.; Fernández-Zurbano, P.; Ferreira, V. Contribution of Nonvolatile Composition to Wine Flavor. *Food Rev. Int.* **2012**, *28* (4), 389–411.

(130) Chira, K.; Teissedre, P.-L. Relation between Volatile Composition, Ellagitannin Content and Sensory Perception of Oak Wood Chips Representing Different Toasting Processes. *Eur. Food Res. Technol.* **2013**, *236* (4), 735–746.

(131) Doussot, F.; Jéso, B. De; Quideau, S.; Pardon, P. Extractives Content in Cooperage Oak

Wood during Natural Seasoning and Toasting; Influence of Tree Species, Geographic Location, and Single-Tree Effects. *J. Agric. Food Chem.* **2002**, *50* (19), 5955–5961.

(132) Petruzzi, L.; Bevilacqua, A.; Ciccarone, C.; Gambacorta, G.; Irlante, G.; Lamacchia, C.; Sinigaglia, M. Artificial Aging of Uva Di Troia and Primitivo Wines Using Oak Chips Inoculated with Penicillium Purpurogenum. *J. Sci. Food Agric.* **2012**, *92* (2), 343–350.

(133) Jordão, A. M.; Ricardo-da-silva, J. M.; Laureano, O.; Adams, A.; Demyttenaere, J.; Verhé, R.; De Kimpe, N. Volatile Composition Analysis by Solid-Phase Microextraction Applied to Oak Wood Used in Cooperage (Quercus Pyrenaica and Quercus Petraea): Effect of Botanical Species and Toasting Process. *J. Wood Sci.* **2006**, *52*, 514–521.

(134) Alanon, M. E.; Dıaz-Maroto, M. C.; Perez-Coello, M. S. Analysis of Volatile Composition of Toasted and Non-Toasted Commercial Chips by GC-MS after an Accelerated Solvent Extraction Method. *Int. J. Food Sci. Technol.* **2012**, *47*, 816–826.

(135) Mosedale, J. R.; Puech, J.-L.; Feuillat, F. The Influence on Wine Flavor of the Oak Species and Natural Variation of Heartwood Components. *Am. J. Enol. Vitic.* **1999**, *50* (4), 503–512.

(136) Campbell, J. I.; Sykes, M.; Sefton, M. A.; Pollnitz, A. P. The Effects of Size, Temperature and Air Contact on the Outcome of Heating Oak Fragments. *Aust. J. Grape Wine Res.* **2005**, *11*, 348–354.

(137) Rodríguez-Rodríguez, P.; Gómez-Plaza, E. Dependence of Oak-Related Volatile Compounds on the Physicochemical Characteristics of Barrel-Aged Wines. *Food Technol. Biotechnol.* **2012**, *50* (1), 59–65.

(138) Prida, A.; Puech, J. L. Natural Variability of Wood Compounds in Relation to Cooperage Oak Quality. *Aust. New Zeal. Wine Ind. J.* **2008**, *23*, 42–46.

(139) Pollnitz, A.; Pardon, K. Gas Chromatograph Injection Techniques on the Accuracy of Measuring Guaiacol, 4-Methylguaiacol and Other Volatile Oak Compounds in Oak Extracts by Stable Isotope Dilution Analysis. *J. Agric. Food Chem.* **2004**, *52*, 3244–3252.

(140) Cano-lópez, M.; Bautista-ortín, A. B.; Pardo-mínguez, F.; López-Roca, J. M.; Gomez-Plaza, E. Sensory Descriptive Analysis of a Red Wine Aged with Oak Chips in Stainless Steel Tanks or Used Barrels: Effect of the Contact Time and Size of the Oak Chips. *J. Food Qual.* **2008**, *31* (2008), 645–660.

(141) De Simón, Brígida Fernández, Muino, I.; Cadahia, E. Characterization of Volatile Constituents in Commercial Oak Wood Chips. *J. Agric. Food Chem.* **2010**, *58* (17), 9587–9596.

(142) Gishen, M.; Dambergs, R. G.; Cozzolino, D. Grape and Wine Analysis - Enhancing the Power of Spectroscopy with Chemometrics. A Review of Some Applications in the Australian Wine Industry. *Aust. J. Grape Wine Res.* **2005**, *11*, 296–305.

(143) Jastrzembski, J. A.; Bee, M. Y.; Sacks, G. L. Trace-Level Volatile Quantitation by Direct Analysis in Real Time Mass Spectrometry Following Headspace Extraction:

Optimization and Validation in Grapes. *J. Agric. Food Chem.* **2017**, *65* (42), 9353–9359.

(144) Yong, W.; Guo, T.; Fang, P.; Liu, J.; Dong, Y.; Zhang, F. Direct Determination of Multi-Pesticides in Wine by Ambient Mass Spectrometry. *Int. J. Mass Spectrom.* **2017**.

(145) Pu, F.; Zhang, W.; Han, C.; Ouyang, Z. Fast Quantitation of Pyrazole Fungicides in Wine by Ambient Ionization Mass Spectrometry. *Anal. Methods* **2017**, *9* (34), 5058–5064.

(146) Schwab, N. V.; Eberlin, M. N. Mass Spectrometry Made Easy: The Quest for Simplicity. *Drug Test. Anal.* **2013**, *5* (3), 137–144.

Chapter 2: Rapid Fingerprinting of Grape Volatile composition using Secondary Electrospray Ionization Orbitrap Mass Spectrometry - A Preliminary Study of Grape Ripening

This chapter has been published as a short communication in Food Control, 81 (2017) 107-112. All efforts were made to keep the original features of this article except minor changes e.g. layout, numbering, font size and style were carried in order to maintain a consistent formatting style of this thesis.

2.1 Overview

A rapid and sensitive method based on secondary electrospray ionisation mass spectrometry (SESI-MS) for profiling volatile emissions from the intact berries of non-Muscat grape cultivars (Pinot Noir, Chardonnay and Sauvignon Blanc) is presented. The method does not require sample preparation or concentration steps. Grape volatiles were tentatively identified based on accurate mass, the related elemental composition and literature. Approximately 300 peaks were detected in positive ion mode, and fewer (70-100) in negative ion mode. Changes in grape berry volatile composition during ripening were monitored to screen for potential ripeness markers. Ten $[M+H]^+$ peaks and four $[M-H]^-$ peaks were observed that evolved in a significant linear trend ($R^2 \geq 0.80$, $p < .05$) for the combined data across all cultivars either increasing or decreasing in the final four weeks of ripening. Peaks assigned to C_{13}-norisoprenoids and benzenoid derivatives have shown similar trends in previous studies using offline gas chromatography (GC) approaches.

Principal components analysis showed that negative ion mode clearly separated each stage of grape ripeness, whilst positive ion mode only separated berries in the final stage, pre-harvest. From this preliminary study, I conclude that SESI-MS holds promise as a tool for rapid screening of grape volatiles. Some potential marker ions

had no interfering peaks within a 1-Da window, such that they could be monitored with simple unit-resolution instruments in future studies. This implies that SESI-MS in combination with portable MS instrumentation has potential for field analysis where real-time analysis is key.

2.2 Introduction

Grape maturity is an important issue in winemaking because the grape chemical composition at harvest time is a key determinant of the resultant wine quality[1–4]. The grape ripening period from post-véraison (i.e. color change) to harvest is the most critical stage[5] because many compounds of oenological importance (free and bound aroma compounds, phenolics, sugar and organic acids) undergo complex changes in this growth phase reaching an "optimal" quality (for a given style of wine) at a certain point in time[6].

Even though sugar and acidity measurements are the most common indices of grape maturity, it is well recognized that they provide only basic information related to wine quality[7] and no information on the aromatic quality of the grapes. Furthermore, as there is no physiological basis for the general inverse correlation between sugar and acidity during ripening[8] many exceptions have been observed[9]. Accordingly, there is a need to complement sugar and acidity indices with other measures to better reflect the multifaceted nature of grape quality[10].

Grape-related wine aromas are derived from volatile organic compounds (VOC's) present in grapes as "free" aroma compounds and indirectly from non-volatile "bound" aroma precursors that are released during the winemaking process. Volatile emissions play a key role in fruit ripening[11] and therefore, VOC emissions from grape berries (whether directly related to wine aroma quality or not) may provide indicators of grape maturity and ripeness[1]. Previous studies regarding the evolution of free grape berry VOC's have focused on aromatic Muscat grape varieties in part because of the low concentration of VOC's in neutral non-Muscat grape cultivars[12–14]. Furthermore, most studies analyzed grape must (crushed grapes) rather than the

intact berries. Sensitive analysis of VOC's directly from intact grapes could ultimately facilitate the deployment of miniature mass spectrometer systems on all-terrain autonomous mobile robots in precision viticulture applications[15].

In this preliminary study we use a numerically optimized Secondary Electrospray ionization Mass Spectrometry (SESI-MS) ion-source[16] (SEADM, Spain) to analyze VOC's directly from intact grapes without sample concentration steps. SESI-MS has already demonstrated promise in the real-time analysis of VOC's[17,18], including monitoring VOC emissions from plants[19]. Furthermore, a similar technique was previously shown to discriminate different stages of ripeness in a variety of fruits including table grapes[20].

Grape berry volatiles from three non-Muscat cultivars (Pinot Noir, Chardonnay and Sauvignon Blanc) were monitored over a four-week period in the lead-up to harvest date. The aims were to determine: (i) the VOC signals (i.e. high resolution m/z and elemental composition) that can be detected directly from intact grapes in real-time (ii) whether clear trends in the evolution of specific ion signals can be identified as potential candidates for grape ripeness markers. We utilize a high resolution Orbitrap™ MS (Thermo Fisher, Bremen) in this preliminary study to maximize the chemical information collected. We note however, that a SESI source can be readily interfaced to a mini-MS for portable applications[21]. Compound identification in this preliminary untargeted study, relied on high resolution MS. Future studies could target the noteworthy peaks identified here by using tandem MS to aid identification of compounds.

2.3 Materials and Methods

2.3.1 Chemicals

Triethylamine (99.5% purity) and chromatography grade water (Sigma-Aldrich, Buchs, Switzerland). A standard solution was prepared 10 µg/mL in water for the MS sensitivity checks and stored at 4°C. External mass calibration was performed using

the standard positive and negative ion calibration solutions from Thermo-Fisher (Bremen, Germany).

2.3.2 Grape Berry Sampling and Pre-measurement Handling Procedures

The volatile composition of intact berries from three non-Muscat grape cultivars was measured weekly, over a four-week period in the lead-up to harvest. The Pinot Noir, Sauvignon Blanc and Chardonnay grape samples were collected from a research vineyard located at Au, Wädenswil, Zurich canton, Switzerland (8°38'43.272"E, 47°14'56.136"N) in the 2015 vintage. Véraison was August 5th for all cultivars and harvest dates were September 25th (Chardonnay), September 29th (Sauvignon Blanc) and October 5th (Pinot Noir). Grape samples were collected weekly from September 4th to September 25th. Approximately, 200 grape berries were collected for each cultivar, randomly sampled from different grapevines (both shadowed and sun exposed bunch positions) from the same rows of vines each week. Picked grapes (pedicel removed) were immediately placed in food-grade plastic bags, stored in a cooler and delivered to the lab for analysis within three hours of picking. Approximately 50 berries were used for classical ripeness assessment conducted by Vinalytik (Seewen, Schwyz, Switzerland); pH and total acidity were measured by a potentiometer whilst glucose, fructose, tartaric and malic acid were measured using high-performance liquid chromatography (HPLC).

2.3.3 SESI-Orbitrap-Mass Spectrometry

Grapes were counted, weighed and equilibrated to room temperature (21^{o}C) prior to SESI-MS analysis. The assessment of grape volatiles was conducted on the same day as sample collection avoiding freezing and storage steps. A random sample of the collected grapes (~ 80 berries) was measured per cultivar over a 2 min period. Grapes were placed in a 500 ml Schott bottle, closed using a modified cap that enabled the headspace of the bottle to be continuously swept (1 L/min, air) into the SESI source (SEADM, S.L.). The SESI source was interfaced to a Thermo-Fisher LTQ-Orbitrap XL mass spectrometer (Thermo Fisher Scientific, Bremen, Germany). The ion source, and MS settings were as previously described[19]. Grapes were also measured in negative mode in the final three weeks prior to harvest (September

11th, 18th and 24th, 2015) to explore a wider range of VOC's. In negative mode, lock masses were m/z 61.98837 and m/z 115.07645, corresponding to NO_3^- and $C_6H_{11}O_2^-$ respectively. External mass calibration was performed weekly prior to grape VOC analysis. MS sensitivity was checked weekly (post-measurement) using triethylamine as a standard.

After a 2 min blank measurement the bottle was opened, filled with sample grapes and closed. Grape berry VOC's were swept from the sample bottle headspace into the ion source. The headspace was measured continuously (3 micro-scans per scan, maximum injection time of 0.2 s) for two minutes, after which the bottle was removed and replaced with an empty, clean bottle. The ion source was flushed with clean air for 10 min between samples to avoid carryover. Negative-ion mode measurements were conducted on the same grape berry samples, following a 15 min equilibrium period.

2.3.4 Data Processing and Analysis

MS acquisition files (.raw format) were converted to .mzml files via ProteoWizard software[22]. Subsequent data processing was performed using python modules based on pymzML[23]. Data processing steps included; peak picking (measured precision 1 ppm, minimum counts 5,000), averaging spectra, m/z binning (2 ppm tolerance), removal of contaminants[24] and inter-quartile range normalization. Average spectra were calculated over a 1 min period in the 2nd min of measurement. The first minute was discarded due to unstable signals from pressure changes in the ion source when opening and closing the sample bottle. Peak intensities were adjusted according to number of grape berries providing results on a per berry basis. Finally, peak intensities over the four weekly measurements were z-score standardized to facilitate comparison of the evolution profiles for the different m/z peaks. Principal components analysis was performed using XLstat (Addinsoft, Paris, France, version 2015.2.01.16529).

2.3.5 Compound and m/z Selection

The standardized evolution profiles for all detected peaks were assessed to determine those with a significant increasing or decreasing linear trend ($R^2 \geq 0.80$, p

< .05) during the ripening process. Data was analyzed by individual cultivar and as a grouped dataset (all cultivars) to detect potential ripeness markers. Detected peaks were tentatively assigned to compounds based on accurate mass (yielding the elemental composition) and those identified in previous studies by GC.

2.4. Results and Discussion

2.4.1 Classical Maturity Measures of Ripening.

Table 2 shows the classical measures of grape ripeness during the four weeks leading to harvest. The sugar related parameters increase over the four-week period. Sugar content for Chardonnay plateaued by week three. Total sugar levels for all cultivars were 220-230 g l^{-1} at week four (prior to harvest). Total acidity generally decreased for both Sauvignon Blanc and Chardonnay, however, Pinot Noir showed little change in the final four weeks of ripening.

2.4.2 Detection of compounds from intact grapes using high resolution mass spectrometry.

The average peak area of the external standard infusions deviated by <10% week-to-week (see *Chapter 2 Supplementary Table 1, in Appendices*) verifying that instrument sensitivity was stable over the four-week measurement period.

Following data processing, 280-300 mass spectral peaks were detected at each ripening period (depending on cultivar) in positive ion mode. Fewer peaks (70-100) were detected in negative ion mode. The average root mean square (rms) error for the detected peaks was 0.62 ppm in positive mode (m/z 59-310) and 0.22 ppm in negative mode (m/z 59-283), indicating that the elemental composition can be uniquely assigned with high confidence. Peaks were tentatively assigned across a range of compound classes previously identified in grapes or grape must including C_{13}-norisoprenoids, monoterpenes, sesquiterpenes, C_6-aldehydes and alcohols, benzene derivatives and fatty acids. For all cultivars, m/z 99.0805 detected in positive mode, i.e. protonated [$C_6H_{10}O$] tentatively assigned to (E)-2-hexenal), was among the most abundant peaks in accordance with previous findings[2,3,14,25]. Negative mode spectra

were dominated by m/z 59.0139, deprotonated [$C_2H_4O_2$], tentatively assigned to acetic acid and is the major volatile fatty acid in grapes and wine[26].

Table 2: Classical measures of grape berry ripening for each grape cultivar. Accuracies are ± 2% for sugar and organic acid determinations and + 0.10%, - 1.52% for total acidity and pH.

	Harvest Date		Week 1: 04-Sep	Week 2: 11-Sep	Week 3: 18-Sep	Week 4: 25-Sep
Chardonnay	2015.09.25	Glucose (g/L)	101.3	99.7	113.0	110.0
		Fructose (g/L)	99.9	103.9	108.7	110.1
		Total Sugar (g/L)	201.2	203.6	221.7	220.1
		Tartaric acid (g/L)	3.59	3.01	2.75	2.69
		Malic acid (g/L)	3.8	4.38	3.44	3.99
		Total acidity (g/L)	6.5	5.4	5.3	4.6
		pH	3.3	3.62	3.51	3.77
		Berry weight (g/berry)	1.58	1.74	1.63	1.68
Pinot Noir	2015.10.05	Glucose (g/L)	100.4	107.7	110.6	115.1
		Fructose (g/L)	102.2	106.4	108.4	111.8
		Total Sugar (g/L)	202.6	214.2	218.9	227.0
		Tartaric acid (g/L)	2.89	3.21	3.10	2.97
		Malic acid (g/L)	3.78	3.5	3.52	3.31
		Total acidity (g/L)	4.7	5.2	5.0	5.0
		pH	3.65	3.53	3.59	3.63
		Berry weight (g/berry)	1.23	1.40	1.43	1.39
Sauvignon Blanc	2015.09.29					
		Glucose (g/L)	93.4	110.6	109.2	118.1
		Fructose (g/L)	97.7	106.8	109.2	112.3
		Total Sugar (g/L)	191.1	217.4	218.4	230.4
		Tartaric acid (g/L)	2.52	3.36	2.66	2.87
		Malic acid (g/L)	4.30	4.03	3.88	2.60
		Total acidity (g/L)	5.3	5.8	4.8	4.3
		pH	3.59	3.46	3.7	3.71
		Berry weight (g/berry)	1.41	1.74	1.67	1.62

Means presented (n = 50 randomly selected berries).

In positive mode, considering all cultivars together, the grouped data revealed 10 peaks (^{13}C isotopes removed) with significant linear trends ($R^2 \geq 0.8$, $P < .05$, n= 12), either increasing or decreasing in the last four weeks of ripening (Table 3). These peaks exhibiting significant linear trends for the grouped data are potential markers of the grape berry ripening process. Based on previous literature four of these peaks were tentatively assigned to known grape VOC's (Table 3). The evolution profiles of the four tentatively identified ripeness markers are presented in Figure 9.

Table 3: Detected m/z peaks $[M+H]^+$ with a significant increasing or decreasing evolution profile (linear trend $R^2 \geq 0.8$, $P < .05$, n = 12), during the last four weeks of ripening. Based on grouped data for all cultivars. Measured via positive ion mode secondary electrospray ionization mass spectrometry.

Measured m/z (Da) [M+H]+	Elemental Composition [M]	Exact mass (Da) $[M+H]^+$	Mass accuracy (ppm)	Tentative compound assignment	Coefficient of determination (R^2)[a]	Trend[b]
59.0492	C_3H_6O	59.04914	-1.4	acetone	0.81	+
139.0389	$C_7H_6O_3$	139.03897	0.6	*	0.84	-
151.0753	$C_9H_{10}O_2$	151.07536	0.4	4-vinylguaiacol / benzyl acetate	0.85	-
155.1542	$C_9H_{18}N_2$	155.15427	0.5	*	0.83	-
163.1481	$C_{12}H_{18}$	163.14813	0.4	*	0.90	-
165.0910	$C_{10}H_{12}O_2$	165.09101	0.0	2-phenethyl acetate / eugenol	0.88	-
175.1481	$C_{13}H_{18}$	175.14813	0.4	*	0.86	-
179.1430	$C_{12}H_{18}O$	179.14304	0.3	*	0.89	-
193.1587	$C_{13}H_{20}O$	193.15869	0.0	α-ionone, β-ionone, vitispirane	0.84	-
203.1430	$C_{14}H_{18}O$	203.14304	0.2	*	0.85	-

[a]All R^2 values significant ($p < .001$) [b]+ (increasing trend), - (decreasing trend). *Unassigned peaks.

m/z 193.1587 corresponds with the chemical formula for three isobaric C_{13}-norisoprenoids compounds $[C_{13}H_{20}O_1]^+$; α-ionone, β-ionone and vitispirane. Whilst the grouped data exhibited a significant decreasing trend ($p < .001$), the trends for individual cultivars (Figure 9) were significant for Sauvignon Blanc ($p = .02$) but not for the others (Chardonnay, $p = .07$ and Pinot Noir, $p = .15$).

Other authors have observed a decrease in the concentrations of free β-ionone in the latter stages of ripening in non-Muscat cultivars including Pinot Noir[25,27], and Nebbiolo, Dolcetto and Barbera[28], and in other grape cultivars[2,3]. Furthermore, β-ionone has previously been suggested as a potential indicator for signaling ripeness in *V. vinifera* reproductive tissues[28] and other plant species[11]. No major interfering peaks were observed within a 1 Da window around the m/z 193.1587 peak, protonated $[C_{13}H_{20}O_1]$ for all cultivars (see *Chapter 2 Supplementary Table 1, in Appendices*). This indicates the possibility of monitoring this signal using lower cost, unit resolution, field deployable mass spectrometers in future studies.

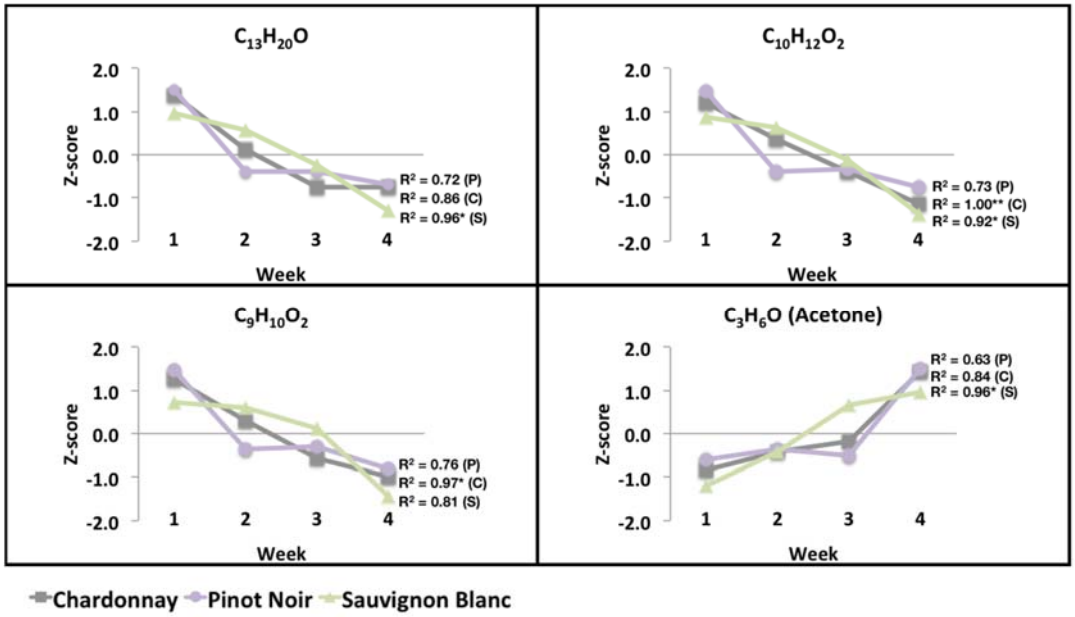

R^2 values shown are for each cultivar treated individually, Pinot Noir (P), Chardonnay (C), and Sauvignon Blanc (S).

** Correlation is significant at the 0.01 level (2-tailed).

* Correlation is significant at the 0.05 level (2-tailed).

Figure 9: Tentatively identified $[M+H]^+$ peaks with a significant linearly increasing or decreasing trend ($R^2 \geq 0.80$, $p < .05$) based on combined data for all cultivars. Measurements via positive ion mode secondary electrospray ionization mass spectrometry.

Two of the peaks in Table 3 correspond to benzene derivatives. m/z 151.0753, protonated [$C_9H_{10}O_2$] and 165.0910, protonated [$C_{10}H_{12}O_2$] were tentatively assigned to 4-vinylguaiacol / benzyl acetate and eugenol / 2-phenylethyl acetate respectively. These compounds have been identified in the canopy of Cabernet Sauvignon[29], and grape must of different cultivars[3,28,30,31]. For protonated [$C_9H_{10}O_2$] the trends for the individual cultivars (Figure 9) were significant for Chardonnay ($p = .01$) but not for the others, Pinot Noir $p = .13$, Sauvignon Blanc $p = .10$ (grouped data $p < .001$). The decreasing trend for protonated [$C_{10}H_{12}O_2$] (Figure 9) was significant for Chardonnay ($p = .001$) and Sauvignon Blanc ($p = .02$), but not for Pinot Noir ($p = .15$). In accordance with our observations these compounds have been observed to decrease with ripening[3,30].

Protonated [C_3H_6O], assigned to acetone was observed to increase in the final four weeks of ripening in contrast to the other compounds that decreased (Table 3). Considering the individual cultivars, the trend (Figure 9) was significant for

Sauvignon Blanc ($p = .02$) but not for the others (Chardonnay $p = .08$, Pinot Noir $p = .20$). Acetone has not been examined in previous studies on grape ripening.

Some positive mode peaks exhibited a cultivar specific evolution trend. For example, m/z 111.0804 protonated [$C_7H_{10}O$] tentatively assigned to (E,E)-2,4-heptadienal, m/z 121.0648 protonated [C_8H_8O] tentatively assigned to 4-vinylphenol and m/z 143.1066 protonated [$C_8H_{14}O_2$] tentatively assigned to isomers of hexenyl acetate exhibited significant linear trends for Pinot Noir but not the other cultivars (see *Chapter 2 Supplementary Figure 2, in Appendices*). The evolution of some benzene derivatives has been found to be cultivar specific[3,28] as we observed for m/z 121.0648, protonated [C_8H_8O].

Fatty acids are found in low abundance in grapes[25] however, we were able to detect fatty acid-related signals directly from the intact grape berries using negative mode SESI-MS. Signals were detected for the series of saturated fatty acids from two-carbon acetic acid to sixteen-carbon hexadecanoic acid, with the exception of pentatonic acid (C_5) and tridecanoic acid (C_{13}) that were not detected (Table 4). Volatile fatty acids were previously detected by negative mode SESI-MS[32].

Considering all cultivars together, the negative mode grouped data revealed four peaks (^{13}C isotopes removed) with significant linear trends ($R^2 \geq 0.8$, $P < .05$, $n= 9$), either increasing or decreasing in the last four weeks of ripening. These peaks were m/z 60.9931 deprotonated [CH_2O_3], m/z 124.0378 deprotonated [$C_3H_9O_5$], m/z 141.0922 deprotonated [$C_8H_{14}O_2$], and m/z 157.0871 deprotonated [$C_8H_{14}O_3$]. No tentative assignment was possible from the literature. The evolution profiles for these peaks over the final three weeks of ripening are provided in *Chapter 2 Supplementary Figure* 3 (see Appendices).

Table 4: Tentative fatty acid peaks, elemental composition and mass accuracy for peaks detected in all cultivars and ripening stages. Measured via negative ion mode secondary electrospray ionization mass spectrometry.

Measured m/z (Da) $[M-H]^-$	Elemental Composition [M]	Exact mass (Da) $[M-H]^-$	Mass accuracy (ppm)	Tentative compound assignment
59.0139	$C_2H_4O_2$	59.01385	-0.7	acetic acid
73.0295	$C_3H_6O_2$	73.02950	-0.3	propanoic acid
87.0452	$C_4H_8O_2$	87.04515	-0.5	butanoic acid
115.0765	$C_6H_{12}O_2$	115.07645	-0.2	hexanoic acid
143.1078	$C_8H_{16}O_2$	143.10775	-0.6	octanoic acid
157.1235	$C_9H_{18}O_2$	157.12340	-0.6	nonanoic acid
171.1392	$C_{10}H_{20}O_2$	171.13905	-0.6	decanoic acid
185.1548	$C_{11}H_{22}O_2$	185.15470	-0.8	undecanoic acid
199.1705	$C_{12}H_{24}O_2$	199.17035	-0.9	dodecanoic acid
227.2019	$C_{14}H_{28}O_2$	227.20165	-1.3	tetradecanoic acid
241.2176	$C_{15}H_{30}O_2$	241.21730	-1.3	pentadecanoic acid
255.2334	$C_{16}H_{32}O_2$	255.23295	-1.6	hexadecanoic acid

[a]Measured mass = the average mass detected (all cultivars and time periods).

The PCA for the negative mode data showed superior separation of the different stages of ripeness in comparison to positive ion mode where grape berries were only separated from the other ripening stages in the final week of measurement, prior to harvest (Figure 10). The utility of negative ion mode in the differentiation of wines[33] and grape musts[34] has been previously demonstrated by direct infusion electrospray ionization (ESI) approaches targeting non-volatile components.

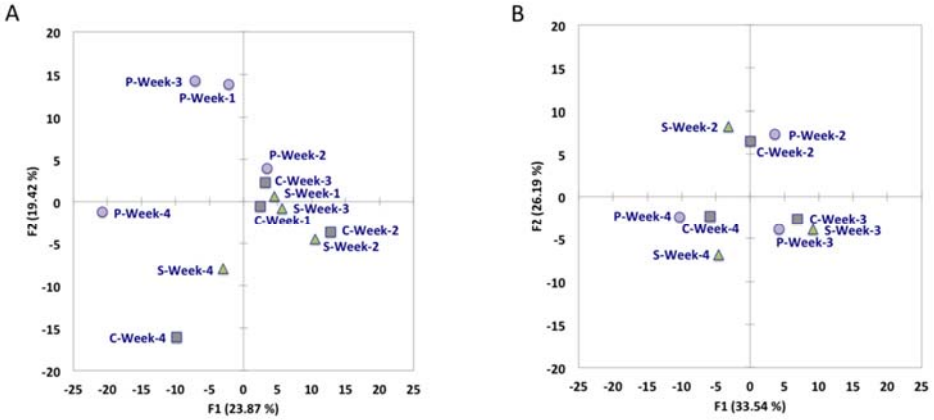

P = Pinot Noir, C = Chardonnay and S = Sauvignon Blanc.

Figure 10: Principal component analysis score plot for first and second components (F1 and F2) for all grape cultivars and measurement time points as measured via positive ion mode (A) and negative ion mode (B) secondary electrospray ionization mass spectrometry.

In conclusion, these preliminary results show that SESI-MS can detect VOC's directly from the headspace of intact grape berries without sample preparation or concentration steps. Ten peaks in positive mode and four peaks in negative mode exhibited significant linear trends ($R^2 \geq 0.8$, $p < .05$) for the combined data across all cultivars either increasing or decreasing in the final four weeks of ripening. These peaks may hold potential as markers of grape maturity, however further investigation over multiple vintages and longer ripening periods is required to test the robustness of the trends observed in this study. Importantly, simple unit resolution MS instrumentation could be used to monitor particular ions of interest indicating that SESI in combination with miniature MS could play a role in field deployable precision viticulture applications in the future.

References

1. Aleixandre, M. *et al.* A Wireless and Portable Electronic Nose to Differentiate Musts of Different Ripeness Degree and Grape Varieties. *Sensors* **15,** 8429–8443 (2015).
2. Coelho, E., Rocha, S. M., Barros, A. S., Delgadillo, I. & Coimbra, M. A. Screening of variety- and pre-fermentation-related volatile compounds during ripening of white grapes to define their evolution profile. *Anal. Chim. Acta* **597,** 257–264 (2007).
3. Vilanova, M., Genisheva, Z., Bescansa, L., Masa, A. & Oliveira, J. M. Changes in free and bound fractions of aroma compounds of four Vitis vinifera cultivars at the last ripening stages. *Phytochemistry* **74,** 196–205 (2012).
4. Giovenzana, V., Civelli, R., Beghi, R., Oberti, R. & Guidetti, R. Testing of a simplified LED based vis/NIR system for rapid ripeness evaluation of white grape (Vitis vinifera L.) for Franciacorta wine. *Talanta* **144,** 584–591 (2015).
5. Geffroy, O. *et al.* Effect of ripeness and viticultural techniques on the rotundone concentration in red wine made from Vitis vinifera L. cv. Duras. *Aust. J. Grape Wine Res.* **20,** 401–408 (2014).
6. Bisson, L. In search of optimal grape maturity. *Pract. Winer. Vineyard* **July/Augus,** 32–43 (2001).
7. González-Barreiro, C., Rial-Otero, R., Cancho-Grande, B. & Simal-Gándara, J. Wine Aroma Compounds in Grapes: A Critical Review. *Crit. Rev. Food Sci. Nutr.* **8398,** 37–41 (2013).
8. Jackson, R. S. in *Wine Science (Third Edition)* (ed. Jackson, R. S.) 50–107 (Academic Press, 2008). doi:http://dx.doi.org/10.1016/B978-012373646-8.50006-8
9. in *Enological Chemistry* (eds. Moreno, J. & Peinado, R.) 137–156 (Academic Press, 2012). doi:http://dx.doi.org/10.1016/B978-0-12-388438-1.00010-8
10. Šuklje, K. *et al.* Optimising harvest date through use of an integrated grape compositional and sensory model: a proposed approach for a better understanding of ripening of autochthonous varieties? *Oenoviti Int. Netw.* 44–49 (2014).
11. Goff, S. A. & Klee, H. J. Plant volatile compounds: sensory cues for health and nutritional value? *Science* **311,** 815–819 (2006).
12. Ferrandino, a., Carlomagno, a., Baldassarre, S. & Schubert, a. Varietal and pre-fermentative volatiles during ripening of Vitis vinifera cv Nebbiolo berries from three growing areas. *Food Chem.* **135,** 2340–2349 (2012).
13. Salinas, M. R., Zalacain, A., Pardo, F. & Alonso, G. L. Stir bar sorptive extraction applied to volatile constituents evolution during Vitis vinifera ripening. *J. Agric. Food Chem.* **52,** 4821–4827 (2004).
14. Kalua, C. M. & Boss, P. K. Comparison of major volatile compounds from Riesling and Cabernet Sauvignon grapes (Vitis vinifera L.) from fruitset to harvest. *Aust. J. Grape Wine Res.* **16,** 337–348 (2010).
15. Lopes, C. M. *et al.* Vineyard yield estimation by vinbot robot preliminary results with the white variety 'Viosinho'. in *XI International Terroir Congress* (2016).
16. Barrios-Collado, C., Vidal-De-Miguel, G. & Martinez-Lozano Sinues, P. Numerical modeling and experimental validation of a universal secondary electrospray ionization source for mass spectrometric gas analysis in real-time. *Sensors Actuators, B Chem.* **223,** 217–225 (2016).
17. Wu, C., Siems, W. F. & Hill, H. H. Secondary Electrospray Ionization Ion Mobility

Spectrometry/Mass Spectrometry of Illicit Drugs. *Anal. Chem.* **72,** 396–403 (2000).

18. Sinues, P. M.-L. *et al.* Mass spectrometry fingerprinting coupled to National Institute of Standards and Technology Mass Spectral search algorithm for pattern recognition. *Anal. Chim. Acta* **755,** 28–36 (2012).

19. Barrios-Collado, C. *et al.* Capturing in vivo plant metabolism by real time analysis of low to high molecular weight volatiles. *Anal. Chem.* (2016). doi:10.1021/acs.analchem.5b04452

20. Chen, H., Sun, Y., Wortmann, A., Gu, H. & Zenobi, R. Differentiation of maturity and quality of fruit using noninvasive extractive electrospray ionization quadrupole time-of-flight mass spectrometry. *Anal. Chem.* **79,** 1447–1455 (2007).

21. Lee, A., Misharin, A., Novoselov, K., Laiko, V. & Doroshenko, V. M. A field deployable ion trap mass spectrometer with atmospheric pressure interface. in *Workshop on Harsh-Environment Mass Spectrometry* (The Harsh Environment Mass Spectrometry Society, Inc., 2013).

22. Kessner, D., Chambers, M., Burke, R., Agus, D. & Mallick, P. ProteoWizard: Open source software for rapid proteomics tools development. *Bioinformatics* **24,** 2534–2536 (2008).

23. Bald, T. *et al.* pymzML - Python module for high throughput bioinformatics on mass spectrometry data. *Bioinformatics* **28,** 1–2 (2012).

24. Keller, B. O., Sui, J., Young, A. B. & Whittal, R. M. Interferences and contaminants encountered in modern mass spectrometry. *Anal. Chim. Acta* **627,** 71–81 (2008).

25. Yuan, F. & Qian, M. C. Development of C13-norisoprenoids, carotenoids and other volatile compounds in Vitis vinifera L. Cv. Pinot noir grapes. *Food Chem.* **192,** 633–641 (2016).

26. Boulton, R.B., Singleton, V.L., Bisson, L.F. and Kunkee, R. E. *Principles and practices of winemaking*. (Springer, 1996). doi:10.1007/978-1-4615-1781-8

27. Yuan, F. & Qian, M. Development of C6 and Other Volatile Compounds in Pinot Noir Grapes Determined by Stir Bar Sorptive Extraction-GC-MS. in *Flavor Chemistry of Wine and Other Alcoholic Beverages* 81–99 (American Chemical Society, 2012).

28. Carlomagno, A., Schubert, A. & Ferrandino, A. Screening and evolution of volatile compounds during ripening of 'Nebbiolo,' 'Dolcetto' and 'Barbera' (Vitis vinifera L.) neutral grapes by SBSE–GC/MS. *Eur. Food Res. Technol.* (2016). doi:10.1007/s00217-015-2626-4

29. Skogerson, K. J. Metabolomics in Agricultural Research: Expanded Applications and Database Capabilities for Volatile Compound Capture and Tracking. (University of California Davis, 2011).

30. Garcia, E., Chacon, J. L., Martinez, J. & Izquierdo, P. M. Changes in volatile compounds during ripening in grapes of Airen, Macabeo and Chardonnay white varieties grown in La Mancha Region (Spain). *Food Sci. Technol. Int.* **9,** 33–41 (2003).

31. Sefton, M. A., Francis, I. L. & Williams, P. J. The Volatile Composition of Chardonnay Juices: A Study by Flavor Precursor Analysis. *Am. J. Enol. Vitic.* **44,** 359–370 (1993).

32. Martínez-Lozano, P. & de la Mora, J. F. Direct Analysis of Fatty Acid Vapors in Breath by Electrospray Ionization and Atmospheric Pressure Ionization-Mass Spectrometry. *Anal. Chem.* **80,** 8210–8215 (2008).

33. Cooper, H. J. & Marshall, A. G. Electrospray ionization Fourier transform mass spectrometric analysis of wine. *J. Agric. Food Chem.* **49,** 5710–5718 (2001).

34. Catharine, R. R. *et al.* Characterization of must and wine of six varieties of grapes by direct infusion electrospray ionization mass spectrometry. *J. Mass Spectrom.* **41,** 185–190 (2006).

Chapter 3: Real-Time Mass Spectrometry Monitoring of Oak Wood Toasting: Elucidating Aroma Development Relevant to Oak-aged Wine Quality

This chapter has been published as a research article in Scientific Reports, 5, 17334 (2015). All efforts were made to keep the original features of this article except minor changes e.g. layout, numbering, font size and style were carried in order to maintain a consistent formatting style of this thesis.

3.1 Overview

A real-time method to monitor the evolution of oak aromas during the oak toasting process is introduced. French and American oak wood boards were toasted in an oven at three different temperatures, while the process-gas was continuously transferred to the inlet of a proton-transfer-reaction time-of-flight mass spectrometer for online monitoring. Oak wood aroma compounds important for their sensory contribution to oak-aged wine were tentatively identified based on soft ionization and molecular mass. The time-intensity profiles revealed toasting process dynamics illustrating in real-time how different compounds evolve from the oak wood during toasting. Sufficient sensitivity was achieved to observe spikes in volatile concentrations related to cracking phenomena on the oak wood surface. The polysaccharide-derived compounds exhibited similar profiles; whilst for lignin-derived compounds eugenol formation differed from that of vanillin and guaiacol at lower toasting temperatures. Significant generation of oak lactone from precursors was evident at 225 ^{o}C. Statistical processing of the real-time aroma data showed similarities and differences between individual oak boards and oak wood sourced from the different origins. This study enriches our understanding of the oak toasting process and demonstrates a new analytical approach for research on wood volatiles.

3.2 Introduction

Oak wood has long been used in wine aging to enhance wine aroma, taste, colour and stability[1,2]. Seasoning and toasting of oak products intended for wine-aging are important to produce oak wood of suitable sensory quality[1]. Freshly sawn oak wood is seasoned in the open air to leach astringent ellagitannins, hydrolyse bitter glycosylated coumarins and increase aroma compounds due to degradation of wood macromolecules by microflora[3–6]. Toasting results in a dramatic alteration of wood chemistry through hydrothermolysis and pyrolysis reactions[1]. Volatile organic compounds produced by thermal degradation of polysaccharides, lignin, and lipids greatly affect the sensory quality of oak-aged wine[7–10].

It is important to understand the chemistry of oak toasting, but previous studies are difficult to compare due to the diversity of extraction methods, the size of the wood samples (chips, boards, barrels), and the use of qualitative descriptions of the toasting process rather than explicit statements of temperature and time[11]. Furthermore, several publications have reported contradictory findings regarding the impact of toasting temperature on the development of oak aroma[11].

It has been difficult to investigate the dynamic process of oak toasting using traditional offline approaches, so limited studies have investigated temporal changes in oak wood chemistry with toasting.

Table 5: List of mass peaks, chemical formulae, tentative identification of compounds and mean peak areas by oak source and toasting temperature.

measured mass	exact mass	error	mass accuracy	tentative identification	chemical formula	two-way ANOVA			peak areas[a]					
(Da)	(Da)	(mDa)	(ppm)			S[b]	T[b]	SxT[b]	FO-175	FO-200	FO-225	AO-175	AO-200	AO-225
97.031	97.0284	2.8	28	furfural	$C_5H_4O_2^+$	n.s.	***	n.s	3.7E+02 ± 2.5E+02[b]	2.5E+03 ± 8.9E+02[b]	2.0E+04 ± 3.9E+03[a]	4.3E+02 ± 2.0E+02[b]	3.2E+03 ± 1.7E+03[b]	2.5E+04 ± 1.7E+04[a]
111.048	111.0441	3.6	33	5-methylfurfural	$C_6H_6O_2^+$	n.s.	***	n.s.	2.5E+01 ± 2.7E+01[b]	2.8E+02 ± 2.4E+02[b]	2.9E+03 ± 2.6E+03[a]	2.1E+01 ± 1.3E+01[b]	2.5E+02 ± 2.2E+02[b]	2.7E+03 ± 2.6E+03[a]
125.064	125.0597	4.6	36	guaiacol	$C_7H_8O_2^+$	*	***	**	6.1E-01 ± 5.2E-01[c]	6.5E+00 ± 3.6E+00[c]	6.8E+01 ± 2.8E+01[b]	1.3E+00 ± 5.4E-01[c]	8.6E+00 ± 5.1E+00[c]	9.9E+01 ± 4.6E+01[a]
127.041	127.0390	2.3	18	5-hydroxy methylfurfural / maltol	$C_6H_6O_3^+$	***	***	***	6.4E+00 ± 5.5E+01[d]	5.5E+01 ± 1.5E+01[cd]	4.1E+02 ± 1.2E+02[b]	8.4E+00 ± 4.7E+00[d]	8.2E+01 ± 3.3E+01[c]	6.3E+02 ± 8.9E+01[a]
153.056	153.0546	1.2	8	vanillin	$C_8H_8O_3^+$	*	***	*	2.7E+00 ± 2.3E+00[c]	3.3E+01 ± 2.7E+01[c]	3.5E+02 ± 1.6E+02[b]	4.8E+00 ± 1.9E+00[c]	5.7E+01 ± 4.7E+01[c]	6.9E+02 ± 5.4E+02[a]
157.122	157.1223	0.2	1	oak lactone	$C_9H_{16}O_2^+$	***	***	***	6.7E+00 ± 4.5E+00[c]	1.9E+01 ± 8.6E+00[bc]	7.9E+01 ± 3.2E+01[b]	1.8E+01 ± 1.2E+01[bc]	5.1E+01 ± 2.0E+01[bc]	2.2E+02 ± 1.3E+02[a]
165.092	165.0910	1.1	7	eugenol	$C_{10}H_{12}O_2^+$	***	***	***	4.7E-01 ± 4.6E-01[c]	3.2E+00 ± 2.2E+00[c]	5.1E+01 ± 1.8E+01[b]	1.1E+00 ± 7.3E-01[c]	9.7E+00 ± 6.5E+00[c]	1.2E+02 ± 8.3E+01[a]

[a] peak areas were calculated by numerical integration at discrete ten second time intervals, FO = French oak, AO = American oak. [b] Oak source effect (S), temperature effect (T) and source x temperature interaction (SxT) significant at the P<0.05*, 0.01**, 0.001*** level, n.s. not significant.

Peak areas given are averages for the four boards within each category. Data followed by different letters (in a row) are significantly different according to ANOVA at the P < 0.05 level

Currently, chemical analysis of oak wood volatiles is performed offline using gas chromatography following lengthy sample preparation[11-17]. Consequently, discrete toasting treatments (one temperature, one toasting period) are currently required for each time period of interest, limiting existing studies to two different time periods for a given toasting temperature[8,11,13].

Different mass spectrometry approaches can be envisaged for real-time monitoring of the oak toasting process. Briefly, these may include proton-transfer-reaction mass spectrometry[14], and laser based methods employing photoionization, including resonance enhanced multiphoton ionization mass spectrometry[15], and single photon ionization mass spectrometry[16].

Given the availability and prior success of proton-transfer-reaction mass spectrometry approaches for online monitoring of the coffee roasting process[17–19], here we take a similar analytical approach. By using online mass spectrometry we illustrate the analysis of oak toasting in real-time. This is achieved by continuous monitoring of volatile compounds during the toasting process. Continuous, real-time data clarify oak aroma development during the toasting process, and generate a new quality of information that is impossible to obtain using the traditional offline approaches. We combine the mass spectrometry data with chemometric protocols to examine differences between individual oak boards and differences between French and American oak.

3.3 Results and discussion

3.3.1 Wood Properties

Oak toasting is a process whereby the wood is brought to a temperature in the range of 150–240 °C[11] for a certain duration. It can be generally divided into two phases: a drying phase, during which water is removed from the hydrophilic wood constituents (hemicellulose and cellulose) and a toasting phase were complex thermal degradation reactions occur transforming non-volatile precursors into aroma active volatile compounds. The moisture content (see *Chapter 3 Supplementary Table 1, in Appendices)* of the oak samples varied minimally, both having average moisture content of 10% (w/w), with standard deviations <0.94%.

Wood density can also affect wood heating rate[20] and energy absorption[21]. However, we found no significant difference ($p > 0.05$, two-tailed t-test) between the oak sources for the small sample size (n=4) used here (see *Chapter 3 Supplementary Table 1, in Appendices*).

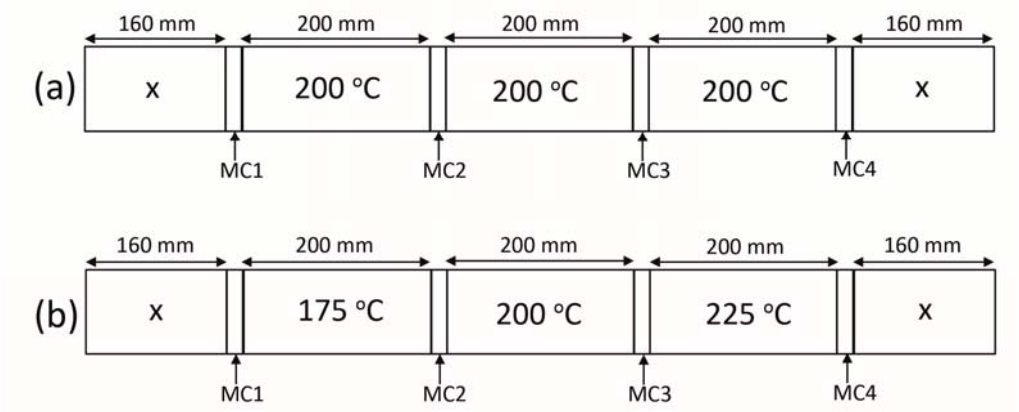

Figure 11: Cutting pattern applied to each board and toasting temperature applied to each sample. (a) Protocol for repeatability experiments. (b) Protocol for toasting temperature experiments. X: sections discarded; MC: sections used for analysing moisture content and density.

3.3.2 Compound Identification.

The measured and theoretical monoisotopic masses for the target compounds, their chemical formulae, tentative identification, corresponding mass errors, and total peak areas are reported in Table 5.

3.3.3 Repeatability Experiments.

The oak samples taken from the same board and toasted at the same temperature (protocol (a) in Figure 11) produced similar time-intensity profiles for the ion traces we studied. Figure 12 shows the time-intensity profiles for the American oak samples taken from the same board. Compared with the American oak profiles for samples taken from different boards (Figure 13) it is clear that between-board variation exceeds within-board variation. The peak area relative standard deviations for within-board samples compared to between-board samples (calculated at 30 minutes) were 6% versus 41%, 9% versus 37% and 4% versus 23% for 5-methylfurfual, vanillin, and oak lactone, respectively. Accordingly, the dimensions of the sample (200 × 50 × 10 mm) appear large enough to provide three samples

representative of each board. Repeatability and precision of the approach is evident in that analysis of samples from the same board result in consistent profiles with a relative standard deviation < 10%. Consequently, observed differences in the aroma profiles can be assigned to differences in oak properties and toasting temperatures, rather than to variability of the analytical method.

3.3.4 Oak aroma time-intensity profiles

The time-intensity profiles shown in Figure 13 and Figure 14 for both American and French oak samples respectively show the dynamic evolution of the selected oak volatiles during toasting. It is important to emphasize that the measured time-intensity profiles reflect the combined effect of three processes;

(a) generation of volatiles from precursors,

(b) diffusion of volatiles through the physical wood structure and

(c) volatilisation from the wood surface.

The time-intensity profiles highlight differences between boards and the oak sources. It is notable that the sudden increase in compound levels observed at approximately 30 min for two of the samples (American oak board three at 200 ^{o}C and French oak board two at 225 ^{o}C) relates to a physical and audible crack in the wood surface. This crack facilitates rapid escape of hot gas from within the wood structure causing a sudden spike in the concentration of the monitored volatiles. A similar phenomenon is observed in the coffee roasting process where spikes in compound concentrations correspond with the first and second “crack”, as cells rupture under high internal pressure[17]. American oak board three, toasted at 225 ^{o}C also displayed evidence of cracking at 15 min.

3.3.5 Polysaccharide-derived compounds.

The time-intensity profiles for furfural, 5-methylfurfural (5MF) and 5-hydroxymethylfurfural (HMF) / maltol reported in Figure 13 and Figure 14 were similar for each toasting temperature. Concentrations of oak volatiles remained low until 10-15 min of toasting (shorter for higher temperatures) and then increased to a maximum, followed by a decrease. The rate of decrease was greater at higher

temperatures. Whilst the shape of the time-intensity profiles remained similar for all temperatures, maximum concentrations increased by approximately one order of magnitude with each 25°C increase in toasting temperature.

The furfural peak was clearly the most intense signal observed for the selected volatiles, indicating that furfural is generated and volatilized in high quantities during the toasting process. Furanic compounds are produced by depolymerization of hemicellulose catalyzed by acetic acid (another compound observed at high intensities) and is formed during heating of wood[11]. Hemicellulose is the most thermo-sensitive wood polymer due to reactive acetyl side groups that are highly susceptible to acid hydrolysis, degrading in the temperature range of 130-194 ^{o}C[21]. When oak wood is heated, pentoses (the main constituents of hemicelluloses) produce furfural, thus explaining the high signal-intensities observed for furfural as toasting progresses. In contrast, 5-methylfurfural and 5-hydroxymethylfurfural / maltol are generated from hexose sugars, a minor constituent of oak wood hemicellulose and mainly found in the more crystalline cellulose[22,23]. The high degree of crystallinity[24,25] provides resistance to acid hydrolysis at the relatively low temperatures (150–240°C[11]) used during oak toasting, hence these compounds would be expected at much lower intensities in toasted oak relative to furfural concentrations. This can be confirmed by the lower intensities observed for these compounds in this study, as shown in Figure 11 and Figure 12. Furthermore, the higher boiling point of 5-hydroxymethylfurfural / maltol (292 ^{o}C and 285 ^{o}C respectively) versus that of 5-methylfurfural (187 ^{o}C) may influence their relative intensities.

3.3.6 Lignin-derived compounds

Time-intensity profiles for vanillin, guaiacol and eugenol (Figure 13 and Figure 14) differed according to temperature. Vanillin and guaiacol had similar profiles, whilst the eugenol profile was different, except at 225 ^{o}C where the profile was similar to that of vanillin and guaiacol. At 225 ^{o}C, the vanillin and guaiacol profiles were similar to the profile of furanic compounds. In accordance with previous findings the time-intensity profile for eugenol is different from that of vanillin and guaiacol[11]: Eugenol levels remained low at 175 ^{o}C (close to background noise levels) and increased to a

maximum at 5-10 min. For French oak, levels remained stable, in contrast to the decreasing intensity trend observed for American oak samples. At 200 °C, signal intensity increased until approximately 40 min. Thereafter, a gradual decrease was observed with time. A similar but more distinct profile was observed at 225 °C.

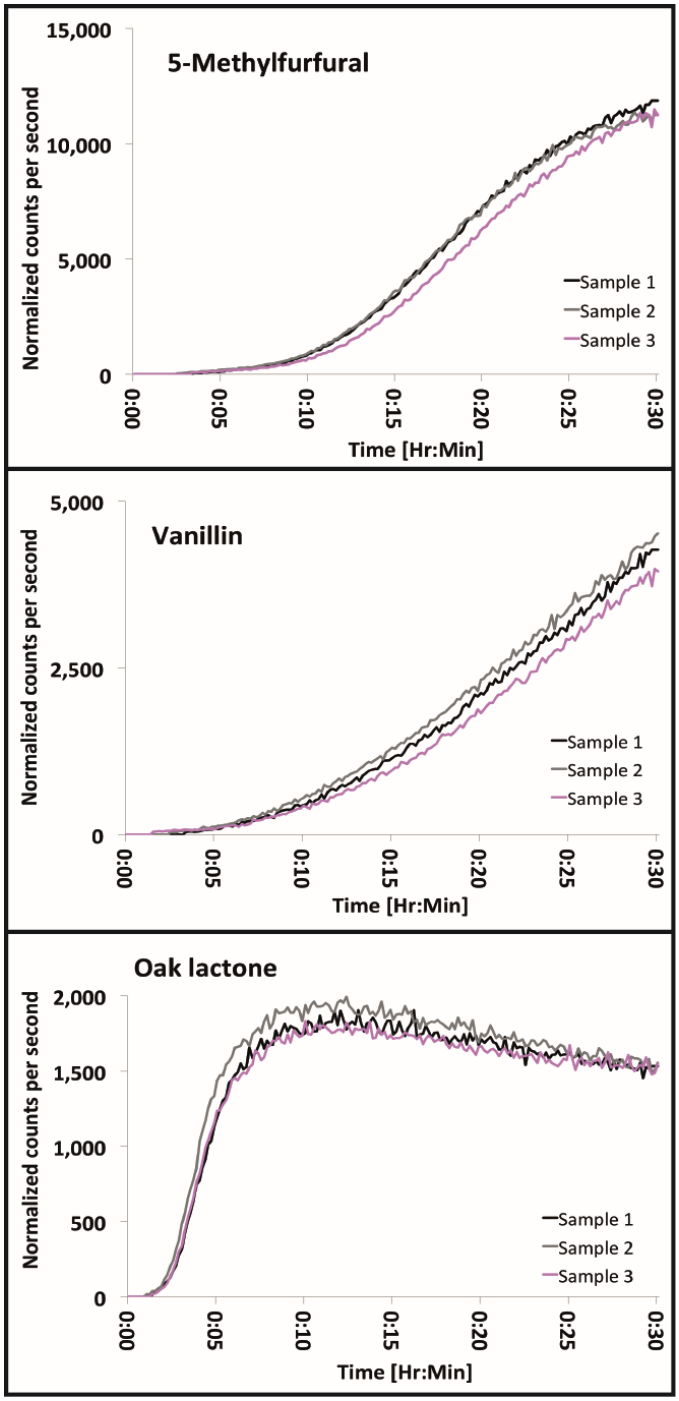

Figure 12: Time-intensity profiles for three compounds evolving from different aroma precursors in American oak wood, showing reproducibility of measurements based on three samples from the same board toasted at 200 °C. Normalised counts per second (ncps) are plotted against toasting time.

Although lignin is generally considered to be the most thermally stable wood polymer (degrading at 280-500 ^{o}C)[25], some degradation of lignin has been shown to occur at relatively low temperatures (e.g. 165 ^{o}C)[26]. This is consistent with our results, where the concentrations of lignin-derived compounds (vanillin, guaiacol and eugenol) clearly increase with temperature, by approximately one order of magnitude for each 25 °C increase in toasting temperature, as illustrated in Figure 11 and Figure 12. Considering the volatility of these compounds (boiling point of vanillin 283 ^{o}C, guaiacol 205 ^{o}C and eugenol 255 ^{o}C) we observe the highest intensities for vanillin (at all temperatures) even though vanillin has the lowest volatility. This confirms a higher concentration of vanillin relative to the other lignin-derived compounds.

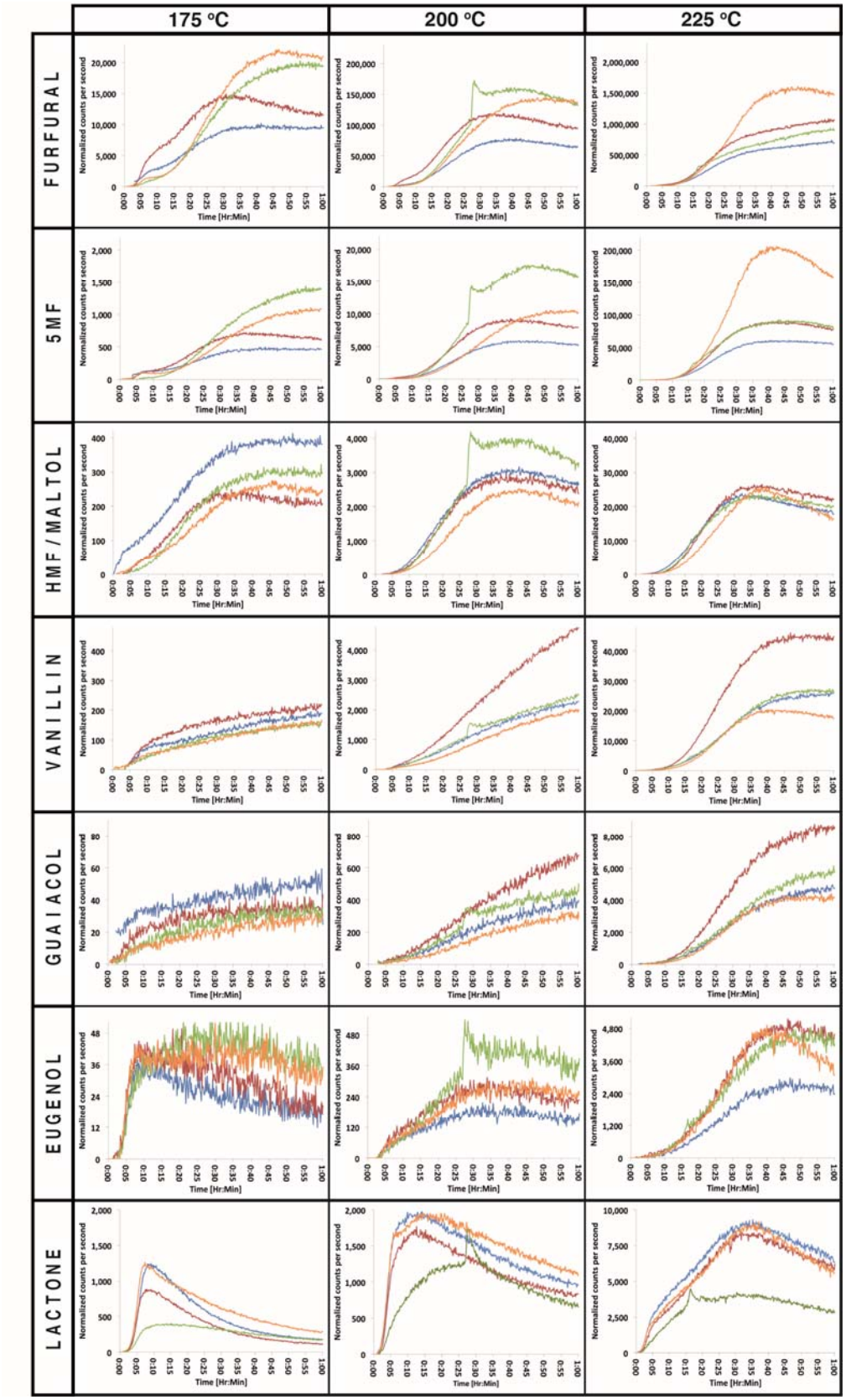

Figure 13: American oak time-intensity profiles for the target compounds at three different temperatures for individual board samples (Board 1: blue, Board 2: red, Board 3: green, Board 4: orange). Normalised counts per second (ncps) are plotted against toasting time. Note that y-axis scaling increases by one order of magnitude for each increase in toasting temperatures.

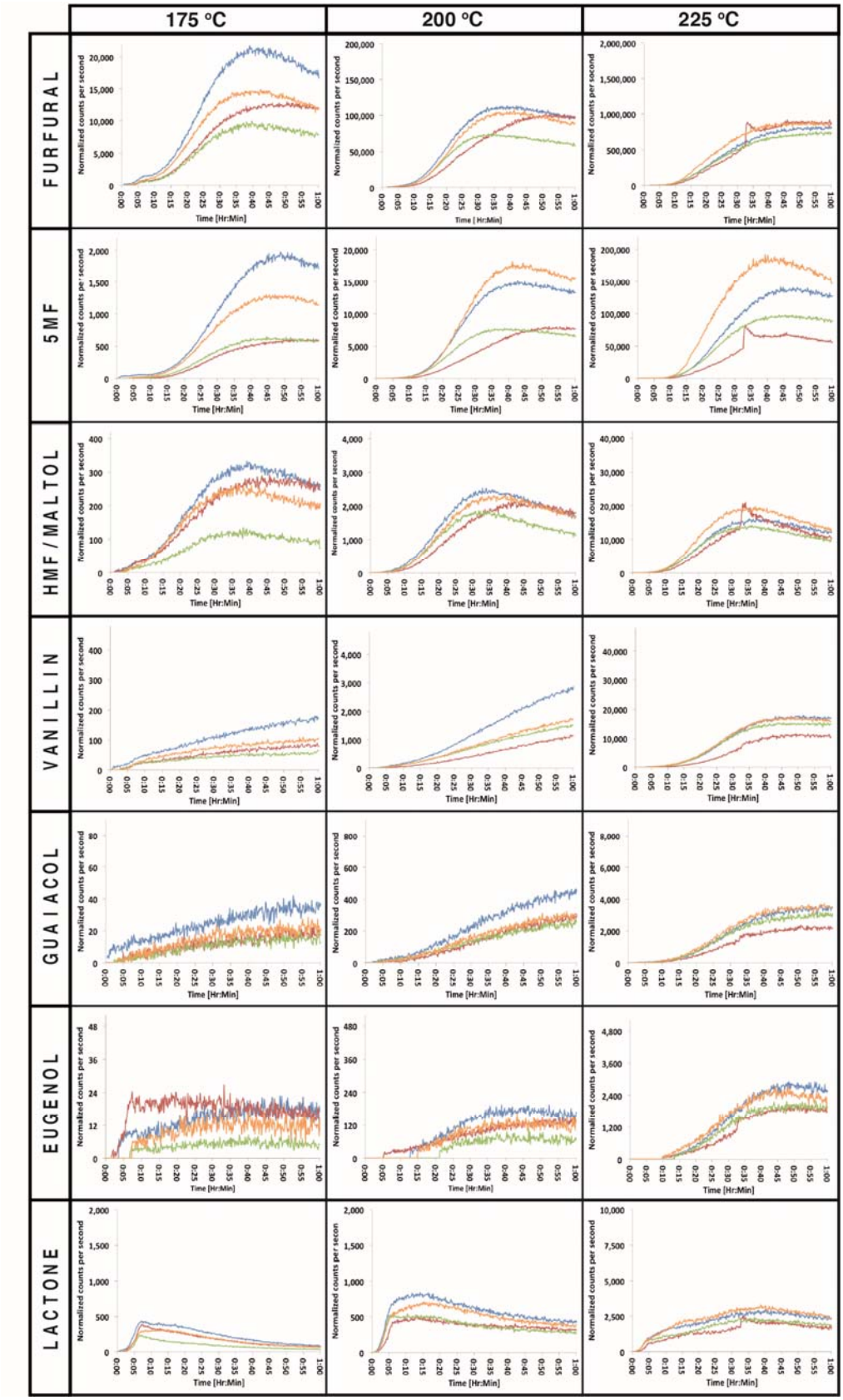

Figure 14: French oak time-intensity profiles for the target compounds at three different temperatures for individual board samples (Board 1: blue, Board 2: red, Board 3: green, Board 4: orange). Normalised counts per second (ncps) are plotted against toasting time. Note that y-axis scaling increases by one order of magnitude for each increase in toasting temperatures.

3.3.7 Lipid-derived compound oak lactone.

Temperature had a notable effect on the shape of the time-intensity profiles for oak lactone, particularly considering the differences between profiles at 175 ^{o}C and 225 ^{o}C (Figure 13 and Figure 14). At 175 ^{o}C, lactone intensity increased rapidly (0-6 min), and then decreased with time. At 200 ^{o}C, the initial rapid increase was again evident, followed by a second (moderate) increase until approximately 15 min. Signal intensities then decreased steadily with time. At 225 ^{o}C, the initial rapid increase was followed by a notable increase that continued and reached a maximum at approximately 35-40 min. Lactone signal intensity then decreased over time, more slowly than the rate of decrease observed at 175 ^{o}C and 200 ^{o}C. For American oak, board three had notably lower lactone intensity across all investigated temperatures. Furthermore, the profile deviated from the trend observed for the other American oak boards. Compared to the compounds derived from polysaccharides and lignin, there was a less pronounced increase in signal intensity with increased temperature.

Toasting treatments have been reported to have different effects on lactone levels (no effect, decreasing at high temperature, increasing then decreasing, or to decrease then increase)[11]. Recently, Wilkinison[13] helped clarify the formation of oak lactone by investigating the thermodegradation of oak lactone glycoconjugate precursors. They examined precursor levels at two toasting temperatures (100 ^{o}C and 200 ^{o}C) conducted for two different time periods (5 and 30 min). Their results showed thermal degradation of the lactone precursor (implying generation of volatile free lactone), but only after toasting at 200 ^{o}C for 30 min. In the current study we observe that oak lactone signal intensities exceed 175 ^{o}C levels after 10 min of toasting at 200 ^{o}C, reaching a maximum after 15 min. Lactone intensities at 200 ^{o}C are approximately double that observed at 175 °C. This increase in lactone at 200 ^{0}C could relate to greater volatilization of free-lactone (boiling point 247 ^{o}C), increased diffusion from deeper in the board sample and / or to the generation of lactone from the precursors (as indicated by Wilkinson[13]).

At 225 ^{o}C the maximum signal intensity is approximately 5-10 times higher than that observed at 175 °C (for French and American oak, respectively). The remarkably

different time-intensity profile observed at 225 °C supports the view that high quantities of free lactone are generated from precursors at temperatures above 200 °C.

3.3.8 Between-board variation.

The time-intensity profiles described above Figure 13 and Figure 14 also illustrate differences in the volatilized compounds between individual oak boards. For example, comparing the boards with the highest and lowest lactone peak areas, the greatest difference was observed at 175 °C, 224 % for American oak, and 249% for French oak. 5-methylfurfural showed the highest between-board variability with relative standard deviations as high as 55%. The lowest variation was observed for 5-hydroxymethylfurfural / maltol with relative standard deviations as low as 7%. In general the ranking of a board changed according to the compound. For example, American oak board 1 (blue) was ranked high for oak lactone and 5-hydroxymethylfurfural / maltol, intermediate for vanillin and guaiacol and low for 5-methylfurfural, furfural and eugenol. These findings show that individual oak boards may react differently under similar toasting conditions, even when the analysis is limited to boards of the same origin, moisture content and density.

3.4 Statistical analysis

3.4.1 Toasting Effects

According to their relative contents (area under the curve after one hour of toasting) the ANOVA for all 24 samples (Table 5) showed that the temperature effect was highly significant for all compounds. However, 5-hydroxymethylfurfural / maltol was the only compound that showed significant differences between all three toasting temperatures (Supplementary Table 2). The other compounds were differentiated by two groups, one related to the 225 °C toasting treatment (high compound concentrations), and another grouping the 200 °C and 175 °C treatments (exhibiting lower compound concentrations).

3.4.2 Oak Source Effects

With the exception of furfural and 5-methylfurfural all compounds were significantly higher in American oak (Tukey's pairwise comparisons, see *Chapter 3 Supplementary*

Tables 3 –9, in Appendices). As reported in Table 5, there was a significant interaction effect between oak source and temperature for most compounds (excluding furfural and 5-methylfurfural), i.e. the toasting effect depended on the oak source for most of the compounds we studied. Caldeira et al[22] also reported similar results for a "wood origin" effect for the compounds targeted in the current work.

3.4.3 Oak Lactone Content

The oak lactones are among the most important volatile compounds with a high sensory impact on oak-aged wines[27]. In agreement with the documented literature we observed significantly higher quantities of oak lactone in the American oak samples (see *Chapter 3 Supplementary Table 9, in Appendices*)[28]. Oak boards could be separated into three groups according to their oak lactone quantities (Tukey's pairwise comparisons, see *Chapter 3 Supplementary Table 10, in Appendices*): American oak 225 °C with high levels, French oak 175 °C with low levels and the remaining categories displaying "medium" lactone levels.

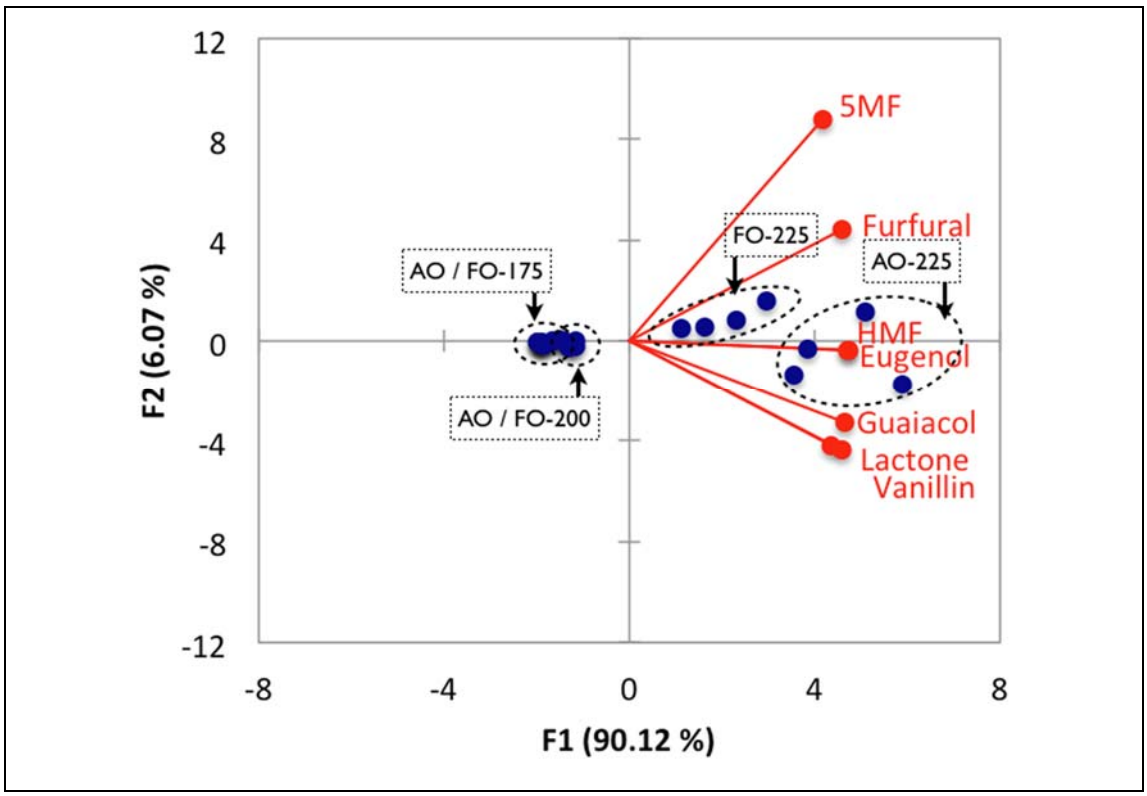

Figure 15: Principal component analysis score and loadings plot for first and second components (F1 and F2) for all oak categories and variables. Note, 5MF refers to 5-methylfurfural and HMF to 5-hydroxymethylfurfural / maltol. The dashed ellipses are used

to visualise the species and temperature groupings and do not represent a confidence interval.

3.5 Principal Component Analysis

The principal component analysis for all oak categories (i.e. oak source and toasting temperatures) presented in Figure 15 demonstrated little separation between the 175 °C and 200 °C toasting treatment. However, the 225 °C treatment was clearly differentiated from the others and separation of the oak source (i.e. French from American oak) was also evident at this temperature. The first principal component (F1), accounting for 90% of the total variance, relates to the increase in compound intensity with increasing temperature. F1 is strongly associated with 5-hydroxymethylfurfural / maltol and eugenol, and separates low temperature treatments (175 °C and 200 °C) from the 225 °C toasting treatment. F1 also provides separation between the oak sources with American oak exhibiting higher signal intensities. The second principal component (F2) accounts for only 6% of the variation separating boards that are high in furanic compounds (particularly 5-methylfurfural and furfural) versus those high in vanillin and oak lactone.

Caldeira et al.[22] observed separation of oak species based on principal component analysis of the volatile composition for untoasted wood, but not when toasted samples were included in the analysis. They did not observe separation based on toasting level, only separating untoasted from toasted samples. Their study used traditional barrel toasting over open fire however with no disclosure of the toasting temperature applied. The “strong” toast they applied was 25 min compared to the 60 min applied herein. Furthermore, the oven toasting method used in the current work (as opposed to standard industry toasting of barrels over open fire) would likely provide better control of the heat applied to the board samples, reducing variation at a given temperature. Probably, a combination of a longer toasting period, potentially higher temperature and greater control of the toasting process in the current work helps separate the “high” versus “low” temperature toasts. The principal component analysis shows that the 175 °C and 200 °C toasting treatments produce toasted oak boards with similar aroma profiles in contrast to clear differences observed when the toasting temperature is increased to 225 °C.

3.5.1 Agglomerative Hierarchical Clustering Analysis

Considering toasting temperatures individually (Figure 16 a, c, e) agglomerative hierarchical clustering grouped the eight oak boards into three clusters at each temperature. However, the composition of the three clusters varied depending on the temperature. At 175 ^{o}C (Figure 16a) French oak boards were clearly separated from American oak, with the exception of French oak Board 1 that was classified with the American oak. American oak Board 1 was placed in a unique, separate cluster. The profile plot (Figure 16b) showed that this cluster was characterized by low levels of furfural, and high levels of guaiacol and lactone. American oak boards were differentiated from the French oak by higher concentrations of the selected volatiles. At 200^{o} C French oak boards were separated from the American oak (Figure 16c) again generally based on higher compound concentrations in American oak. The American oak boards were separated into two groups based on higher levels of oak lactone and lower levels of the other compounds (Figure 16d). At 225^{o} C, once again French oak boards were separated from American oak (Figure 14e), whilst American oak Board 4 was differentiated from the other American oak boards primarily based on high furfural and 5-methylfurfural levels (Figure 16f). When agglomerative hierarchical clustering was applied to all boards (across all temperatures) three clusters were identified (Figure 16g); one grouping all boards toasted at 175^{o} C and 200 ^{o}C, a second grouping the French oak boards toasted at 225 ^{o}C and a third grouping all American oak boards toasted at 225^{o}C.

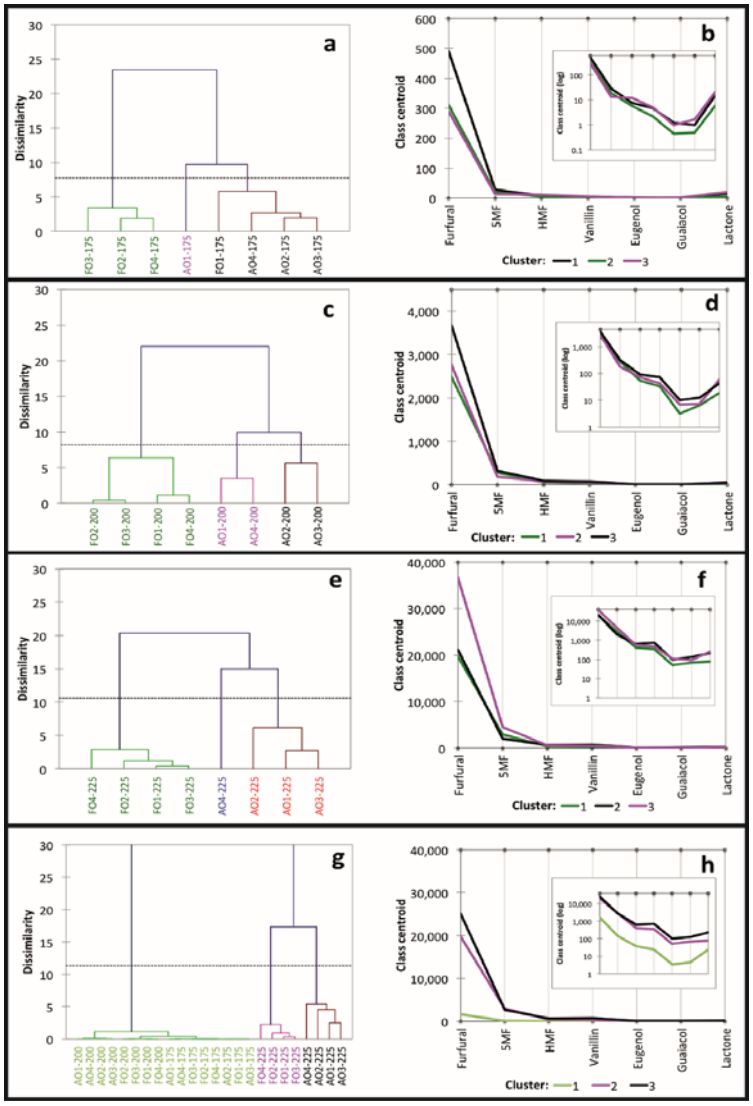

Figure 16: Agglomerative hierarchical clustering dendrogram (a,c,e,g) and compound profile plots (b,d,f,h) showing the aroma composition associated with each cluster (including a log-scale inset). All plots are based on integrated peak area after one hour of toasting.

This was further demonstrated by the Tukey's test pairwise comparisons (see *Chapter 3 Supplementary Table 10, in Appendices*) given the statistical differences between the American oak 225 ^{o}C treatment and the others. Considering these findings, we show that oak boards can be readily classified according to their toasted aroma profiles using chemometric tools.

In summary, a real-time methodology for online monitoring of the oak toasting process based on PTR-ToF-MS is demonstrated. The method requires no sample preparation and entails direct introduction of the oak toasting process gas into the inlet of the mass spectrometer. The results presented show the utility of PTR-ToF-MS

for monitoring the changes in aroma active volatiles during the oak toasting process. Real-time monitoring revealed how aroma compounds derived from different precursors develop over time. This online method circumvents limitations associated with previous gas chromatography based approaches by:

(i) greatly improving the temporal resolution (one measurement was recorded every 2 s) allowing the time-intensity profile for key aroma compounds to be directly monitored in real-time,

(ii) avoiding liquid extractions and lengthy sample preparation protocols,

(iii) reducing sources of error associated with liquid extractions

(iv) avoiding multiple time-discrete toasting treatments by elucidating the time dimension in a single dynamic experiment.

In addition, proton-transfer-reaction mass spectrometers are field-deployable[29], hence this approach is relevant to both laboratory-based and industry-based (*in situ*) research. Portable instrumentation offers a potential route to optimization of (site-specific) toasting systems to achieve targeted aroma profiles.

The combination of real-time monitoring, precise specification and control of toasting temperatures applied in this study helps elucidate the development of important oak aroma compounds during the toasting process. The observations conducted in real-time also highlight the variable nature of oak wood chemistry. Individual oak boards react differently under similar toasting conditions, even when the analysis is limited to boards of the same origin, moisture content and density. Natural variation in oak chemistry is well documented in the prior research conducted offline, using gas chromatography approaches[10,11,30–32]. Combined with chemometric approaches the described PTR-ToF-MS methodology can be used to differentiate or group similar oak boards according to their toasted aroma profiles.

In this work, new insights are provided into the dynamics of the oak toasting process. I anticipate that real-time mass spectrometry approaches could readily be used in many different applications to further our understanding and control of oak

wood flavor chemistry, improving the sensory quality of oak-aged wine, spirits and beer.

3.6 Methods

3.6.1 Oak Samples

Seasoned, non-toasted oak boards classified only by source (American oak from Kentucky and French oak from forests of central France) were provided in "Fan-assembly" form by Canton cooperage (Lebanon, KY, USA). The French oak boards were sawn lengthwise to 50 mm widths to match the dimensions of the American oak boards (10 × 50 × 980 mm). Subsequently, 160 mm sections were cut from each end of the board and discarded ("X"in Figure 9) to improve homogeneity by avoiding sampling from the board ends. Three 200 mm board samples were then cut taking 15 mm wide sections between each sample for determination of sample board moisture content determined by the oven dry method (MC 1-4) Figure 9.[33]. The moisture content samples were also used to calculate density based on the oven dry weight and oven dry volume, with volume determined by the water immersion method[34].

3.6.2 Oak Toasting Experiments

Firstly, three samples from a single American and French oak board were toasted at the same temperature as shown in protocol (a) in (Figure 11).This protocol was used to test the repeatability of the experimental method and to examine potential variation between samples within a given board. Secondly, to investigate the temperature effect, one sample from each of the four boards (for both French and American oak) was toasted at each temperature (175 ^{o}C, 200 ^{o}C and 225 ^{o}C) for 1 h as shown in protocol (b) in Figure 11.

3.6.3 Experimental Setup

Toasting was conducted in a 53 L forced convection oven (model FD-53, Binder GmbH, Tuttlingen, Germany). The oven was preheated to the desired toasting temperature before placing the oak board sample on the middle rack.

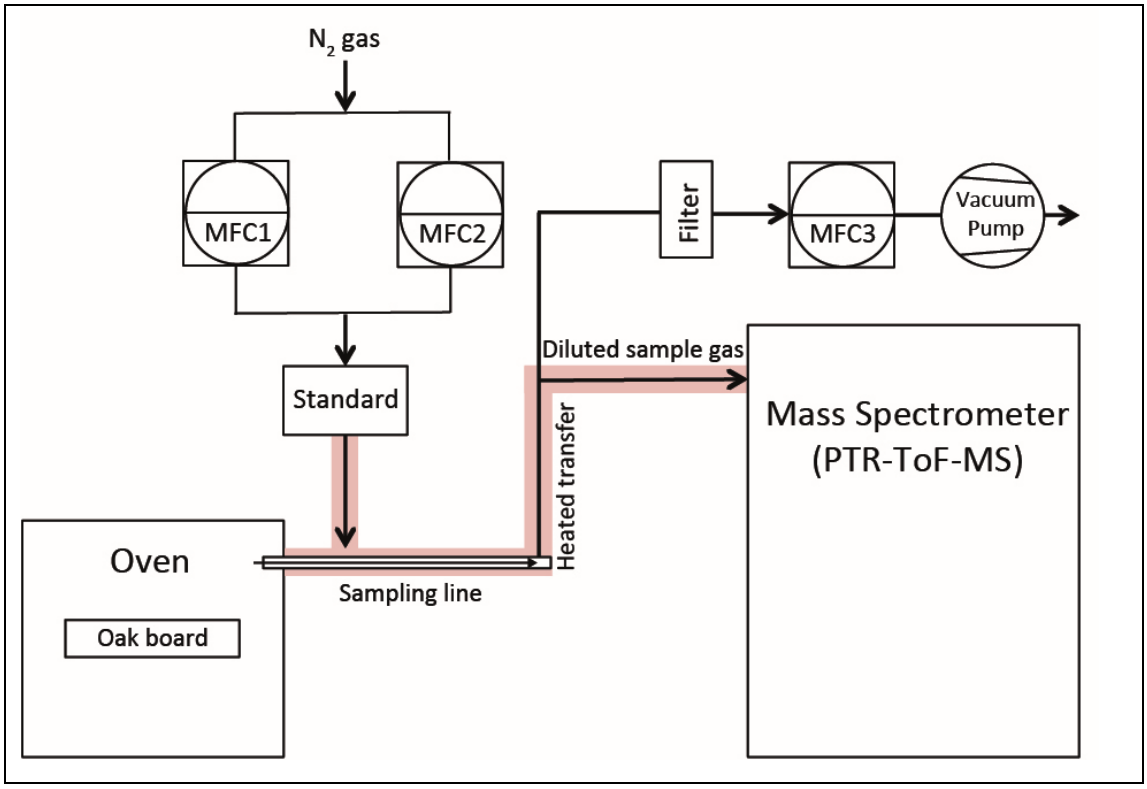

Figure 17: Experimental setup for sampling of oak volatiles generated during the toasting process. Volatiles were continuously drawn into the sampling line by the vacuum pump flow and diluted according to the toasting temperature by a nitrogen gas flow containing the mass calibration standard. The vacuum pump and dilution gas flows were controlled by mass flow controllers (MFC1-3). MFC capacities were MFC1: 5 L, MFC2: 0.2 L and MFC3: 10 L. MFC2 was included in the dilution gas supply to permit accurate adjustment and control of flow via a low capacity MFC.

Volatiles released from the oak board during toasting were measured as shown in Figure 17. This sampling configuration was adapted from Wellinger[35] using a sampling line with an integrated dilution port. The sampling line was inserted into the oven to actively sample and deliver toasting process-gas to the inlet of the mass spectrometer. The process-gas was diluted with nitrogen gas (in the sampling line and outside the oven) at a specific ratio for each toasting temperature to avoid condensation of sampled volatiles in the transfer tube, maintain stable and reproducible ionization conditions in the proton transfer reaction drift tube and to minimize detector saturation. The dilution factors were decreased at lower temperatures to retain sensitivity. Appropriate dilution factors were determined experimentally by monitoring the stability of the primary ion (H_3O^+) during preliminary toasting trials. The gas fractions sampled at each toasting treatment were 92.8% (175 °C), 27.2% (200 °C) and 6.8% (225 °C), resulting in dilution factors of

1.1, 3.7 and 14.6 respectively. The calibrated sampling flow into the mass spectrometer inlet was 249 standard cubic centimetres per minute (sccm) for all toasting experiments. The gas flows were controlled by mass flow controllers (Bronkhorst, Ruurlo, The Netherlands) and quantified for each dilution setting with a calibrated bubble flowmeter (Sigma-Aldrich (St. Louis, USA) and corrected according to operating temperature and atmospheric pressure. The vacuum pump flow was controlled by a 10 L mass flow controller (MFC3 in Figure 15). The dilution gas was controlled by two mass flow controllers of different capacity (MFC1: 5 L and MFC2: 0.2 L). MFC2 enabled fine control of the dilution gas supply. Transfer lines (0.25 in. Silcosteel-CR, 316 grade by Restek) were heated to 120 °C and insulated to minimize condensation and memory-effects. A standard (2-isobutyl-3-methylpyrazine, molecular weight: 150.22 u, Sigma-Aldrich, St Louis, USA) was added to the dilution gas stream for high mass range calibration of the mass spectrometer.

3.6.4 Proton Transfer Reaction Time-of-flight Mass Spectrometry

A PTR-ToF-MS 8000, mass resolution > 5,000 (FWHM) from Ionicon Analytik GmbH (Innsbruck, Austria) was used. The drift tube voltage was set at 600 V, drift tube pressure at 2.3 mbar (E/N 138 Td) and drift tube temperature at 90 °C. A 5 min blank was recorded before and after each toasting experiment to allow for background correction and to check for memory-effects. The time-of-flight extraction frequency was 50 kHz with a data acquisition rate corresponding to one mass-spectrum recorded every 2 s.

3.6.5 Mass Spectral Data Processing

PTR-TOF Data Analyzer (v 4.21)[36] was used for data analysis. The intrinsic $H_3{}^{18}O^+$ and $H_3{}^{18}O^+(H_2O)$ signals (21.022 m/z and 39.033 m/z) as well as the standard 2-isobutyl-3-methylpyrazine (protonated form): $[C_9H_{15}N_2]^+$, 151.123 m/z) were used for mass axis calibration and reference peak shape. Output files were processed according to a targeted mass list based on the protonated form of known oak aroma compounds[9,37–41]. Spectra were averaged during data processing creating result files with a ten second resolution to increase both accuracy and precision of peak fitting. Ion count rates were normalized to 10^6 H_3O^+ primary ions within the software. Ion

counts were then background corrected and adjusted for the dilution factor utilized at each toasting temperature.

3.6.6 Compound and m/z Selection

A targeted approach was used selecting seven ion traces (m/z values) tentatively identified as the $[M+H]^+$ peaks for key aroma compounds derived from the three main aroma precursors in oak wood i.e. polysaccharides (hemicellulose and cellulose), lignin and lipids. These diverse compounds (furanic aldehydes, volatile phenols, phenolic aldehydes, oak lactones and enolic compounds), are widely referred to in the literature and largely dictate the organoleptic quality of toasted oak and sensory impact on oak-aged wine[8,42]. Isomeric species cannot be differentiated by PTR-ToF-MS thus, the *cis* and *trans* isomers of oak lactone are collectively analyzed as the sum of both isomeric forms. Furthermore, as some lactones have been reported to fragment extensively in proton-transfer-reaction mass spectrometry[43], oak lactone fragmentation was checked under the analytical conditions used (see *Chapter 3 Supplementary Table 11, in Appendices*). Although fragmentation was observed sufficient analytical sensitivity was still achieved. Maltol and 5-hydroxymethylfurfural have the same chemical formulae thus results reported (at this m/z) relate to the contribution of both compounds. We assign the signal at 127 m/z to the sum of both 5-hydroxymethylfurfural and maltol. Furfural was generated in large concentrations during the toasting process, resulting in detector saturation for this m/z. Consequently, furfural intensities reported were calculated from the isotopic ratio for the ^{13}C isotope.

3.7 Data Analysis and Statistics

The time-intensity profile for each (m/z) studied (intensity shown as background and dilution corrected normalized counts per second) was plotted to elucidate the compound evolution profile. As the proton-transfer-reaction mass spectral signal is proportional to compound concentration[44], the area under the curve for each ion trace was calculated (numerical integration in discrete time-intervals of 10 s corresponding to the data processed by PTR-ToF data analyzer). The integrated area was used to provide insight on the differences between oak source, individual

boards and temperatures with regards to the total volatilized amount for each compound. The two oak sources and three toasting temperatures created six datasets, each containing four samples. All 24 samples were tested for significant differences using ANOVA followed by Tukey's test ($p < 0.05$). Principal component analysis and agglomerative hierarchical clustering based on dissimilarities (Euclidean distances) and Ward's agglomeration method was performed on the peak areas for the selected compounds. These chemometric approaches were used to visualize correlations and between-board variation and explore classification by statistical means. Statistical analysis was performed using XLstat (Addinsoft, Paris, France, version 2015.2.01.16529).

References

1. Hale, M. D., Mccafferty, K., Larmie, E., Newton, J. & Swan, J. S. The Influence of Oak Seasoning and Toasting Parameters on the Composition and Quality of Wine. *Am. J. Enol. Vitic.* **50 ,** 495–502 (1999).
2. Gougeon, R. D. *et al.* Expressing forest origins in the chemical composition of cooperage oak woods and corresponding wines by using FTICR-MS. *Chemistry* **15,** 600–11 (2009).
3. Sefton, M. A., Francis, I. L., Pocock, K. F. & Williams, P. J. The influence of natural seasoning on the concentrations of eugenol, vanillin, and cis-beta-methyl-gamma-octalactone and trans-beta-methyl-gamma-octalactone extracted from French and American oakwood. *Sci. Aliments* **13,** 629–643 (1993).
4. Martinez, J., Cadahia, E., De Simon, B. F., Ojeda, S. & Rubio, P. Effect of the seasoning method on the chemical composition of oak heartwood to cooperage. *J. Agric. Food Chem.* **56,** 3089–3096 (2008).
5. Masson, E., Baumes, R., Moutounet, M. & Puech, J. L. The effect of kiln-drying on the levels of ellagitannins and volatile compounds of European oak (Quercus petraea Liebl.) stave wood. *Am. J. Enol. Vitic.* **51,** 201–214 (2000).
6. Doussot, F., De Jeso, B., Quideau, S. & Pardon, P. Extractives Content in Cooperage Oak Wood during Natural Seasoning and Toasting; Influence of Tree Species, Geographic Location, and Single-Tree Effects. *J. Agric. Food Chem.* **50,** 5955–5961 (2002).
7. Francis, I. L., Sefton, M. A. & Williams, M. A. A Study by Sensory Descriptive Analysis of the Effects of Oak Origin, Seasoning, and Heating on the Aromas of Oak Model Wine Extracts. *Am. J. Enol. Vitic.* **43,** 23–30 (1992).
8. Cutzach, I., Chatonnet, P., Henry, R. & Dubourdieu, D. Identification of volatile compounds with a 'toasty' aroma in heated oak used in barrelmaking. *J. Agric. Food Chem.* **45,** 2217–2224 (1997).
9. Chatonnet, P., Cutzach, I., Pons, M. & Dubourdieu, D. Monitoring toasting intensity of barrels by chromatographic analysis of volatile compounds from toasted oak wood. *J. Agric. Food Chem.* **47,** 4310–4318 (1999).
10. Doussot, F., Jéso, B. De, Quideau, S. & Pardon, P. Extractives content in cooperage oak wood during natural seasoning and toasting; influence of tree species, geographic location, and single-tree effects. *J. Agric. Food Chem.* **50,** 5955–5961 (2002).
11. Duval, C. J. *et al.* Dry vs soaked wood : Modulating the volatile extractible fraction of oak wood by heat treatments. *Food Chem.* **138,** 270–277 (2013).
12. Chatonnet, P. Discrimination and control of toasting intensity and quality of oak wood barrels. *Am. J. Enol. Vitic.* **50,** 479–494 (1999).
13. Wilkinson, K. L., Prida, A. & Hayasaka, Y. Role of glycoconjugates of 3-methyl-4-hydroxyoctanoic acid in the evolution of oak lactone in wine during oak maturation. *J. Agric. Food Chem.* **61,** 4411–6 (2013).
14. Lindinger, W., Hansel, A. & Jordan, A. On-line monitoring of volatile organic compounds at pptv levels by means of Proton-Transfer-Reaction Mass Spectrometry (PTR-MS) Medical applications, food control and environmental research. *Int. J. Mass Spectrom.* **173,** 191–241 (1998).

15. Hertz-Schünemann, R., Dorfner, R., Yeretzian, C., Streibel, T. & Zimmermann, R. On-line process monitoring of coffee roasting by resonant laser ionisation time-of-flight mass spectrometry: Bridging the gap from industrial batch roasting to flavour formation inside an individual coffee bean. *J. Mass Spectrom.* **48,** 1253–1265 (2013).

16. Hertz-Schünemann, R., Streibel, T., Ehlert, S. & Zimmermann, R. Looking into individual coffee beans during the roasting process: Direct micro-probe sampling on-line photo-ionisation mass spectrometric analysis of coffee roasting gases. *Anal. Bioanal. Chem.* **405,** 7083–7096 (2013).

17. Yeretzian, C., Jordan, A. & Badoud, R. From the green bean to the cup of coffee : investigating coffee roasting by on-line monitoring of volatiles. *Eur. Food Res. Technol.* **214,** 92–104 (2002).

18. Wieland, F. *et al.* Online monitoring of coffee roasting by proton transfer reaction time-of-flight mass spectrometry (PTR-ToF-MS): towards a real-time process control for a consistent roast profile. *Anal. Bioanal. Chem.* **402,** 2531–2543 (2012).

19. Gloess, A. N. *et al.* Evidence of different flavour formation dynamics by roasting coffee from different origins: On-line analysis with PTR-ToF-MS. *Int. J. Mass Spectrom.* **365-366,** 324–337 (2014).

20. Leonardelli, M. J. Regarding barrel toasting levels. *Enology News & Notes* 1 (2012).

21. Dupleix, A., Sousa Meneses, D., Hughes, M. & Marchal, R. Mid-infrared absorption properties of green wood. *Wood Sci. Technol.* **47,** 1231–1241 (2013).

22. Caldeira, I., Clímaco, M. C., de Sousa, R. B. & Belchior, A. P. Volatile composition of oak and chestnut woods used in brandy ageing: Modification induced by heat treatment. *J. Food Eng.* **76,** 202–211 (2006).

23. Garde Cerdan, T., Rodrıguez Mozaz, S. & Ancın Azpilicueta, C. Volatile composition of aged wine in used barrels of French oak and of American oak. *Food Res. Int.* **35,** 603–610 (2002).

24. Shebani, A. N., Reenen, A. J. Van & Meincken, M. The effect of wood extractives on the thermal stability of different wood species. *Thermochim. Acta* **471,** 43–50 (2008).

25. Jin, W., Singh, K. & Zondlo, J. Pyrolysis Kinetics of Physical Components of Wood and Wood-Polymers Using Isoconversion Method. *Agriculture* **3,** 12–32 (2013).

26. Hill, C. A. S. *Wood Modification: Chemical, Thermal and Other Processes*. (John Wiley & Sons, Ltd., 2007).

27. Polášková, P., Herszage, J. & Ebeler, S. Wine flavor: chemistry in a glass. *Chem. Soc. Rev.* 2478–2489 (2008). doi:10.1039/b714455p

28. Maga, J. A. Oak lactones in alcoholic beverages. *Food Rev. Int.* **12,** 105–130 (1996).

29. Holzinger, R., Kasper-Giebl, a., Staudinger, M., Schauer, G. & Röckmann, T. Analysis of the chemical composition of organic aerosol at the Mt. Sonnblick observatory using a novel high mass resolution thermal-desorption proton-transfer-reaction mass-spectrometer (hr-TD-PTR-MS). *Atmos. Chem. Phys.* **10,** 10111–10128 (2010).

30. Prida, A. & Puech, J. Influence of geographical origin and botanical species on the content of extractives in American, French, and East European oak woods. *J. Agric. Food Chem.* **54,** 8115–8126 (2006).

31. Prida, A. & Puech, J. L. Natural variability of wood compounds in relation to cooperage oak quality. *Aust. New Zeal. Wine Ind. J.* **23,** 42–46 (2008).

32. Spillman, P. J., Sefton, M. A. & Gawel, R. The effect of oak wood source, location of seasoning and coopering on the composition of volatile compounds in oak-matured wines. *Aust. J. Grape Wine Res.* **10,** 216–226 (2004).

33. International, A. Standard Test Methods for Direct Moisture Content Measurement of Wood and Wood-Base Materials. (2007).

34. *Standard test methods for density and specific gravity (relative density) of wood and wood-based materials*. (ASTM International, West Conshohocken, PA, 2014, 2014). doi:10.1520/D2395-14

35. Wellinger, M., Biollaz, S. & Ludwig, C. Sampling and Online Analysis of Alkalis in Thermal Process Gases with a Novel Surface Ionization Detector. *Energy & Fuels* **25,** 4163–4171 (2011).

36. Müller, M., Mikoviny, T., Jud, W., D'Anna, B. & Wisthaler, A. A new software tool for the analysis of high resolution PTR-TOF mass spectra. *Chemom. Intell. Lab. Syst.* **127,** 158–165 (2013).

37. De Simón, Brígida Fernández, Muino, I. & Cadahia, E. Characterization of Volatile Constituents in Commercial Oak Wood Chips. *J. Agric. Food Chem.* **58,** 9587–9596 (2010).

38. Díaz-maroto, M. C., Guchu, E., Castro-vázquez, L., Torres, C. De & Pérez-coello, M. S. Aroma-active compounds of American , French , Hungarian and Russian oak woods , studied by GC–MS and GC–O. 93–98 (2008). doi:10.1002/ffj

39. Cabrita, M. J. B., Garcia, R., Martins, N., Gomes da Silva, M. D. R. & Freitas, A. M. C. in *Advanced gas chromatography - Progress in agricultural, biomedical and industrial applications* (ed. Mohd, M. A.) 185–208 (2012).

40. Simón, B. F. De, Cadahía, E., Muiño, I., Álamo, M. Del & Nevares, I. Volatile Composition of Toasted Oak Chips and Staves and of Red Wine Aged with Them. *Am. J. Enol. Vitic.* **61,** 157–165 (2010).

41. Estrella Cadahia, Brigida Fernandez de Simon, Raul Vallejo, Miriam Sanz, and M. B. Volatile Compound Evolution in Spanish Oak Wood (Quercus petraea and Quercus pyrenacia) during Natural Seasoning. *Am. J. Enol. Vitic.* **58,** 163–172 (2007).

42. Prida, A. & Chatonnet, P. Impact of Oak-Derived Compounds on the Olfactory Perception of Barrel-Aged Wines. *Am. J. Enol. Vitic.* **3,** 408–413 (2010).

43. Buhr, K., Buettner, A. & Schieberle, P. Analysis of Lactones by Proton Transfer Reaction - Mass Spectrometry (PTR-MS). Fragmentation Patterns and Detection Limits. in *3rd International Conference on Proton Transfer Reaction Mass Spectrometry and Its Applications* (eds. Armin, H. & Timann, M.) 149–153 (innsbruck university press, 2007).

44. Lindinger, W., Hansel, A. & Jordan, A. On-line monitoring of volatile organic compounds at pptv levels by means of proton-transfer-reaction mass spectrometry (PTR-MS) medical applications, food control and environmental research. *Int. J. Mass Spectrom. Ion Process.* **173,** 191–241 (1998).

Chapter 4: Rapid Screening of Oak Wood Volatiles by Dielectric Barrier Discharge Ionisation Mass Spectrometry

4.1 Overview

A thermal desorption dielectric barrier discharge ionisation mass spectrometry system (TD-DBDI-MS) for rapid analysis of volatile organic compounds (VOC's) from oak wood shavings is introduced. The system employs a novel thermal desorption unit (TDU) comprising two heated aluminium blocks separated by a central PTFE slider that acts as a sample introduction device via a manually activated sliding action. Oak VOC's were tentatively identified by high resolution Orbitrap mass spectrometry. Known oak wood VOC's from different chemical classes were detected including furanic aldehydes, volatile phenols, phenolic aldehydes, oak lactones and norisoprenoids. 287 peaks were detected across all fifteen oak samples measured in triplicate. Screening of oak VOC's could be conducted with an analysis time of ten seconds. The system was also used to monitor the oak toasting process. The oak toasting process evolved from inherent compounds such as oak-lactone to furanic compounds derived from hemicellulose degradation and in the latter stages to phenolic compounds derived from lignin degradation. High sensitivity was demonstrated for oak-lactone with a gas phase limit of detection of 26 part per trillion. Furthermore, the benefit of high resolution mass spectrometry for the analysis of oak wood VOC's was exemplified by the observation of seven peaks within a 0.3 Da window for m/z 225.

4.2 Introduction

4.2.1 Oak aromas and wine quality

The sensory experience of wine relates to the interplay of complex flavours derived from the grape, from fermentation and those extracted during maturation in oak wood. Oak wood maturation increases aromatic complexity through the extraction of many different volatile compounds including furanic aldehydes, volatile phenols, phenolic aldehydes, oak lactones and enolic compounds.

Table 6: Summary of sources of variation in oak flavour found in wine. *Reproduced from Wine Science[1] (page 455)*

- Oak species (coarse/fine grain, tyloses, chemistry, rays) - Geographic origin (rate of growth and ratio of spring to summer wood) - Location along length of tree trunk - Method of drying/seasoning (kiln drying versus the climatic conditions prevalent in the location where external seasoning occurred) - Type of barrel production (steaming versus firing) - Level of toasting - Nature of barrel conditioning prior to use Oak species (coarse/fine grain, tyloses, chemistry, rays) Geographic origin (rate of growth and ratio of spring to summer - Size of cooperage, duration, and cellar conditions during maturation - Repeated use (with or without shaving and retoasting)

Current methods for the analysis of oak wood volatiles are mostly based on gas chromatography in combination with mass spectrometry (GC-MS). Despite the high analytical performance achieved by GC methods, they have several disadvantages and limitations. For example, GC methods often require laborious sample preparation protocols requiring a high degree of technical skill and increasing the analytical time per sample analysed. Furthermore, the poor temporal resolution (i.e. runs of 30-40 mins for a single analysis) limits sample throughput and restricts the application of GC methods to “offline” analysis. Direct MS approaches offer a route towards simpler (e.g. using compact, unit resolution mass spectrometers), faster chemical analysis, holding great promise for rapid screening and the analysis of highly dynamic processes such as oak wood toasting.

4.2.2 Ambient Ionisation Mass Spectrometry

Ambient ionisation techniques coupled to mass spectrometry have been well

developed since the introduction of desorption electrospray ionization (DESI) in 2004[2]. This breakthrough technique demonstrated the direct desorption and ionisation of untreated samples freeing sample introduction from the vacuum environment of the mass spectrometer. Since DESI, over 40 different ambient ionisation sources have been developed[3], with at least seven being commercially available including (DESI, DART, LAESI, ASAP, SESI, DBDI and paper spray). Dielectric barrier discharge ionisation (DBDI) offers a low cost, compact, low power ion-source that can be readily applied to samples in the gas, liquid or solid state[4]. The DBDI ion source utilised here was first described by Zenobi's group as "active capillary plasma ionisation" whereby the ion source is effectively an extension of the MS inlet[5].

In this study, a rapid ambient ionisation method coupled to a high-resolution Orbitrap mass spectrometer was explored for the direct analysis of oak wood volatiles. The method promises rapid, sensitive and selective analysis, overcoming several limitations associated with traditional GC approaches.

4.3 Method

4.3.1 Chemicals

A d_3-oak-lactone standard was synthesised in-house by the Bode research group ETH-Zurich (unpublished work, Figure 18). A 1 ppm solution of the synthesised d3-lactone was prepared in HPLC-grade methanol and was continually infused as an internal standard during the analysis via a heat-assisted nanospray procedure similar to that previously described[6].

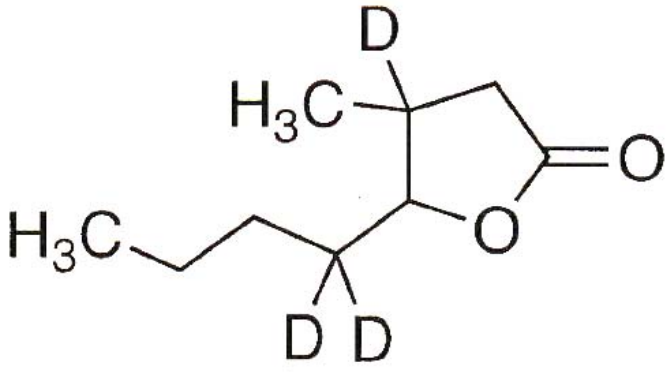

Figure 18: d_3-oak-lactone standard used to monitor ion suppression for oak lactone.

4.3.2 Oak Samples

Sections of seasoned oak wood staves (approximately 10 cm in length) were obtained from Vicard Cooperage in France. The 15 sample staves were a mix of European oak (*Quercus pedunculata* and *Quercus petraea,* species not determined) from different origins (France, Germany, Romania and Caucasus region) selected to cover a range of oak wood typically processed at the cooperage. Seasoning was at least 24 months. Oak shavings where produced using a hand plane, cut into small sections (< 10 mm in any dimension) and mixed.

4.3.3 Dielectric Barrier Discharge Ionisation Mass Spectrometry (DBDI-MS)

The DBDI source used in this work can be easily interfaced to any MS with an atmospheric pressure interface and has been described in detail in previous reports[5,6]. In this work a DBDI ion source was coupled to a thermal desorption unit to introduce volatiles from the oak wood samples. The ion source has previously been coupled to SPME for direct SPME-MS[7], to nano-liquid chromatography[8] and has been used as an atmospheric pressure soft ionisation source for GC[9].

In brief, the ion source consists of two concentric electrodes, onto which an alternating current is applied. The configuration of the DBDI source used in this work consisted of a quartz glass capillary (ID 0.7 mm, OD 1.0 mm) connected to the inlet of the mass spectrometer. A stainless-steel capillary (ID 0.5 mm, OD 0.6 mm) inserted into the glass capillary served as the first electrode. The counter-electrode was a 5 mm wide copper ring (ID 1.0 mm) surrounding the capillary. By applying a sine modulated (5.75 kHz) high voltage (1.5 kV, peak to peak) to the electrodes, a plasma ignites inside the capillary by dielectric discharge. The plasma then ionizes the passing gas molecules continuously drawn through the inlet capillary via the MS vacuum.

Air or nitrogen can be used as the reagent gas. In this work clean lab air was used. The resultant ionization is soft, inducing little fragmentation due to the characteristics of the low-temperature plasma that generates mostly protonated molecules $[M+H]^+$ (in positive mode). The air was humidified via bubbling through a gas wash bottle to maximise ionisation efficiency. The direct coupling of the ion source to the inlet capillary of the MS, results in a highly efficient ionization *and* ion transfer into the MS. This is in contrast with alternative

DBDI ion sources that employ an “open” configuration such as a plasma jet[10] or DART[11] ion source.

Preliminary optimization of the thermal desorption conditions, compound identification and calibration were performed on an LCQ Deca XP (Thermo Fisher Scientific, Bremen, Germany). The final, high-resolution mass spectra were acquired using an LTQ-Orbitrap XL (Thermo Fisher Scientific, Bremen, Germany), in full scan mode with a resolution setting of 60,000. The LTQ interface parameters were as follows: capillary voltage, 11 V; tube lens voltage, 100 V; capillary temperature, 200 °C. The acquisition was performed with a mass window of 60 to 500 m/z, with 1 micro scan, and with a maximum injection time of 200 ms. Automatic gain control was used.

4.3.4 Identification and Calibration

Compounds were tentatively identified based on accurate mass (yielding elemental composition) and based on known oak wood volatile organic compounds (VOC’s) identified in the previous literature. A calibration curve was conducted for oak-lactone using single reaction monitoring (SRM) after collision induced dissociation (CID) to determine the sensitivity of the DBDI-MS approach for oak wood VOC analysis. The heat-assisted nanospray procedure previously described[6] was used, taking three replicate measurements for each concentration. The average intensity of the most abundant fragment was then plotted against the corresponding gas-phase concentration. The LOD was then calculated according to IUPAC[12] using the 3s blank method.

4.3.5 Thermal Desorption Unit and Instrumentation

The thermal desorption unit (TDU) designed and developed in this work was based on a Polytetrafluoroethylene (PTFE) slider sandwiched between two heated aluminium blocks (Figure 19). The PTFE slider (160 x 60 x 15 mm) contained two opposed sample holders. The sample holders consisted of a circular brass ring with a 48 mm diameter hole and a 6 mm lower ledge supporting a stainless-steel mesh. The sample holders create a 42 mm diameter area through which gas phase volatiles from the sample pass through enroute to the ion-source and MS inlet. The aluminium blocks contained two holes to house heating cartridges. A one mm hole in the aluminium block was used to insert a thermocouple to maintain the desired desorption temperature. As shown in Figure 19 the aluminium blocks were

machined with a central conical section with a gas inlet and outlet that permitted clean heated gas to enter the TDU, and thermally desorbed volatiles to exit the TDU and transfer to the ion source and MS inlet.

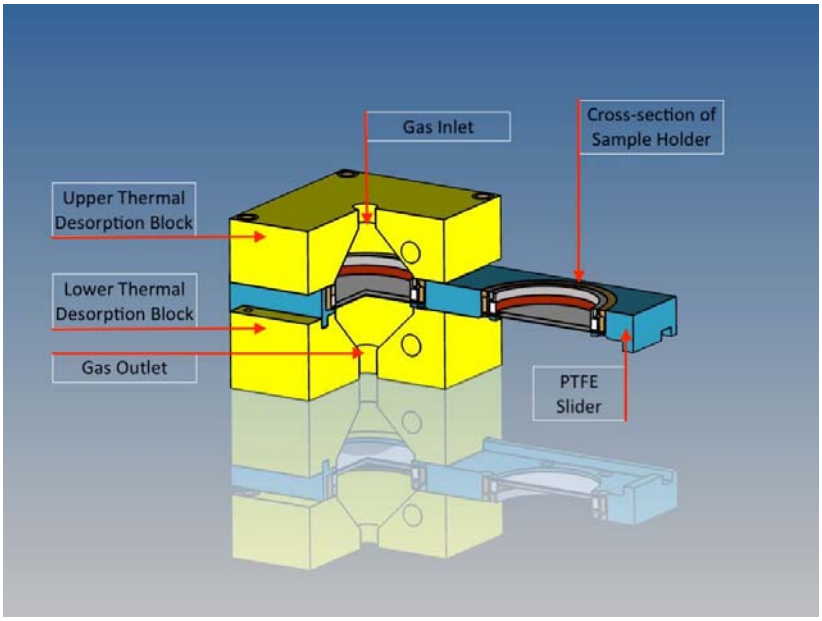

Figure 19: Drawing of the thermal desorption unit for introducing solid samples into a preheated chamber. In the chamber, samples are exposed to a hot gas that flows to the dielectric barrier discharge ion source and the inlet of the mass spectrometer allowing thermally desorbed volatiles to be monitored in real-time. Each desorption block measures 70 x 80 x 25 mm.

As shown in Figure 20, a gas heater (21 mm diameter heating cartridge wrapped with stainless-steel tubing) was used to deliver preheated gas to the TDU. A make-up gas flow was used to deliver hot clean gas to the ion source and MS allowing the gas from the TDU to be diluted. The gas flows were controlled by mass-flow controllers (Bronkhorst High Tech B.V., Ruurlo, Netherlands). Optimisation of the gas flows was conducted to determine the best dilution setting, i.e. to minimise ion suppression whilst retaining sufficient sensitivity for oak VOC's. In this work a dilution factor of twenty was used (one part sample : 20 parts dilution gas). Excess flow from the TDU exited the system through an exhaust line. Finally, a pressure-assisted nanospray setup as previously described[6] was used to introduce a known quantity of d_3-oak-lactone, used as an internal standard through the dilution line to monitor potential ion suppression effects.

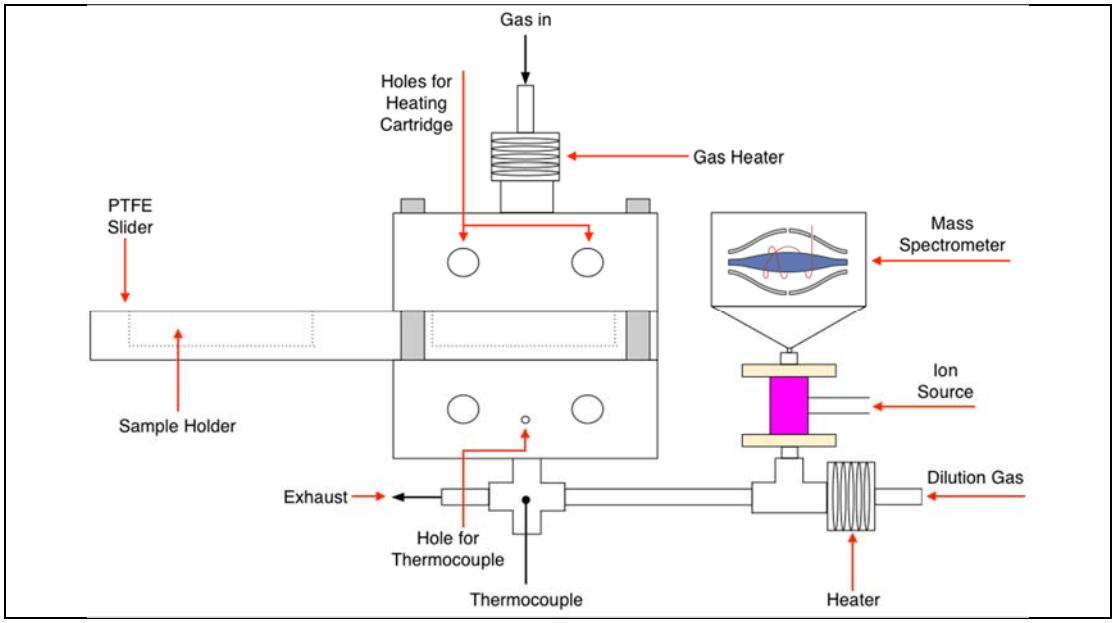

Figure 20: Schematic drawing of the thermal desorption dielectric barrier discharge ionisation mass spectrometry setup, including the thermal desorption sample introduction unit, dilution gas flow, internal standard delivery system, ion source and Orbitrap mass spectrometer. Note: Not to scale for better representation.

The effective desorption temperature was 200 °C as determined via a thermocouple inserted through a Swagelok cross piece at the exit of the TDU (Figure 18).

4.3.6 Temperatures

- Desorption gas supply to TDU: 225 °C
- TDU: 225 °C
- Dilution / internal standard gas supply: 200 °C

4.3.7 Gas Flows

- Desorption gas supply (lab supply air) to TDU: 3.0 L/min
- Dilution / internal standard gas supply (lab supply air): 1.0 L/min

4.3.8 Internal Standard

- 1 ppm solution (in methanol) infused via pressurised (1.0 bar) nanospray via a 40 µm (internal diameter) quartz capillary, 400 mm in length.

4.3.9 TD-DBDI-MS Sample Introduction

The TDU allowed solid or liquid samples to be introduced to the system. Once inserted into the TDU and exposed to the hot flowing gas, VOC's were desorbed via thermal desorption

and swept to the DBDI ion source and subsequently into the MS. Repeatability of the thermal desorption system was tested by spotting 2 µl of a 100 µg/ml 5-butyl-4-methyloxolan-2-one (oak lactone) solution in methanol (i.e. 200 ng) onto a mesh sample holder. The mesh was allowed to dry for two minutes before being placed in the sample slider and inserted into the TDU.

Solid samples were introduced by simply placing fragments of oak wood shavings onto the sample holder and pushing the slider with the loaded sample into the TDU. For each oak wood sample in this work, approximately 12 mg of oak wood shavings were placed onto the sample holder and the sample weight recorded via an analytical balance (readability 0.1 mg). Three independent samples from each oak wood stave were analysed.

The oak wood samples were inserted into the TDU for five minutes and the thermally desorbed volatiles continuously measured, after which the sample was removed. The TDU was flushed with clean air for 10 minutes between samples to prevent carryover. The process undertaken allowed high resolution mass spectrum fingerprints of oak wood VOC's to be obtained and the toasting process to be monitored in real-time.

4.3.10 Data Processing and Analysis

A lock mass calibration was applied to the data using RecalOffline (Thermo Fisher Scientific, Bremen, Germany) using the protonated d_3-oak-lactone internal standard, recalibrating per scan, and using Param C. Further data processing was similar to that discussed in Chapter 2. MS acquisition files (.raw format) were converted to .mzml files via ProteoWizard software [13]. Peak picking (measured precision 1 ppm, minimum counts 10,000), spectra averaging, m/z binning (5 ppm tolerance), and inter-quartile range normalization was performed using in-house python modules based on pymzML [14].

Average spectra were calculated over different time periods, 1-10 s, 0-30 s, 30-60 s and 60-120 s to investigate oak wood VOC fingerprints and monitor the toasting process. Peak intensities were adjusted according to sample weight. Oak lactone peak intensity was adjusted according to observed suppression of the deuterated d3-oak-lactone standard. Multivariate analyses were performed using XLstat (Addinsoft, Paris, France, version 2015.2.01.16529).

4.3.11 Compound and m/z Selection

Oak wood VOC's were tentatively identified by elemental composition from accurate mass and the previous literature. For multivariate analysis a targeted approach was used selecting 16 peaks related to compounds believed to be key drivers of oak expression in oak-aged wines. These 16 compounds are henceforth referred to as the impact aroma compounds.

Isomeric species cannot be differentiated by direct MS approaches that forego a chromatography "pre-separation" step prior to mass analysis. Consequently, the *cis* and *trans* isomers of oak lactone are collectively analysed as the sum of both isomeric forms. The literature also revealed several oak wood VOC's with identical elemental compositions. The results for these protonated molecules may relate to the contribution of multiple compounds and are reported as such.

4.4 Results and Discussion

4.4.1 Repeatability Experiments

Repeated measures of an oak-lactone standard spotted on a sample mesh was acceptable with a relative standard deviation (RSD) of 15%, n=9 (Figure 21). The observed variation is not only related to the TD-DBDI-MS instrumentation but also to;

(i) manual spotting of the sample solution on the mesh

(ii) evaporation during the drying of the sample solution on the mesh

(iii) rate of sample insertion via the manual actuation of the slider

Given the RSD was acceptable for a direct ambient MS method no further study into the significance of the sources of variation was undertaken.

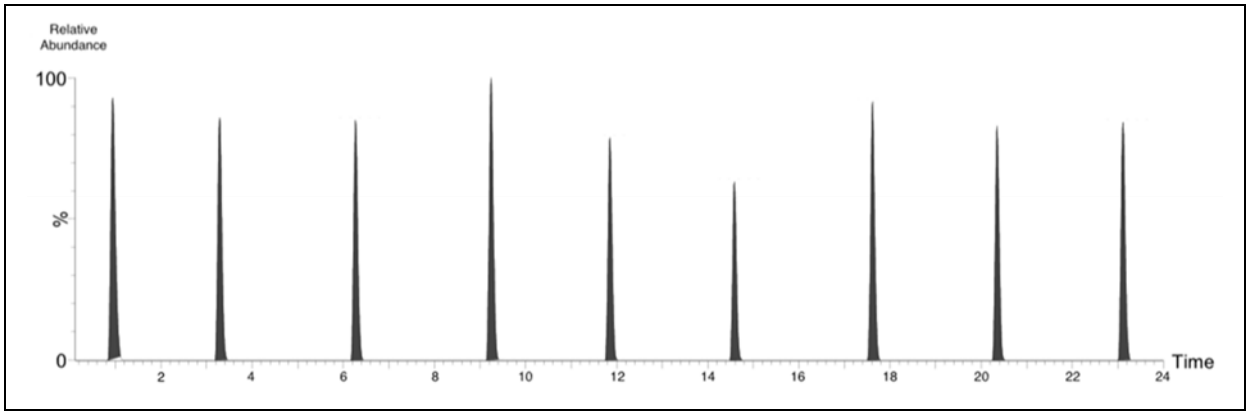

Figure 21: TD-DBDI-ORBITRAP-MS extracted ion chromatogram signals for eight consecutive measurements of 200 ng of oak lactone loaded on a stainless-steel mesh via manual spotting of 2 µl of 100 µg/ml oak lactone standard. After drying of the solvent, the mesh was placed in the sample slider and manually pushed into the thermal desorption unit.

4.4.2 Continuous Infusion of a Deuterated Standard Allows Ion Suppression to be Monitored

Figure 22 shows how the continuous infusion of a deuterated standard can be used to monitor ion suppression for target compounds such as oak-lactone. The internal standard also allows the sample gas dilution factor to be optimised by monitoring changes of signal intensity for the infused standard. By minimising and accounting for ion suppression effects (a potential drawback of DBDI-MS and ambient MS approaches in general) robust, quantitative data can be acquired.

Ion suppression for oak lactone (as determined via the d_3-oak-lactone standard) was typically less than 15 % (e.g. sample 7, Figure 22). The maximum level of ion suppression was 39 % (sample 11, Figure 23). The short spikes in the d_3-oak-lactone signal was due to build-up of the internal standard at the capillary end likely due to tip damage and deterioration in spray quality. However, the signal was generally stable and served its function as an ion suppression monitor.

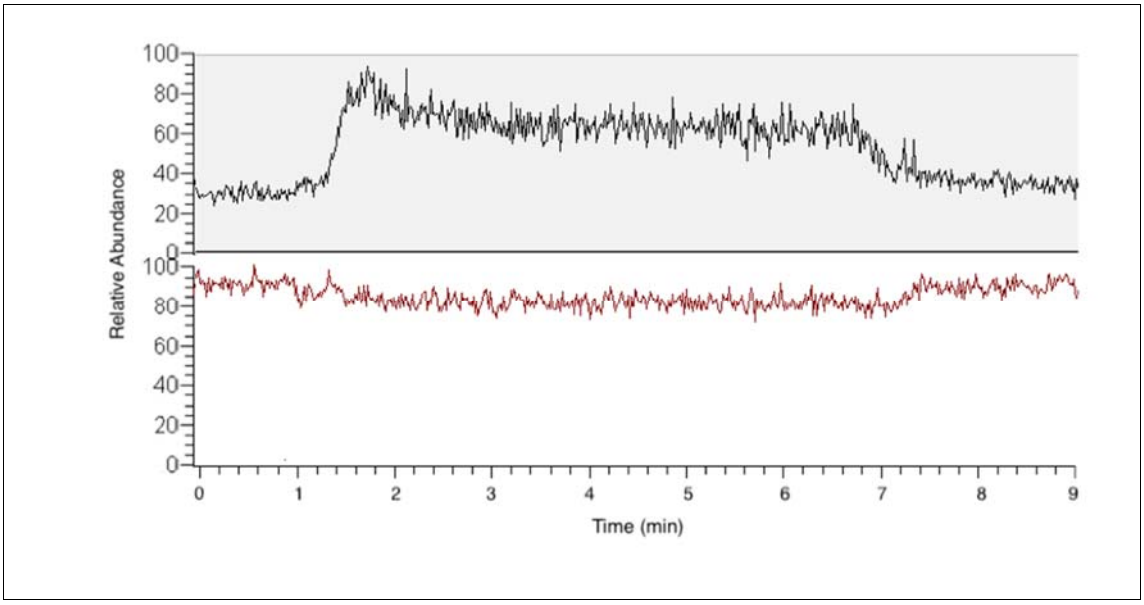

Figure 22: Extracted ion traces for sample 7 showing m/z 157.1223, oak lactone (upper pane) and the continually infused internal standard m/z 160.1411, d_3-oak-lactone (lower pane).

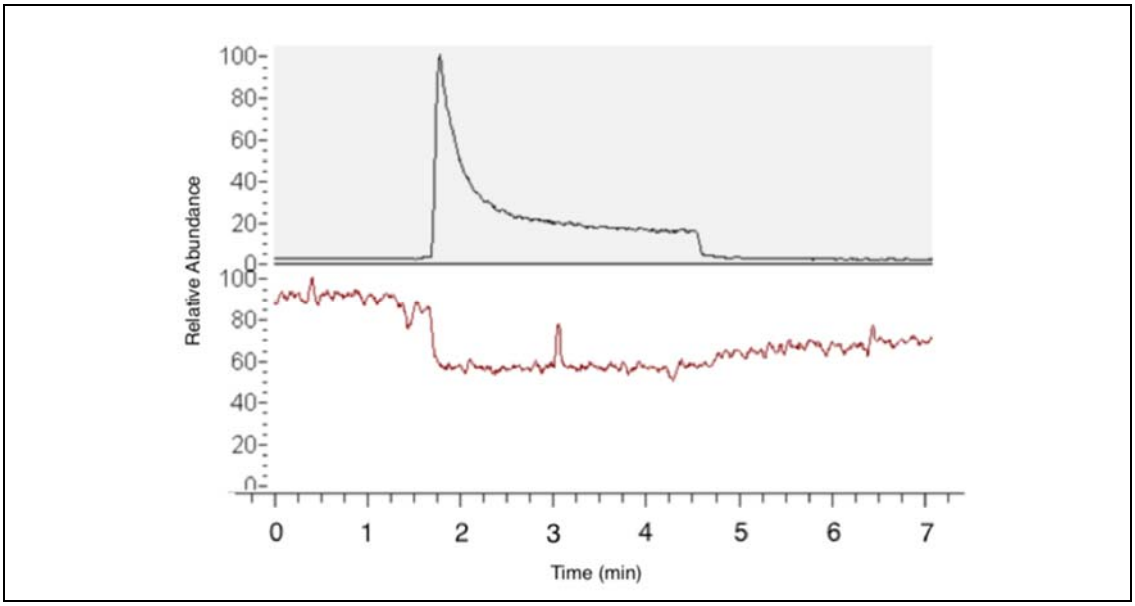

Figure 23: Extracted ion trace for sample 11 showing m/z 157.1223, oak lactone (upper pane) and the continually infused internal standard m/z 160.1411, d_3-oak-lactone (lower pane).

4.4.3 High Sensitivity Detection of Oak-lactone Using DBDI-MS

To examine the sensitivity of the DBDI-MS approach for analysis of oak wood volatiles a five-point calibration curve was conducted for one of the primary oak VOC's, oak-lactone. The calibration curve was based on the introduction of gas phase concentrations of oak lactone ranging from 18 ppt to 1.8 ppb. The resultant

calibration curve based on the m/z 157→139 SRM transition (Figure 24) demonstrates the high sensitivity of the DBDI-MS approach. The absolute gas-phase detection limits show that oak lactone can be detected at low parts-per-trillion levels using DBDI-MS. This is below the sensory threshold for oak lactones which is reported to be in the part-per-billion (20-370 µg/L) range[15].

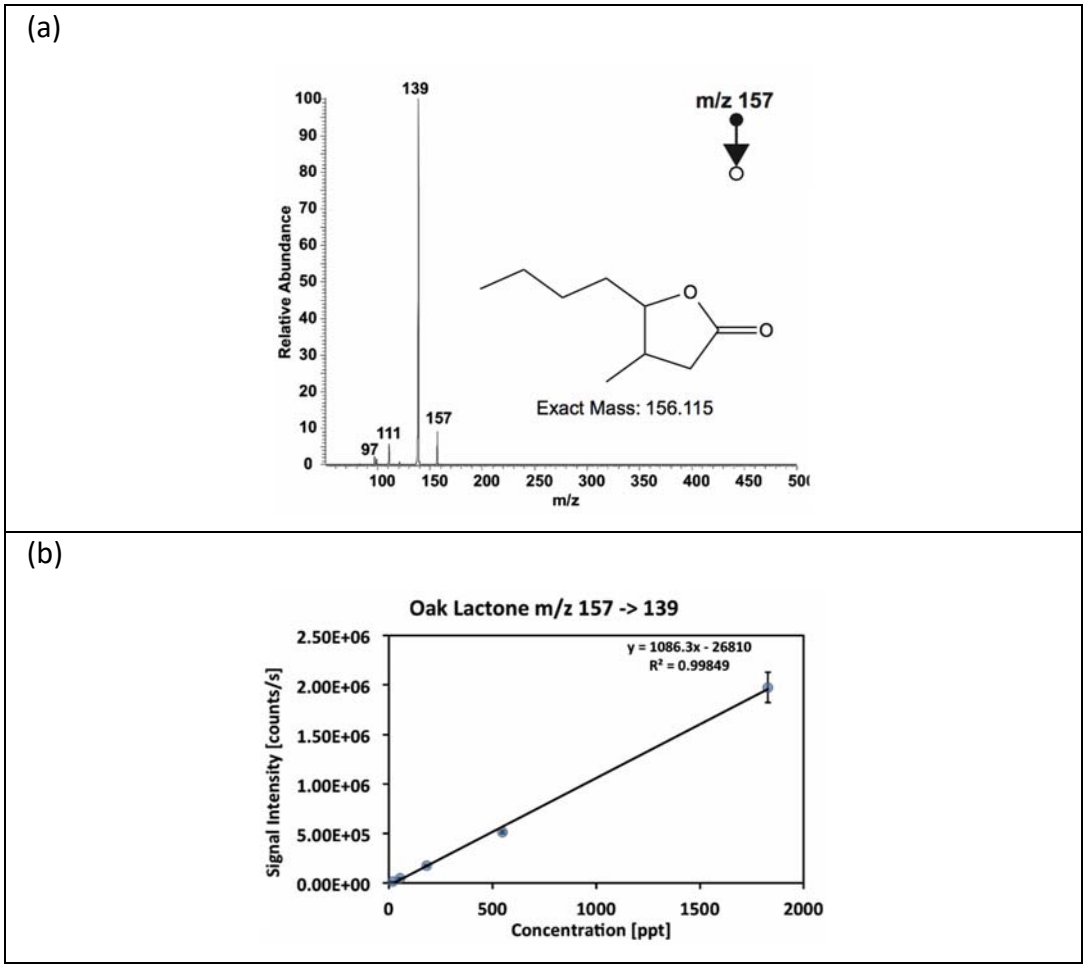

Figure 24: Quantification of oak lactone by DBDI-MS/MS. (a) MS/MS spectra for oak lactone and (b) corresponding calibration plot monitoring transition m/z 157 – m/z 139 performed on an LCQ Deca XP ion trap mass spectrometer.

4.4.4 High Resolution DBDI-MS Analysis of Oak Wood Volatiles

In addition to exceptional sensitivity, a second advantage of the instrumentation used in this work is the high-resolution mass spectrometry data. The maximum resolution of the Orbitrap XL used in this work was >100,000 at m/z 400, greatly exceeding the highest resolution offered by current PTR-MS instrumentation e.g. 5,000 – 10,000, Ionicon Analytik GmbH (Innsbruck, Austria) and Tofwerk AG (Thun, Switzerland) respectively. An example spectrum is displayed in Figure 8a-c below, showing the complex nature of the VOC

fingerprint from a French oak wood sample. The benefit of high resolution is exemplified by the seven peaks within a 0.3 Da window (225.0000 – 225.3000 *m/z*) in Figure 23 (c).

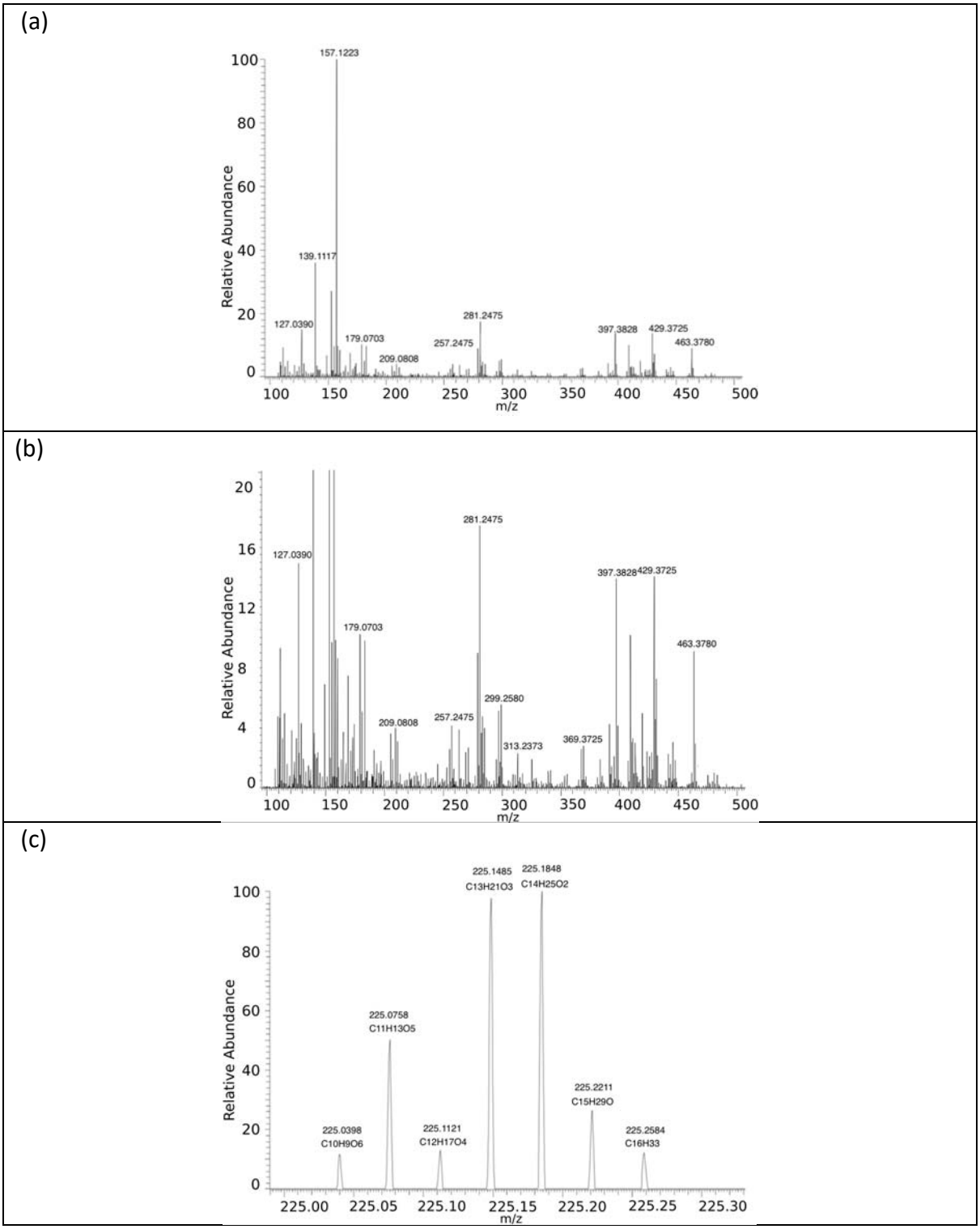

Figure 25 (a, b, and c): Positive mode TD-DBDI-Orbitrap MS spectra of untoasted oak wood calculated by averaging the spectra over the first 10s of sample introduction showing (a) typical mass spectrum between 100 and 500 m/z, (b) mass spectrum between 100 and 500 m/z zoomed in to 20% relative abundance, (c) Five peaks in the zoomed region of 225.00 to 225.30 m/z.

Figure 26 shows a simulated mass spectrum using the highest (theoretical) resolution available via PTR-MS (R = 10,000) versus a resolution set to 60,000 – readily achievable with the Orbitrap XL mass spectrometer. As shown in Figure 26 a resolution of 10,000 would not resolve the seven peaks detected by the TD-DBDI-ORBITRAP-MS approach at m/z 225.

4.4.5 TD-DBDI-MS Reveals European Oak Wood's Chemical Complexity and Diversity

The average mass spectrum acquired over 1-10s of analysis provides a chemical fingerprint of the oak wood in its untoasted state. Example spectra from two different oak wood samples (both of French origin) are displayed in Figure 27. The high-resolution mass spectra demonstrate both the chemical complexity and the natural variation in oak wood volatiles with 573 peaks and 388 peaks observed for sample 13A and sample 3A respectively. The MS spectra for these samples are strikingly different with sample 13A dominated by m/z 157.1223 (protonated $C_9H_{16}O_2$) oak lactone, whereas the MS spectra of sample 3A is dominated by m/z 160.1411 the internal standard (d_3-oak-lactone, same concentration in both spectra). In sample 3A, m/z 153.0546 protonated $C_8H_8O_3$ (tentatively assigned to vanillin) is among the most prominent peaks related to the oak sample.

287 peaks were observed in the volatile fingerprint common to all oak wood (n=15) samples measured by TD-DBDI-Orbitrap-MS (average spectra 1-10s). Of the numerous peaks detected across a range of compound classes including aldehydes, phenols, lactones and norisoprenoids, 23 were tentatively assigned to known oak wood volatile compounds (Table 7) based on their elemental composition derived from accurate mass and based on previous literature.

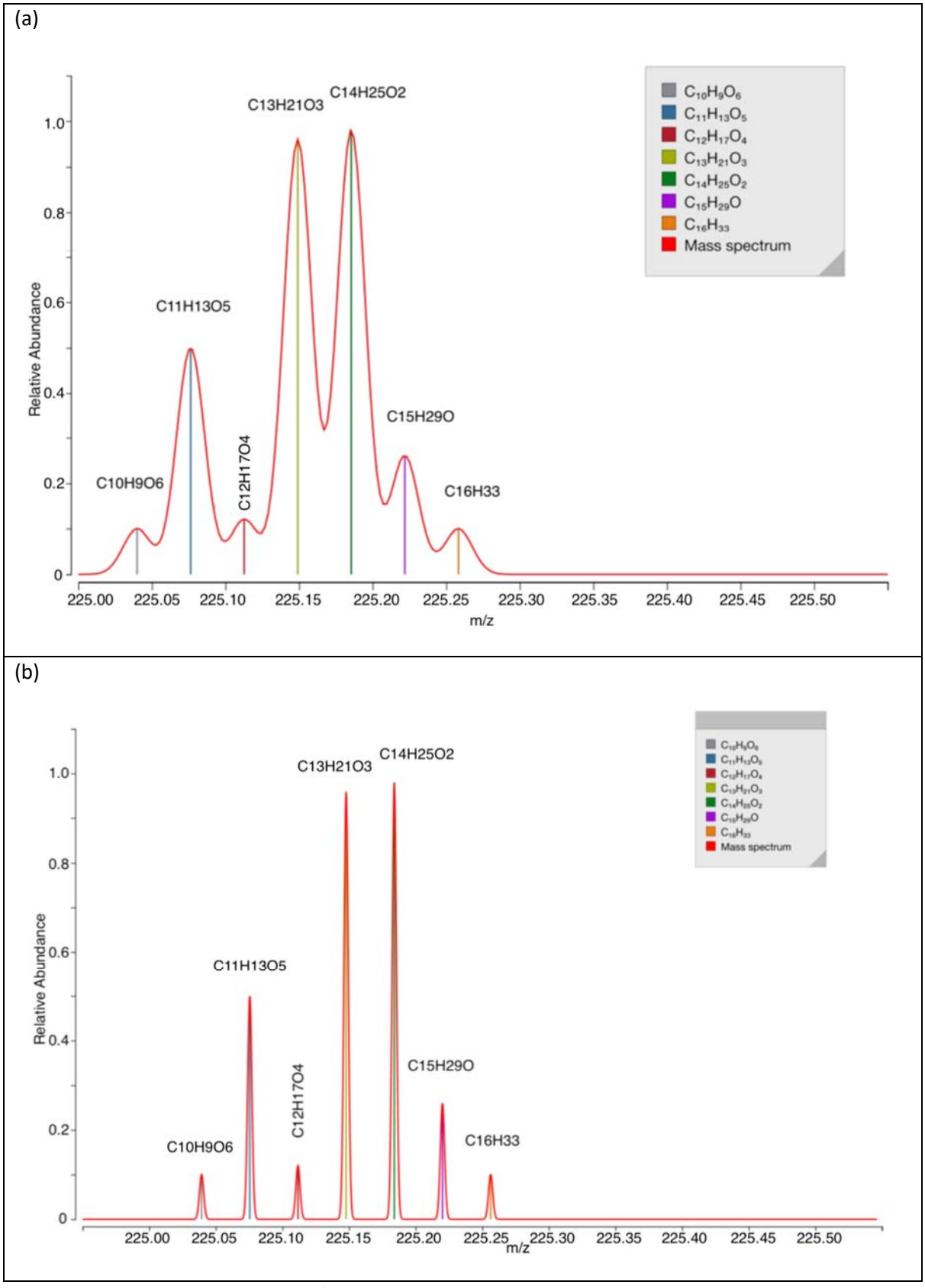

Figure 26: Simulated mass spectra for the 7 peaks detected in the 225.0000 to 225.3000 Da range, showing (a) Mass spectrum at resolution = 10,000. (b) Mass spectrum at resolution = 60,000. Spectra simulated using Prot pi[16].

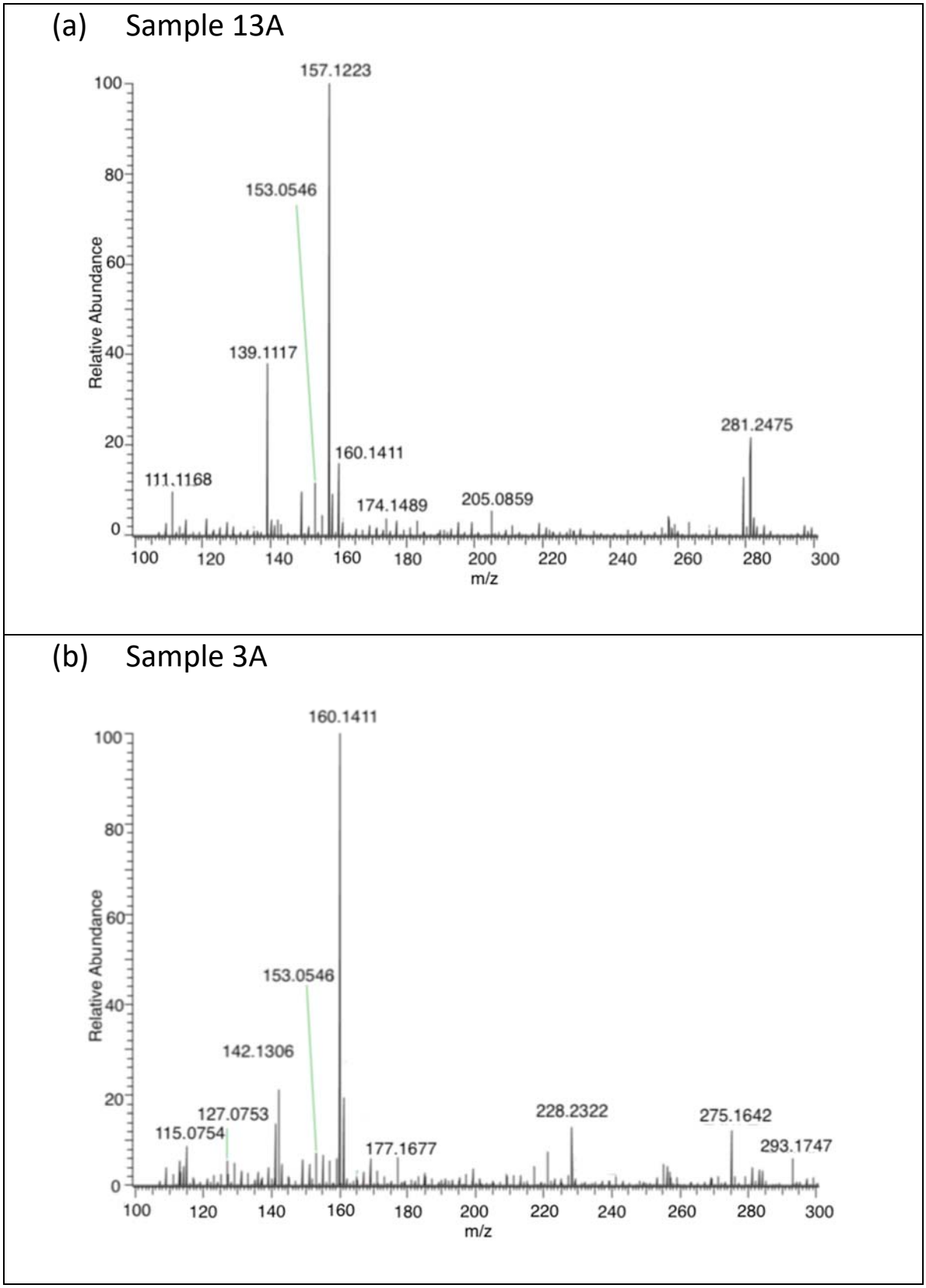

Figure 27: Positive mode TD-DBDI-Orbitrap-MS spectra of samples 13A and 3A showing mass spectrum between 100 and 300 *m/z*.

Table 7: Subset of molecular formulae of important oak wood aroma compounds observed across all samples. Associated absolute errors of assignment in ppm and tentative compound identification based on known chemistry of oak wood volatiles.

Measured m/z (Da) $[M+H]^+$	Elemental Composition [M]	Exact mass (Da) $[M+H]^+$	Mass accuracy (ppm)	Possible compound assignment
111.0441	$C_6H_6O_2$	111.04406	0.0	5-methyl-furfural
123.0804	$C_8H_{10}O$	123.08044	0.1	4-ethylphenol*
125.0597	$C_7H_8O_2$	125.05971	0.1	guaiacol
127.0390	$C_6H_6O_3$	127.03897	0.1	HMF, maltol*
139.0753	$C_8H_{10}O_2$	139.07536	0.1	4-methylguaiacol*
141.1273	$C_9H_{16}O$	141.12739	0.6	trans-2-Nonenal
143.0339	$C_6H_6O_4$	143.03389	0.2	5-Hydroxymaltol
145.0495	$C_6H_8O_4$	145.04954	0.2	DDMP
151.0753	$C_9H_{10}O_2$	151.07536	0.1	4-vinylguaiacol
153.0546	$C_8H_8O_3$	153.05462	0.0	vanillin
153.0910	$C_9H_{12}O_2$	153.09101	0.1	4-ethylguaiacol
157.1223	$C_9H_{16}O_2$	157.12231	0.0	oak lactone
165.0910	$C_{10}H_{12}O_2$	165.09101	0.2	eugenol*
179.0703	$C_{10}H_{10}O_3$	179.07027	0.1	coniferaldehyde
183.0652	$C_9H_{10}O_4$	183.06519	0.1	syringaldehyde*
183.1015	$C_{10}H_{14}O_3$	183.10157	0.2	4-ethylsyringol*
191.1430	$C_{13}H_{18}O$	191.14304	0.2	megastigmatrienone*
193.1587	$C_{13}H_{20}O$	193.15869	0.1	β-ionone / vitispirane
207.1379	$C_{13}H_{18}O_2$	207.13796	0.3	4-oxo-β-ionone
209.0808	$C_{11}H_{12}O_4$	209.08084	0.2	sinapaldehyde
209.1536	$C_{13}H_{20}O_2$	209.15361	0.2	3-oxo-α-ionol*
211.1692	$C_{13}H_{22}O_2$	211.16926	0.1	blumenol C*
225.1485	$C_{13}H_{20}O_3$	225.14852	0.1	Blumenol A, Vomifoliol

*Note: * indicates there are other isobaric compounds that have previously been identified in oak wood and thus are other potential candidates*

Interestingly, protonated $C_{13}H_{18}O$ (tentatively assigned to megastigmatrienone) and protonated $C_{13}H_{20}O$, $C_{13}H_{18}O_2$, $C_{13}H_{20}O_2$, $C_{13}H_{22}O_2$, $C_{13}H_{20}O_3$ (tentatively assigned to norisoprenoid compounds, Table 7) were observed in the high-resolution TD-DBDI-MS spectra. These important oak wood aroma compounds impart tobacco and floral notes to oak-aged wine and were not detected in the previous work utilising PTR-MS for real-time monitoring of oak wood (see Chapter 3).

Possible reasons that norisoprenoid compounds were detected by TD-DBDI-MS and not by the PTR-MS methodology may relate to differences in the limits of detection (LOD) of the two methods. However, the different volumes of the thermal desorption setups and the different sample formats (200 mm board sections versus shavings) mean that it is difficult to quantify the effective concentration of sample gas delivered to the ion source in each study.

4.4.6 Multivariate Statistical Analysis of the TD-DBDI-MS Data Highlights Variation in Oak Wood Aroma Profiles

Figure 28 shows a principal component analysis (PCA) biplot showing both the observations and the influencing variables for the untoasted oak wood VOC fingerprint based on an average of the first ten seconds in the TDU. The 16 impact aroma compounds that contribute strongly to aroma in oak-aged wine are used as the variables. A squared cosine of greater than or equal to 0.5 between indicates a strong influence of the variable on the PC[18] (Table 8). The spread of the observations over each of the four quadrants indicates the high degree of variability in oak wood VOC composition as reported in previous research[19–21].

Principal component 1 (PC1) accounts for 63% of the observed variation in the data. It is observed that PC1 is linked to 13 of the 16 aroma compounds as shown by the squared cosine of the variables in Table 8. Oak boards with high content of the 13 influencing VOC's are in the positive direction of PC1 (Figure 26a), whilst those with low content (for the 13 VOC's) are generally in the negative direction.

PC2 is strongly linked to m/z 127.0390 (Table 8), protonated [$C_6H_6O_3$] tentatively assigned to HMF / maltol, contributing 27% to PC2 (Table 9). PC3 is strongly linked to m/z 157.1223, protonated [$C_9H_{16}O_2$] i.e. oak lactone, contributing 68% to PC3. PC4 is strongly linked to m/z 165.0910, protonated [$C_{10}H_{12}O_2$] eugenol / iso-eugenol, contributing 51% to PC4.

(a)

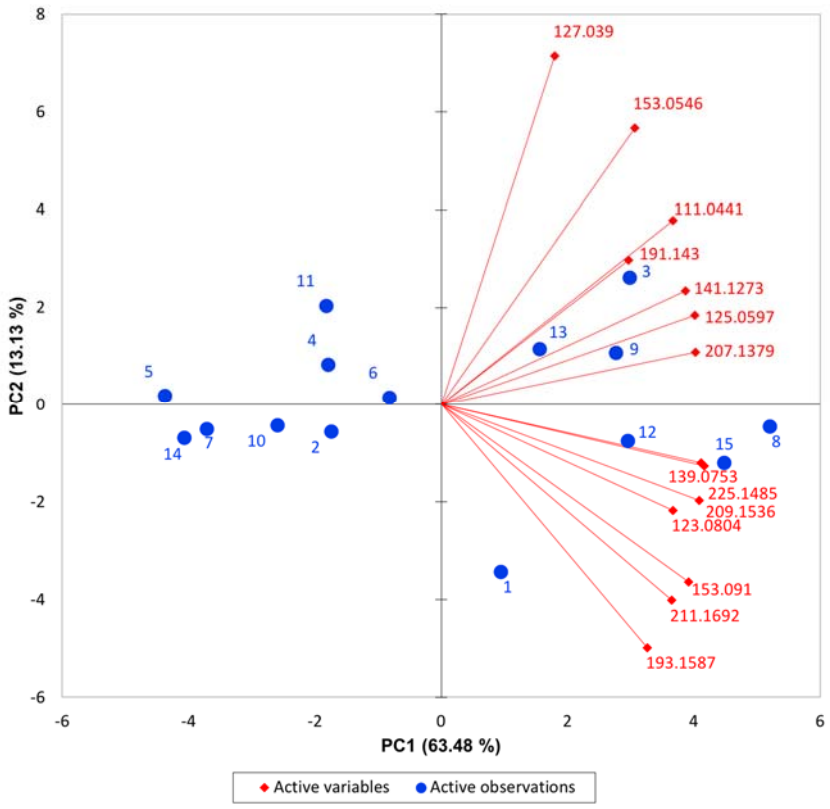
127.039
153.0546
111.0441
191.143
141.1273
125.0597
207.1379
139.0753
225.1485
209.1536
123.0804
153.091
211.1692
193.1587
PC2 (13.13 %)
PC1 (63.48 %)
Active variables
Active observations

(b)

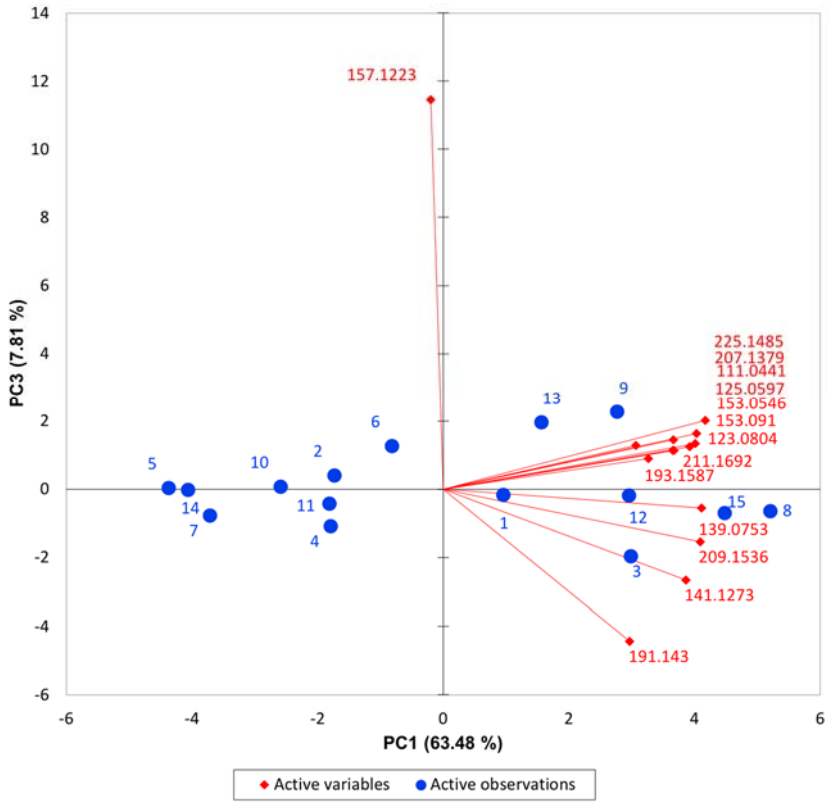
157.1223
225.1485
207.1379
111.0441
125.0597
153.0546
153.091
123.0804
211.1692
193.1587
139.0753
209.1536
141.1273
191.143
PC3 (7.81 %)
PC1 (63.48 %)
Active variables
Active observations

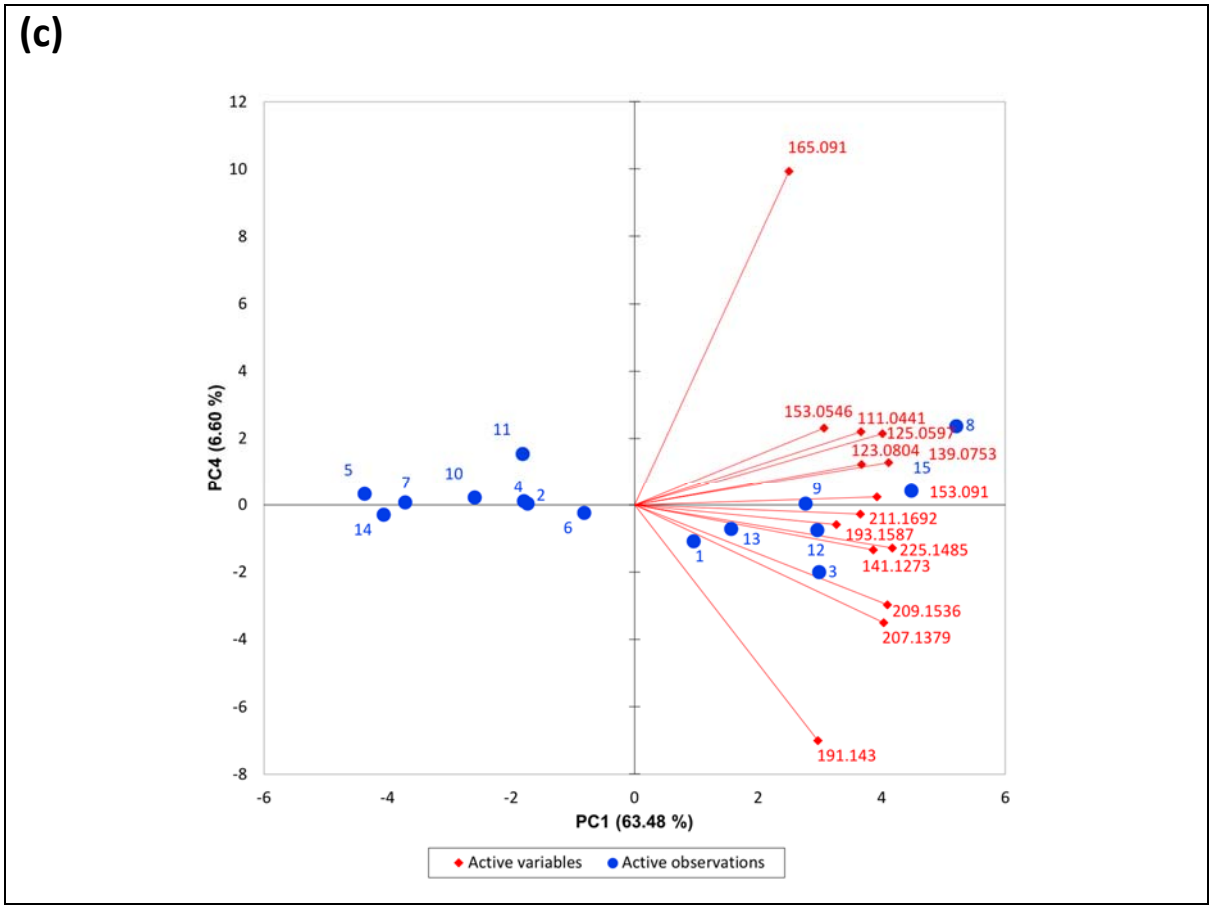

Figure 28: Principal Components Analysis (16 impact aroma compounds as variables) of the untoasted oak wood aroma fingerprints based on inter-quartile range normalised spectra averaged over the three replicates for each sample. (a) PC1 Vs PC2, (b) PC1 Vs PC3, (c) PC1 Vs PC4.

Table 8: Squared cosine of the variables for the PCA (16 impact aroma compounds as variables) of the untoasted oak wood aroma fingerprints. Values in bold correspond for each variable to the factor for which the squared cosine is the largest.

Variable	PC1	PC2	PC3	PC4
111.0441	**0.710**	0.156	0.013	0.026
123.0804	**0.712**	0.052	0.008	0.008
125.0597	**0.851**	0.037	0.011	0.025
127.0390	0.170	**0.557**	0.051	0.003
139.0753	**0.893**	0.016	0.002	0.009
141.1273	**0.789**	0.060	0.046	0.010
153.0546	**0.496**	0.351	0.011	0.029
153.0910	**0.812**	0.145	0.010	0.000
157.1223	0.002	0.107	**0.853**	0.007
165.0910	0.329	0.004	0.043	**0.542**
191.1430	**0.466**	0.096	0.128	0.270
193.1587	**0.564**	0.272	0.005	0.002
207.1379	**0.858**	0.013	0.017	0.067
209.1536	**0.883**	0.043	0.015	0.049
211.1692	**0.703**	0.176	0.008	0.000
225.1485	**0.917**	0.018	0.026	0.009

Table 9: Contribution of the variables (%) to each principal component. The variables with greatest contribution are shown in bold.

Measured m/z (Da) $[M+H]^+$	Elemental composition	Tentative compound assignment	Principal component 1 (63%)	Principal component 2 (13%)	Principal component 3 (8%)	Principal component 4 (7%)
111.0441	C6H6O2	5-methyl-furfural	7.0	7.4	1.1	2.5
123.0804	C8H10O	4-ethylphenol*	7.0	2.5	0.7	0.8
125.0597	C7H8O2	guaiacol	8.4	1.8	0.9	2.4
127.0390	C6H6O3	HMF, maltol*	1.7	**26.5**	4.1	0.3
139.0753	C8H10O2	4-methylguaiacol*	8.8	0.7	0.2	0.8
141.1273	C9H16O	trans-2-Nonenal	7.8	2.9	3.7	0.9
153.0546	C8H8O3	vanillin	4.9	16.7	0.9	2.8
153.0910	C9H12O2	4-ethylguaiacol	8.0	6.9	0.8	0.0
157.1223	C9H16O2	oak lactone	0.0	5.1	**68.3**	0.6
165.0910	C10H12O2	eugenol*	3.2	0.2	3.4	**51.2**
191.1430	C13H18O	megastigmatrienone*	4.6	4.6	10.2	25.6
193.1587	C13H20O	β-ionone / vitispirane	5.6	12.9	0.4	0.2
207.1379	C13H18O2	4-oxo-β-ionone	8.5	0.6	1.4	6.4
209.1536	C13H20O2	3-oxo-α-ionol*	8.7	2.0	1.2	4.6
211.1692	C13H22O2	blumenol C*	6.9	8.4	0.7	0.0
225.1485	C13H20O3	Blumenol A, Vomifoliol	**9.0**	0.8	2.1	0.9

*Note: * indicates there are other isobaric compounds that have previously been identified in oak wood and thus are other potential candidates exist*

An agglomerative hierarchical clustering (AHC) analysis using the 16 impact oak aroma compounds as variables grouped the oak samples into three clusters (Figure 29). The compound profile plot (Figure 30) shows the aroma composition associated with each cluster. Cluster one (blue) consisting of six samples grouped oak wood with higher concentrations of furanic and norisoprenoid compounds including 5MF and HMF (m/z 111.0441 and 127.0390), megastigmatrienone (m/z 191.1430), β-ionone (m/z 193.1587) and other norisoprenoid related peaks at m/z 209.1536, 211.1692 and 225.1485. Oak lactone (m/z 157.1223) levels were observed to be lowest for this cluster.

Cluster two (red) consisting of seven samples generally exhibited the opposite trend being characterised by high levels of oak lactone and low levels of the furanic and norisoprenoid related peaks. Cluster three (green) consisting of two samples was characterised by the

highest levels of vanillin and generally intermediate levels of oak lactone and the remaining impact aroma compounds.

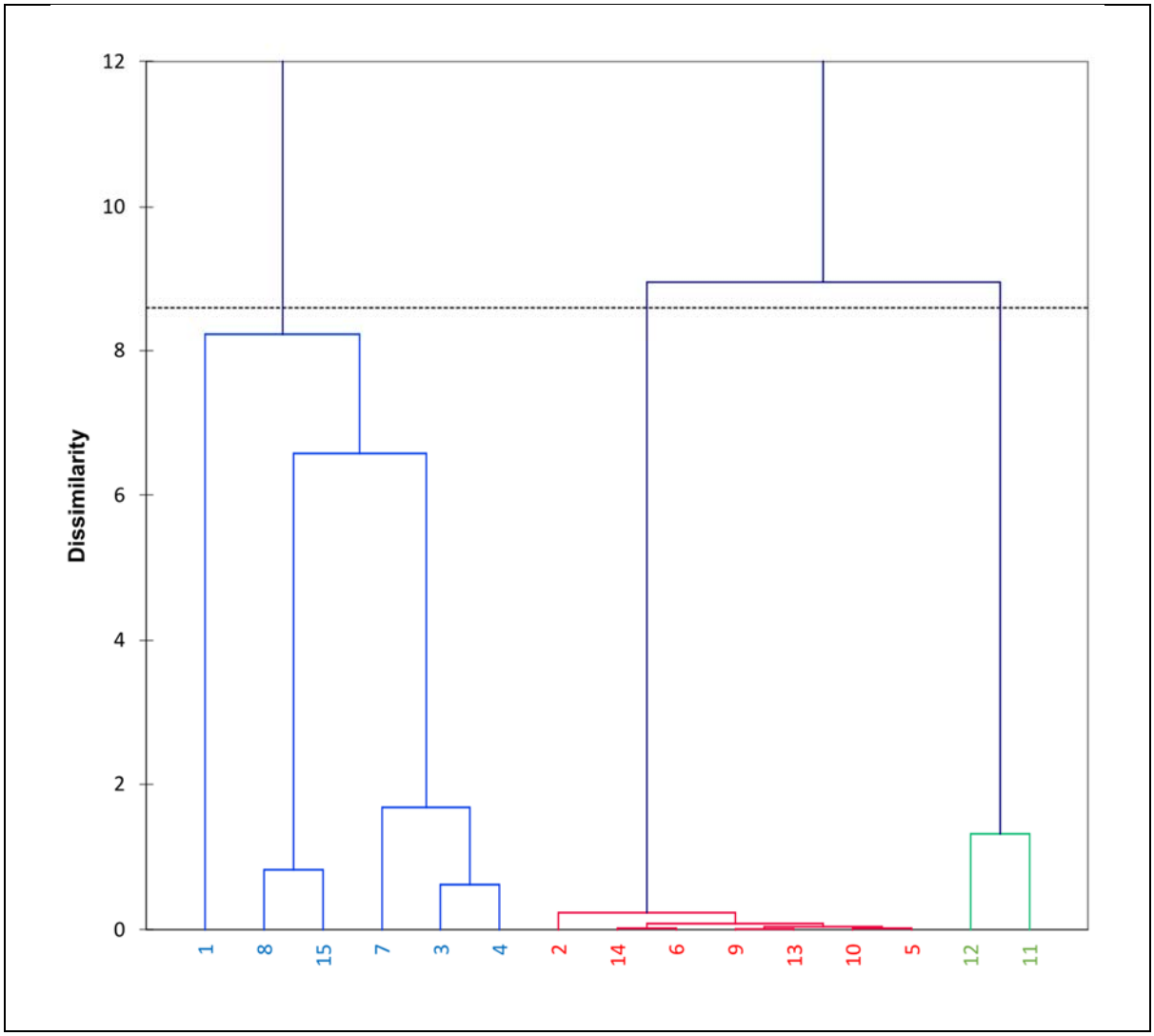

Figure 29: Agglomerative hierarchical clustering dendrogram based on the 0-10 s average mass spectrum using inter-quartile range normalised spectra averaged over the three replicates for each sample with 16 impact aroma compounds used as variables

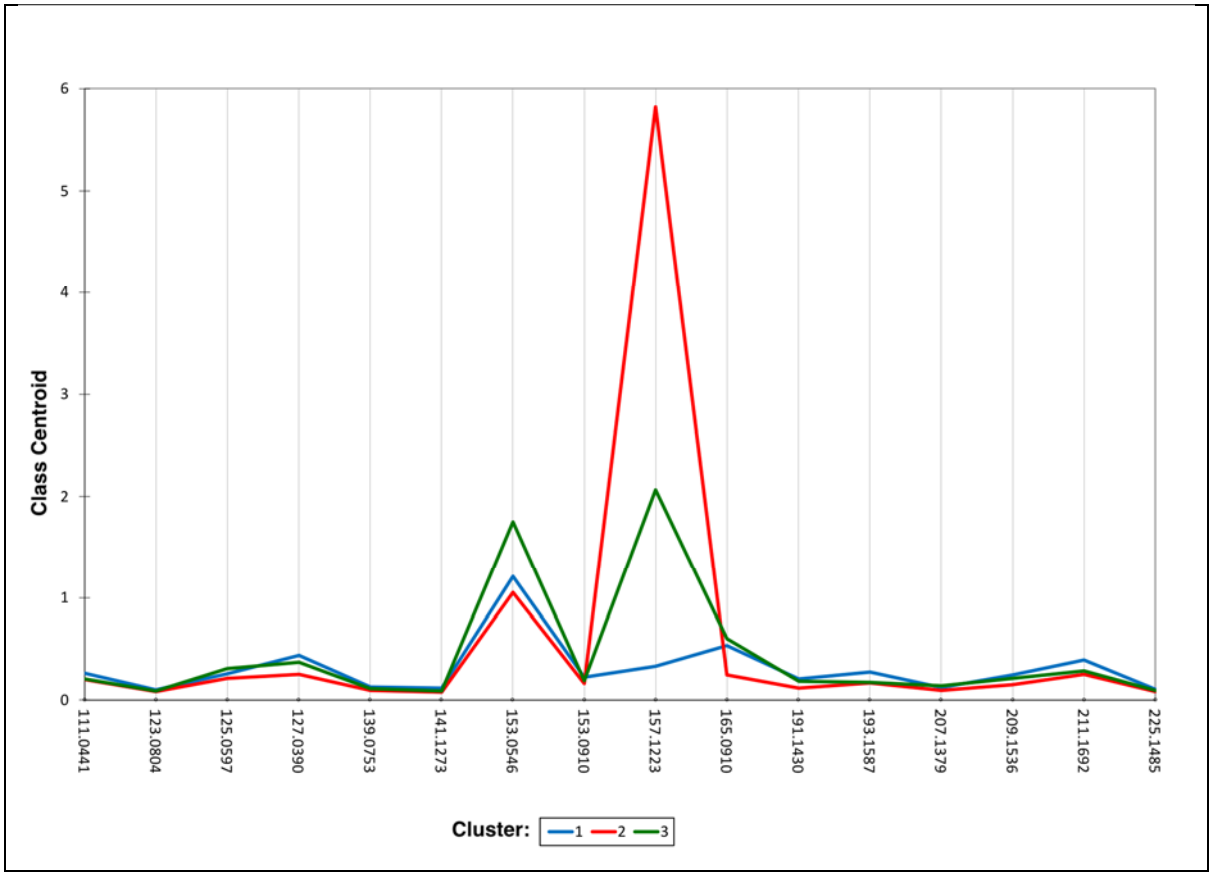

Figure 30: Profile plot showing the aroma composition associated with each cluster, all plots are based on the 0-10 s average spectrum using inter-quartile range normalised spectra averaged over the three replicates for each sample with 16 impact aroma compounds used as variables.

4.4.7 Real-time Monitoring of Oak Wood Toasting by TD-DBDI-MS

In the cooperage process oak wood boards (staves) undergo a toasting process prior to final construction of the wine barrel. This toasting process leads to a dramatic alteration of the wood chemistry through hydrothermolysis and pyrolysis reactions[22]. The analysis of oak wood volatiles is traditionally based on gas chromatography methods. Such “offline” approaches are of limited utility for the analysis of highly dynamic processes such as coffee roasting or oak wood toasting. Consequently, direct mass spectrometry approaches are highly advantageous as previously discussed in Chapter 3.

In the previous study (Chapter 3) an oven coupled to a PTR-MS (resolving power 5,000) accommodating large solid sections of oak wood (200 mm) was used to monitor the oak wood toasting process. The current study employs a novel, compact thermal desorption device coupled to a highly sensitive DBDI ion source and high-resolution Orbitrap mass spectrometer (resolving power > 60,000) to rapidly analyse VOC’s from oak wood shavings.

By leaving the oak sample in the TDU for several minutes the thermally induced changes indicative of the toasting process could be observed with high temporal resolution (1 Hz). Figure 29 shows the time-intensity profiles for selected oak wood VOC's over a five min period with the effective desorption temperature of 200 ^{o}C.

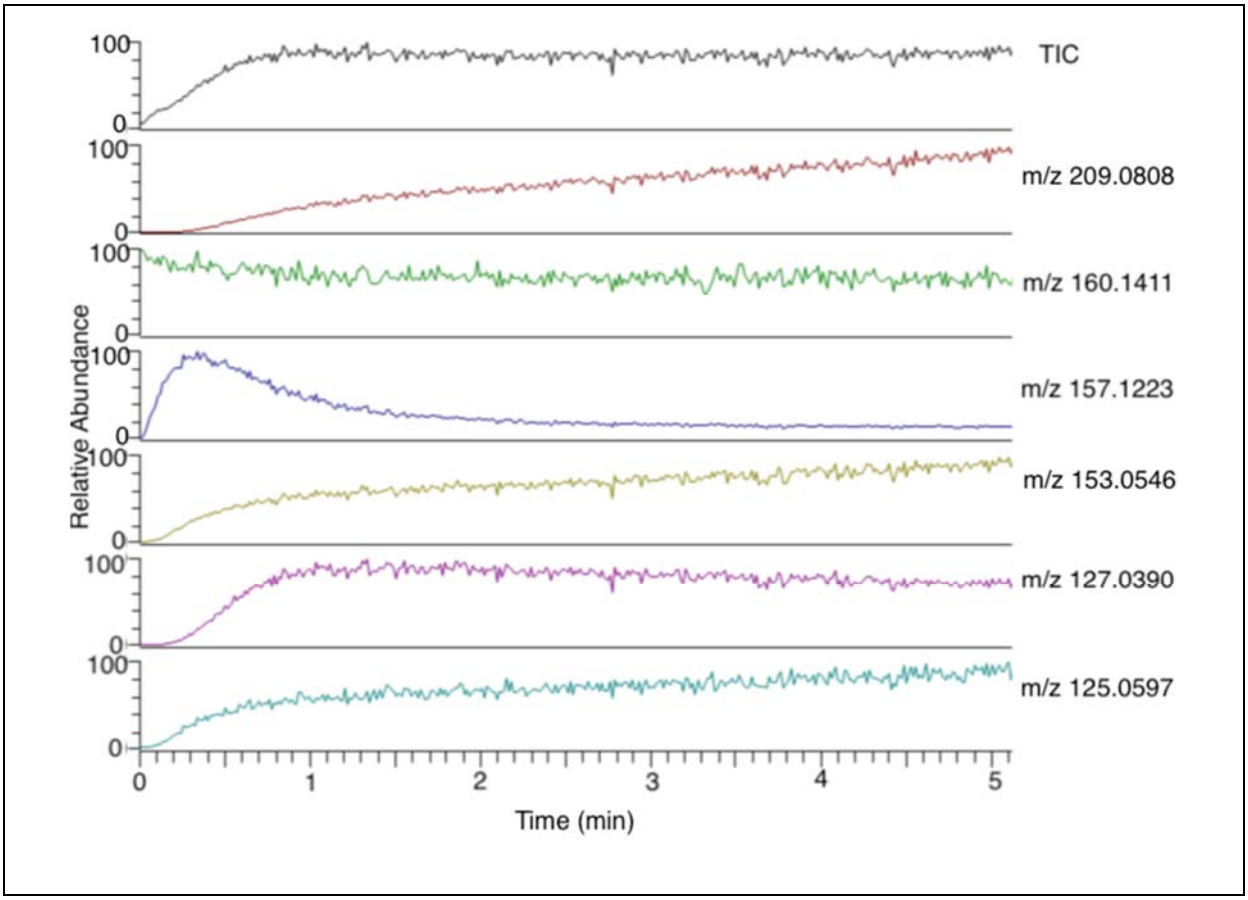

Figure 31: Time-intensity profiles for oak wood VOC's as measured by TD-DBDI-Orbitrap-MS over a five minute time period with an effective desorption temperature of 200 ^{o}C. Oak samples were inserted into the TDU at time zero.

Figure 31 shows time-intensity plots for selected m/z values (m/z 209.0808, Sinapaldehyde; m/z 160.1411 d_3-oak lactone standard, m/z 157.1223, oak lactone; m/z 153.0546, vanillin; m/z 127.0390, HMF / maltol and m/z 125.0597, guaiacol. Lignin derived compounds (m/z 209.0808, 153.0546 and 125.0597) increase with time. Oak lactone (m/z 157.1223) is initially volatilised reaching a maximum and then decreases (a balance between volatilisation and generation from lactone glycosidic precursor as discussed in Chapter 3). The furanic compound (m/z 127.0390) reaches a maximum at early stage then slowly declines in intensity.

Figure 32 shows the changes in the mass spectrum over time, indicating the evolution of different compounds as the toasting process progresses. In the first 30s the spectrum for sample 13 is dominated by *m/z* 157.1223 (oak lactone) which is the prominent base peak. In the following 30-60s, *m/z* 127.0390 is the base peak, tentatively assigned to the furanic compounds HMF and / or maltol derived from the degradation of hemicellulose. From 60-120 s further changes are observed in the spectra with *m/z* 179.0703 (tentatively assigned to coniferaldehyde and derived from lignin degradation) becoming the base peak.

The observed evolution of toasting related VOC's exhibits a transition from compounds already present in the untoasted oak wood such as oak lactone, towards compounds derived from thermal degradation of the wood polymers (e.g. furanic compounds derived from hemicellulose, and phenolic aldehydes from lignin degradation). These observations are in agreement with the findings of the PTR-MS study (Chapter 3) and fits with the general understanding that lignin is the most thermally stable wood polymer[23].

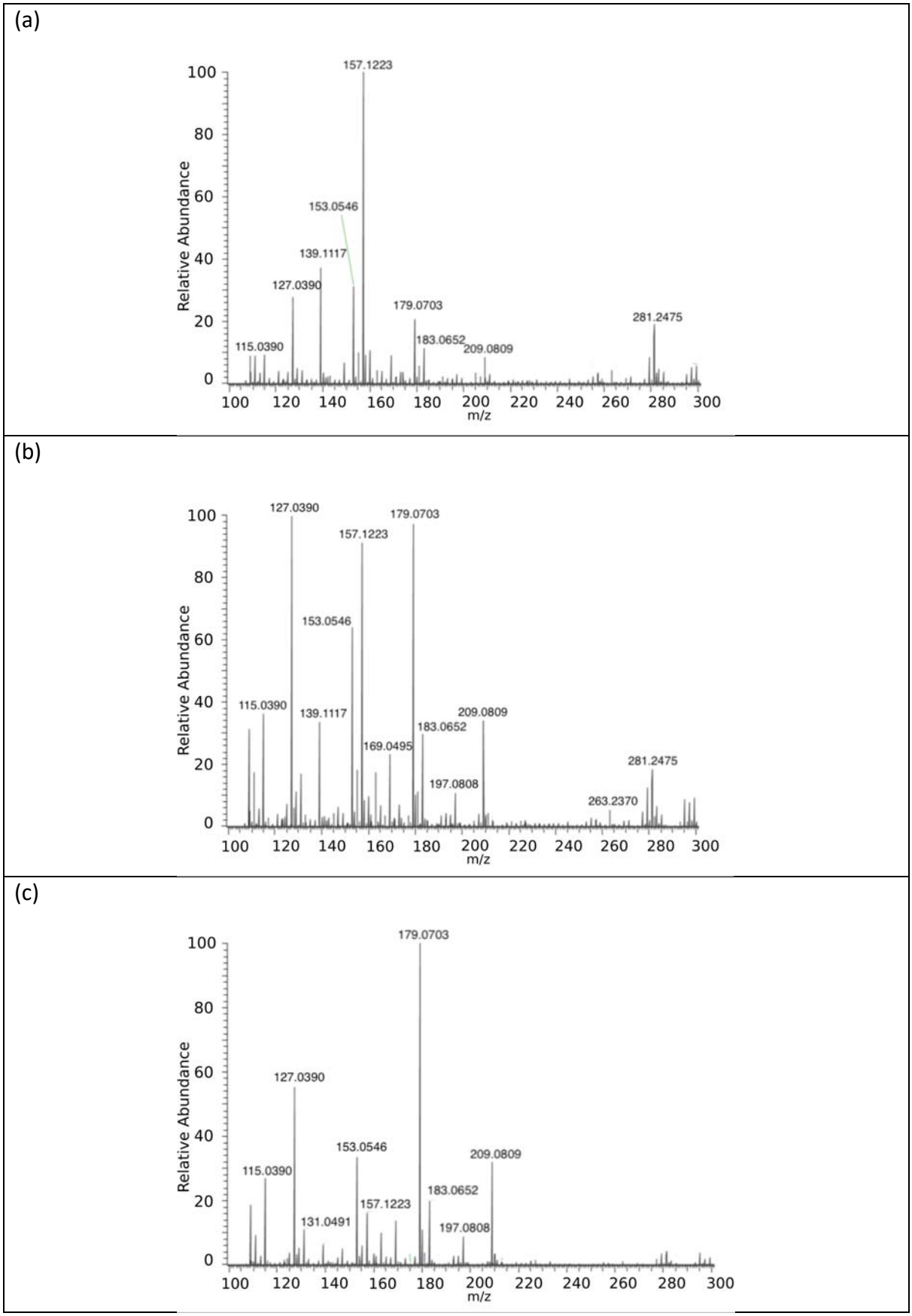

Figure 32: Average TD-DBDI-Orbitrap-MS spectra of sample 13 at (a) 0-30 s, (b) 30-60 s and (c) 60-120 s showing evolution of the oak toasting process through time.

4.5 Conclusion

A novel ambient mass spectrometry approach based on TD-DBDI-MS has been developed for the analysis of oak wood volatiles. The method does not require laborious sample preparation steps or lengthy chromatography separations associated with traditional (GC) approaches.

This study showed how the TD-DBDI-MS system could be used to rapidly analyse oak wood VOC's by simply placing a wood shaving in a pre-heated thermal desorption unit, providing results within seconds. The sample slider allowed oak shavings to be introduced and removed rapidly without altering the desorption temperature. Furthermore, the oak toasting process could be monitored in real-time by leaving the oak sample to desorb in the TDU unit for several minutes. The limit of detection for oak-lactone was 26 ppt on an LCQ Deca ion-trap MS demonstrating the high sensitivity of the approach.

The ability to easily couple the DBDI source to any mass analyser with an atmospheric pressure interface, provides analytical flexibility and overcomes limitations with alternative direct MS approaches such as PTR-MS that are currently restricted to unit mass resolution quadrupoles or, time-of-flight analysers with resolution < 10,000. Complex spectra were observed in the oak wood samples by the DBDI-Orbitrap-MS approach, exemplified by seven peaks found within a 0.3 Da window for *m/z* 225.

Whilst norisoprenoid related peaks were detected by the DBDI-MS and not by the previous PTR-MS study, it is not clear whether this observation was due to differences in the sampling setup, ion source sensitivity or different ionisation mechanisms.

Ion suppression phenomena could be minimized and accounted for by:

(i) diluting the sample gas

(ii) continuous infusion of a suitable chemical analogue as an internal standard (in this case d_3-oak-lactone)

The spectra observed by TD-DBDI-MS generally agree with the previous thermal desorption PTR-MS findings (Chapter 3), i.e. inherent compounds such as oak lactone dominate the initial spectra, giving way to furanic compounds derived from hemicellulose degradation and

ultimately to phenolic compounds derived from lignin degradation as the toasting process advances.

Based on the observations in this study I believe that the TD-DBDI-MS approach provides a simple, sensitive and selective analytical approach for the rapid analysis of oak wood aroma chemistry.

References

1. Jackson, R. S. in *Wine Science (Third Edition)* (ed. Jackson, R. S.) 418–519 (Academic Press, 2008). doi:http://dx.doi.org/10.1016/B978-012373646-8.50011-1
2. Takáts, Z., Wiseman, J. M., Gologan, B. & Cooks, R. G. Mass Spectrometry Sampling Under Ambient Conditions with Desorption Electrospray Ionization. *Science (80-.).* **306,** 471–473 (2004).
3. Monge, M. E., Harris, G. a., Dwivedi, P. & Fernandez, F. M. Mass spectrometry: Recent advances in direct open air surface sampling/ionization. *Chem. Rev.* **113,** 2269–2308 (2013).
4. Chen, J., Tang, F., Guo, C., Zhang, S. & Zhang, X. Plasma-based ambient mass spectrometry: a step forward to practical applications. *Anal. Methods* **9,** 4908–4923 (2017).
5. Nudnova, M. M., Zhu, L. & Zenobi, R. Active capillary plasma source for ambient mass spectrometry. *Rapid Commun. Mass Spectrom.* **26,** 1447–1452 (2012).
6. Wolf, J., Schaer, M., Siegenthaler, P. & Zenobi, R. Direct Quanti fi cation of Chemical Warfare Agents and Related Compounds at Low ppt Levels: Comparing Active Capillary Dielectric Barrier Discharge Plasma Ionization and Secondary Electrospray Ionization Mass Spectrometry. (2015).
7. Mirabelli, M. F., Wolf, J. C. & Zenobi, R. Direct Coupling of Solid-Phase Microextraction with Mass Spectrometry: Sub-pg/g Sensitivity Achieved Using a Dielectric Barrier Discharge Ionization Source. *Anal. Chem.* **88,** 7252–7258 (2016).
8. Mirabelli, M. F., Wolf, J. C. & Zenobi, R. Pesticide analysis at ppt concentration levels: coupling nano-liquid chromatography with dielectric barrier discharge ionization-mass spectrometry. *Anal. Bioanal. Chem.* **408,** 3425–3434 (2016).
9. Mirabelli, M. F., Wolf, J.-C. & Zenobi, R. Atmospheric pressure soft ionization for gas chromatography with dielectric barrier discharge ionization-mass spectrometry (GC-DBDI-MS). *Analyst* **142,** 1909–1915 (2017).
10. Schütz, A. *et al.* Dielectric Barrier Discharge Ionization of Perfluorinated Compounds. *Anal. Chem.* **87,** 11415–11419 (2015).
11. Cody, R. B., Laramée, J. A. & Durst, H. D. Versatile New Ion Source for the Analysis of Materials in Open Air under Ambient Conditions. *Anal. Chem.* **77,** 2297–2302 (2005).
12. Wilkinson, A. D. M. and A. *IUPAC. Compendium of Chemical Terminology, (the 'Gold Book').* (Blackwell Scientific Publications, 1997).
13. Kessner, D., Chambers, M., Burke, R., Agus, D. & Mallick, P. ProteoWizard: Open source software for rapid proteomics tools development. *Bioinformatics* **24,** 2534–2536 (2008).
14. Bald, T. *et al.* pymzML - Python module for high throughput bioinformatics on mass spectrometry data. *Bioinformatics* **28,** 1–2 (2012).
15. Brown, R. C., Sefton, M. A., Taylor, D. K. & Elsey, G. M. An odour detection threshold determination of all four possible stereoisomers of oak lactone in a white and a red wine. *Aust. J. Grape Wine Res.* **12,** 115–118 (2006).
16. Josuran, R. Prot pi. Available at: https://www.protpi.ch/Calculator/MassSpecSimulator. (Accessed: 21st April 2018)

17. Wolf, J. C. *et al.* A Radical-Mediated Pathway for the Formation of [M + H]+ in Dielectric Barrier Discharge Ionization. *J. Am. Soc. Mass Spectrom.* **27,** 1468–1475 (2016).

18. David, C. C. & Jacobs, D. J. Principal Component Analysis: A Method for Determining the Essential Dynamics of Proteins. *Methods Mol. Biol.* **1084,** 193–226 (2014).

19. Doussot, F., Jéso, B. De, Quideau, S. & Pardon, P. Extractives content in cooperage oak wood during natural seasoning and toasting; influence of tree species, geographic location, and single-tree effects. *J. Agric. Food Chem.* **50,** 5955–5961 (2002).

20. Prida, A. & Puech, J. Influence of geographical origin and botanical species on the content of extractives in American, French, and East European oak woods. *J. Agric. Food Chem.* **54,** 8115–8126 (2006).

21. Prida, A. & Puech, J. L. Natural variability of wood compounds in relation to cooperage oak quality. *Aust. New Zeal. Wine Ind. J.* **23,** 42–46 (2008).

22. Hale, M. D., McCafferty, K., Larmie, E., Newton, J. & Swan, J. S. The Influence of Oak Seasoning and Toasting Parameters on the Composition and Quality of Wine. *Am. J. Enol. Vitic.* **50,** 495–502 (1999).

23. Jin, W., Singh, K. & Zondlo, J. Pyrolysis Kinetics of Physical Components of Wood and Wood-Polymers Using Isoconversion Method. *Agriculture* **3,** 12–32 (2013).

Chapter 5: Concluding Remarks and Future Perspectives

This chapter will examine the findings of each of the three studies in this thesis, make conclusions on the basis of the results and highlight possibilities for future research.

In this thesis, the utility of three direct MS approaches was investigated for different wine industry quality control applications. Firstly, a numerically optimized secondary electrospray ionization mass spectrometry (SESI-MS) ion-source, interfaced to an Orbitrap MS was used to monitor the latter stages of grape ripening by analysing VOC's directly from intact grapes (Chapter 2).

Previous studies regarding the evolution of free grape berry VOC's have focused on aromatic Muscat grape varieties in part because of the low concentration of VOC's in "neutral" non-Muscat grape cultivars. On the contrary, this study investigated VOC's from non-Muscat grape cultivars. The SESI-MS approach detected approximately 300 mass spectral peaks at each ripening period in positive ion mode, and 70-100 peaks in negative ion-mode. This indicates that a rich chemical dataset can be acquired from intact, non-Muscat grape berries with unrivalled temporal resolution and without requiring sample preparation or concentration steps.

Trends for peaks assigned to C_{13}-norisoprenoids and benzenoid derivatives (based on accurate mass) showed similar trends in previous studies using offline gas chromatography (GC) approaches. Ten peaks in positive mode and two peaks in negative mode exhibited significant linear trends ($R^2 \geq 0.8$, $p < 0.05$) for the combined data across all cultivars, either increasing or decreasing in the final four weeks of ripening. These peaks may hold potential as markers of grape maturity. However, further investigation is required over multiple vintages and longer ripening periods to determine the robustness of the trends observed in this first preliminary study.

Given the simplicity, sensitivity and temporal resolution of the SESI-MS approach, I believe that such direct MS approaches hold great promise for a multitude of next generation precision viticulture applications.

Secondly, the oak toasting process was monitored in real-time using a proton transfer reaction mass spectrometer (PTR-MS), (Chapter 3). This online method circumvents limitations associated with previous GC based approaches by:

(i) greatly improving the temporal resolution (one measurement was recorded every 2 s) allowing the time-intensity profile for key aroma compounds to be directly monitored in real-time;
(ii) avoiding liquid extractions and lengthy sample preparation protocols;
(iii) reducing sources of error associated with liquid extractions; and
(iv) avoiding multiple time-discrete toasting treatments by elucidating the time dimension in a single dynamic experiment.

Some important compounds (e.g. norisoprenoids) were not detected in the PTR-MS experiments. Future work should examine whether this was due to the experimental setup that may have limited the sensitivity for these compounds typically present in oak wood at trace concentrations.

This first study of online monitoring of the oak toasting process showed that individual oak boards react differently under similar toasting conditions, even when the analysis is limited to boards of the same origin, moisture content and density. The direct PTR-MS study elucidated the development of important oak aroma compounds during the toasting process. I believe that such direct MS approaches could readily be used in many different applications to further our understanding and control of “oak expression” in aged wine. This is particularly important considering the high degree of natural variability in oak wood and the current lack of objective real-time measurements of oak wood aroma potential.

Thirdly, a thermal desorption dielectric barrier discharge ionisation mass spectrometry system (TD-DBDI-MS) for rapid analysis of volatile organic compounds (VOC’s) from oak wood shavings was introduced (Chapter 4). Screening of oak VOC’s

from a sample of shavings could be conducted with an analysis time of ten seconds. Known oak wood VOC's from different chemical classes were detected, including furanic aldehydes, volatile phenols, phenolic aldehydes and oak lactones. Norisoprenoid compounds were also detected by TD-DBDI-MS, tentatively identified from accurate mass via Orbitrap MS.

The TD-DBDI-MS system was also used to monitor the oak toasting process. The oak toasting process evolved from inherent compounds such as oak-lactone to furanic compounds (from hemicellulose degradation) and phenolic compounds (from lignin degradation) in agreement with the PTR-MS study and previous investigations on oak toasting. The novel sample introduction device based on a "sample-slider" facilitated rapid analysis but could be improved by use of an electrically controlled motor allowing hands-free functionality and avoiding potential inconsistencies due to manual operation.

As mentioned above, future work should investigate whether the detection of norisoprenoid compounds by DBDI-MS and not PTR-MS was due to differences in the experimental setup or whether it relates to sensitivity or ionisation mechanisms of the different ion-sources.

A limitation of all three direct MS approaches is the inability to differentiate isomeric species. For example, m/z 165.0910, protonated [$C_{10}H_{12}O_2$] was tentatively assigned to eugenol and / or 2-phenylethyl acetate (Chapter 2) as both compounds have been reported as grape VOC's. This disadvantage may be overcome by the addition of an ion mobility spectrometry (IMS) step prior to MS detection, providing an orthogonal dimension of separation whilst maintaining the real-time nature of the analysis[1]. Another strategy to enable separation of isomers by direct MS include selective reagent ionisation mass spectrometry (SRI-MS)[2]. Such developments in combination with innovations in miniaturised, portable mass spectrometer systems will advance the adoption of direct MS by non-technical users.

The direct mass spectrometry methods developed and outlined in this thesis provide an initial step towards harnessing the power of mass spectrometry in wine industry

quality control applications. The three ionisation approaches differ in their ionisation mechanisms, sensitivity and mode of operation.

Consequently, the choice of one approach over another may depend on the specific application. For example, DBDI and SESI will ionise a wider range of compounds than PTR, whilst PTR is more suitable for quantitative analysis. For portable applications DBDI appears a better candidate than SESI, due to the simplicity of the ion source that does not require any solvent system and is compact in size. The medical and security industries have been early adopters of direct mass spectrometry approaches. The wine industry could benefit greatly from powerful, real-time chemical sensors due to the complexity and variability of the wine-making process.

References

1. Cumeras, R., Figueras, E., Davis, C. E., Baumbach, J. I. & Gràcia, I. Review on ion mobility spectrometry. Part 2: hyphenated methods and effects of experimental parameters. *Analyst* **140,** 1391–1410 (2015).
2. Lanza, M. *et al.* Distinguishing two isomeric mephedrone substitutes with selective reagent ionisation mass spectrometry (SRI-MS). *Journal of mass spectrometry : JMS* **48,** (2013).

Appendices

Supplementary information to Chapter 2

Chapter 2 - Supplementary Table 1: External standard infusions for mass spectrometer sensitivity tests.

Week	Measurement date	Average peak area	Residual standard deviation	Peak area change
1	09-04-2016	3.57E+05	11%	-
2	09-11-2016	3.26E+05	4%	-9%
3	09-18-2016	3.53E+05	5%	-1%
4	09-25-2016	3.34E+05	27%[a]	-6%

[a]A blocked capillary in the infusion set-up resulted in a high RSD (27%) in the final week.

P

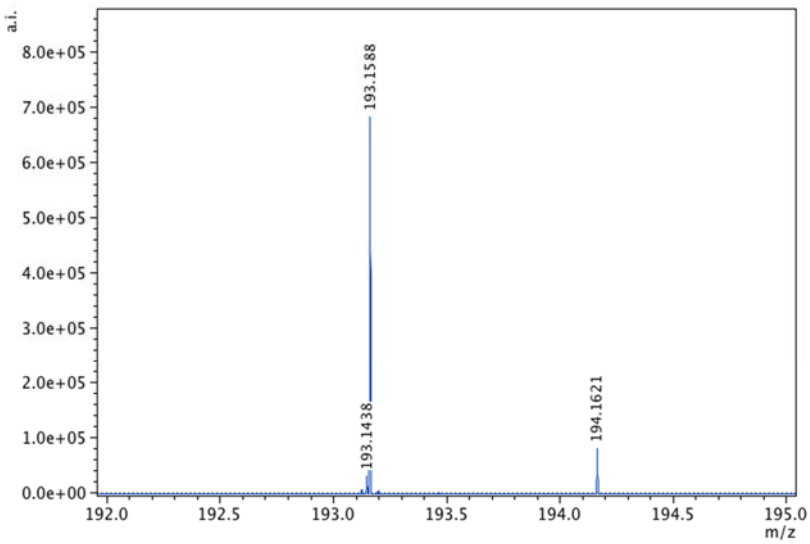

C

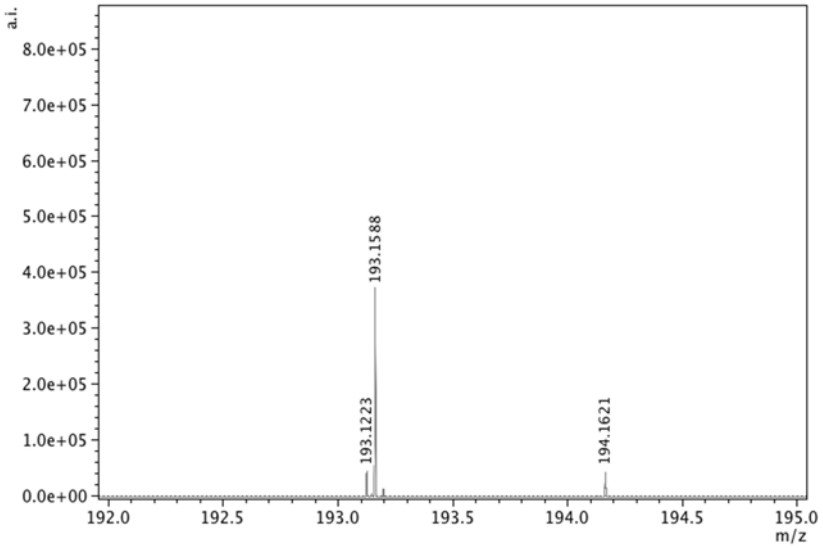

S

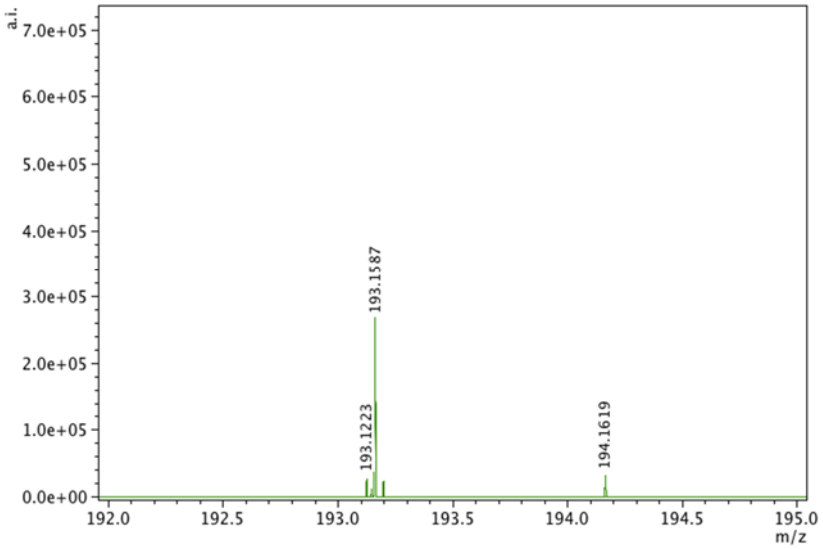

Chapter 2 - Supplementary Figure 1: High-resolution positive ion mode SESI-MS spectra for m/z = 192-195 showing no major interfering peaks at m/z = 193.1587. P, Average spectra Pinot Noir; C, Average spectra Chardonnay; S, Average spectra Sauvignon Blanc.

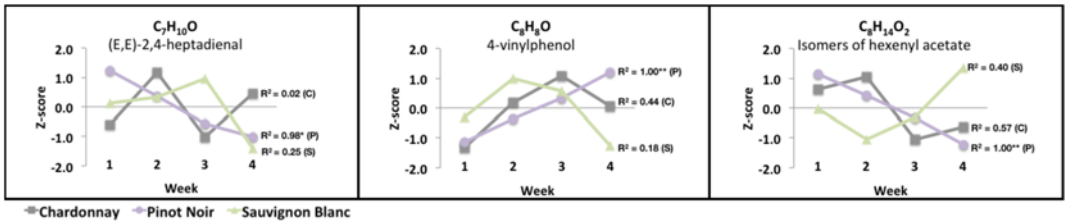

R^2 values shown are for each cultivar treated individually, Pinot Noir (P), Chardonnay (C), and Sauvignon Blanc (S).

** Correlation is significant at the 0.01 level (2-tailed).

* Correlation is significant at the 0.05 level (2-tailed).

Chapter 2 - Supplementary Figure 2: Tentatively identified $[M+H]^+$ peaks with a cultivar specific (Pinot Noir) linear increasing or decreasing trend ($R^2 \geq 0.80$, $p < .05$) during the final four weeks of grape berry ripening based on combined data for all cultivars. Measured by positive ion mode secondary electrospray ionization mass spectrometry.

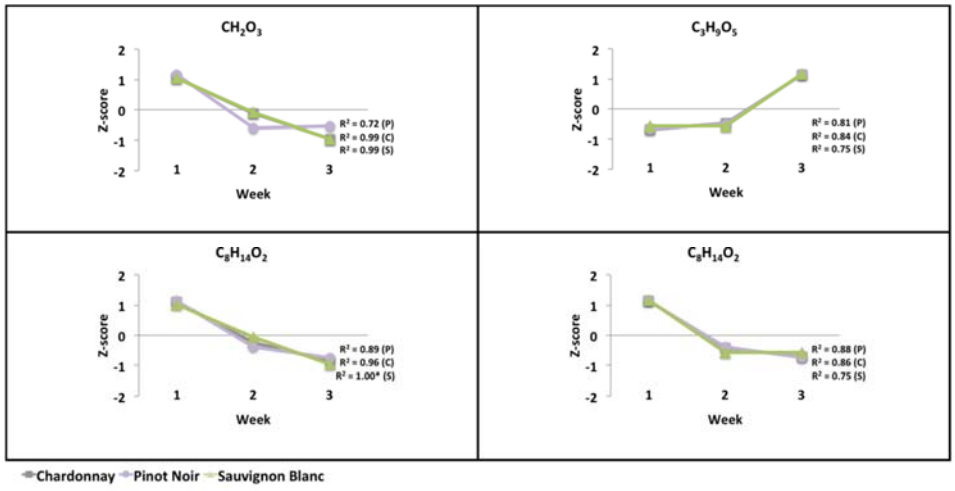

R^2 values shown are for each cultivar treated individually, Pinot Noir (P), Chardonnay (C), and Sauvignon Blanc (S).

* Correlation is significant at the 0.05 level (2-tailed).

Chapter 2 - Supplementary Figure 3: Tentatively identified $[M-H]^-$ peaks with a significant linearly increasing or decreasing trend ($R^2 \geq 0.80$, $p < .05$) during the final three weeks of grape berry ripening based on combined data for all cultivars. Measurements via negative ion mode secondary electrospray ionization mass spectrometry.

Supplementary information to Chapter 3

Chapter 3 - Supplementary Table 1: Moisture content and density properties for the oak staves measured prior to the toasting process.

French Oak			American Oak		
Board	Moisture content (%)	Oven-dry density (g/cm^3)	Board	Moisture content (%)	Oven-dry density (g/cm^3)
1	10.8	0.689	1	9.5	0.707
2	11.1	0.755	2	8.4	0.736
3	10.0	0.682	3	9.6	0.771
4	9.8	0.701	4	10.7	0.782
Average	10.4	0.707	Average	9.5	0.749
Standard deviation	0.6	0.033	Standard deviation	0.9	0.034

Chapter 3 - Supplementary Table 2: Summary of temperature effects according to ANOVA (least square means) for each compound.

	Furfural	5MF	HMF	Vanillin	Eugenol	Guaiacol	Lactone
225	22413.690 a	2774.267 a	521.328 a	518.353 a	74.999 a	95.993 a	151.628 a
200	2854.985 b	266.119 b	68.469 b	45.297 b	5.867 b	8.125 b	34.919 b
175	399.158 b	22.803 b	7.420 c	3.730 b	0.878 b	0.877 b	12.296 b
Pr > F	<0.0001	<0.0001	<0.0001	<0.0001	<0.0001	<0.0001	<0.0001
Significant	Yes	Yes	Yes	Yes	Yes	Yes	Yes

Data followed by different letters (in a column) are significantly different according to ANOVA at the $P < 0.05$ level.

Chapter 3 - Supplementary Table 3: Summary of pairwise comparisons for species for furfural according to Tukey's Honestly Significantly Different test.

Category	LS means(Furfural)	Groups
AO	9574.848	A
FO	7537.041	A

Categories (rows) with different letters are significantly different according at the $P < 0.05$ level.

Chapter 3 - Supplementary Table 4: Summary of pairwise comparisons for species for 5-methylfurfural (5MF) according to Tukey's Honestly Significantly Different test.

Category	LS means(5MF)	Groups
FO	1064.329	A
AO	977.797	A

Categories (rows) with different letters are significantly different according at the $P < 0.05$ level.

Chapter 3 - Supplementary Table 5: Summary of pairwise comparisons for species for 5-hydroxymethylfurfural (HMF) according to Tukey's Honestly Significantly Different test.

Category	LS means(HMF)	Groups	
AO	240.532	A	
FO	157.613		B

Categories (rows) with different letters are significantly different according at the P < 0.05 level.

Chapter 3 - Supplementary Table 6: Summary of pairwise comparisons for species for vanillin according to Tukey's Honestly Significantly Different test.

Category	LS means(Vanillin)	Groups	
AO	249.696	A	
FO	128.557		B

Categories (rows) with different letters are significantly different according at the P < 0.05 level.

Chapter 3 - Supplementary Table 7: Summary of pairwise comparisons for species for eugenol according to Tukey's Honestly Significantly Different test.

Category	LS means(Eugenol)	Groups	
AO	36.205	A	
FO	18.291		B

Categories (rows) with different letters are significantly different according at the P < 0.05 level.

Chapter 3 - Supplementary Table 8: Summary of pairwise comparisons for species for guaiacol according to Tukey's Honestly Significantly Different test.

Category	LS means(Guaiacol)	Groups	
AO	45.117	A	
FO	24.880		B

Categories (rows) with different letters are significantly different according at the P < 0.05 level.

Chapter 3 - Supplementary Table 9: Summary of pairwise comparisons for species for oak lactone according to Tukey's Honestly Significantly Different test.

Category	LS means(Lactone)	Groups	
AO	97.634	A	
FO	34.929		B

Categories (rows) with different letters are significantly different according at the P < 0.05 level.

Chapter 3 - Supplementary Table 10: Summary of pairwise comparisons for each species x temperature category according to Tukey's Honestly Significantly Different test.

Category	LS means(Lactone)	Groups		
AO*225	223.918	A		
FO*225	79.338		B	
AO*200	51.076		B	C
FO*200	18.763		B	C
AO*175	17.906		B	C
FO*175	6.686			C

Categories (rows) with different letters are significantly different according at the $P < 0.05$ level.

Chapter 3 - Supplementary Table 11: Fragmentation of oak lactone under proton-transfer-reaction mass spectrometry conditions utilized in this work.

Compound	Molecular weight	Relative abundance[a] of major ions[b] [(relative abundance)]			
Oak lactone	156	**157** (100)	139 (48)	97 (11)	55 (10)

[a] data presented as the background corrected counts per second normalized to the most abundant mass fragment (relative abundance 100). All other intensities are calculated relative to the most abundant mass fragment.

[b] Mass fragments with intensity less than 10 not shown. $[M+H]^+$ in bold.